

CELLULARITY OF KLR AND WKLRW ALGEBRAS VIA CRYSTALS

ANDREW MATHAS AND DANIEL TUBBENHAUER

ABSTRACT. We prove that the wKLRW algebras of finite type, and their cyclotomic quotients, are sandwich cellular algebras. The sandwich cellular bases are explicitly described using crystal graphs. As a special case, this proves that the KLR algebras of finite type are sandwich cellular. As one of our applications, we give explicit formulas for some graded decomposition numbers of the cyclotomic algebras in level one.

CONTENTS

1. Introduction	1
2. Sandwich cellularity	4
3. wKLRW algebras	6
4. Main example	12
5. Finite types and crystal graphs	16
6. Sandwich cellular bases	25
7. Proof of sandwich cellularity	39
8. Some consequences of sandwich cellularity	47
References	55

1. INTRODUCTION

This introduction is organized as follows. We begin with a historical overview in [Section 1A](#), followed by a technicality-free summary in [Section 1B](#); [Section 1C](#) then provides the full details for experts.

1A. A historical overview. In 1996, Lascoux, Leclerc and Thibon [[LLT96](#)] made their now-famous LLT conjecture that predicted deep connections between the representation theory of Iwahori-Hecke algebras of type A and the canonical bases Kac-Moody algebras. Soon afterwards, Ariki [[Ari96](#)] proved their conjecture, not just for the Hecke algebras of type A but for the Ariki-Koike algebras at complex roots of unity.

Rather than resolving the LLT conjecture, Ariki's work opened new questions because the LLT conjecture says that the decomposition numbers of the Iwahori-Hecke algebras of the symmetric groups can be computed by evaluating certain parabolic Kazhdan-Lusztig polynomials at 1. Interpreting the polynomial variable as a grading parameter, this is precisely what one would expect if the decomposition numbers were shadows of graded multiplicities. This strongly suggests that there should be a nontrivial grading on these algebras, but no such grading was known.

The first significant step towards finding such a grading was made by Chuang and Rouquier [[CR08](#)], who introduced \mathfrak{sl}_2 -categorifications, which are a family of derived equivalences that categorify the action of the simple reflections in the affine Weyl group on the Fock spaces underlying the LLT conjecture. As an application, Chuang and Rouquier showed that Broué's abelian defect group conjecture [[Bro90](#)] holds for the symmetric groups. Motivated in part by the LLT conjecture and Ariki's work, they further suggested the existence of stronger Kac-Moody categorifications.

Independently, Khovanov-Lauda [[KL09](#), [KL11](#)] and Rouquier [[Rou08](#)] introduced the KLR algebras, which are a family of \mathbb{Z} -graded algebras attached to a Kac-Moody quiver. These algebras can be defined both by generators and relations and diagrammatically, with the grading of these algebras being determined by the underlying quiver and its Cartan matrix. They proved that the (affine) KLR algebras categorify the positive part of the corresponding quantised Kac-Moody algebra.

The cyclotomic KLR algebras are finite dimensional quotients of the KLR algebras, indexed by dominant weights of the corresponding Kac-Moody algebra, which are defined in exactly the same way as the cyclotomic quotients of the affine Hecke algebras. For affine quivers of type A , Lauda and Vazirani [[LV11](#)] proved that the simple modules of these algebras categorify the crystal graph of the associated highest weight module. Varagnolo-Vasserot [[VV11](#)] and Rouquier [[Rou12](#)] proved that the cyclotomic KLR algebras of finite type

2020 *Mathematics Subject Classification.* Primary 18M30, 20C08; Secondary 05E10, 17B10, 18N25.

Key words and phrases. KLR and wKLRW algebras, sandwich cellular algebras, crystal graphs.

categorify the highest weight modules and their crystal graphs. For the simply laced quivers, Varagnolo–Vasserot [VV11] and Kang–Kashiwara [KK12] proved that the simple modules of the cyclotomic KLR algebras categorify the dual canonical bases, and the projective indecomposable modules categorify the canonical bases, of the corresponding highest weight modules.

In the special case of affine quivers of type A , Brundan and Kleshchev [BK09a] and Rouquier [Rou12] proved that the cyclotomic KLR algebras are isomorphic to the cyclotomic Hecke algebras of type A . Indeed, before the work of Varagnolo–Vasserot and Kang–Kashiwara mentioned above, [BK09b, Rou12] proved that the canonical bases categorification theorem in type A . Consequently, these results for the KLR algebras can be viewed as a vast generalisation of Ariki’s categorification theorem. In particular, the grading on the KLR algebras fully explain the appearance of q in the LLT conjecture.

In 2012, Kleshchev, Loubert and Miemietz [KLM13] conjectured that the KLR algebras are graded (affine) cellular algebras. Some progress was made towards this conjecture for the infinite dimensional KLR algebras [KL15], but the conjecture for the cyclotomic quotients proved to be much harder, except in type $A_e^{(1)}$ [HM10].

In spite of the wealth of strong categorification theorems describing the representation theory of the cyclotomic KLR algebras, surprisingly little is known about these algebras, except in affine type A where the Brundan–Kleshchev isomorphism to the ungraded Hecke algebras made it possible to classify the blocks of these algebras [BK09a, LM07] and construct cellular bases for them [HM10].

In order to understand categorifications of tensor products, Webster [Web17a, Web19, Web17b] introduced the *weighted KLRW algebras*, which include the KLR algebras as a special case. These algebras admit a diagrammatic presentation and Bowman [Bow22] was able to use these algebras to construct new graded cellular bases for the cyclotomic KLR and weighted KLRW algebras of affine type A . Extending these ideas, the authors proved that the weighted KLRW algebras and their cyclotomic quotients are graded (affine) cellular algebras in types $C_{e>1}^{(1)}$, $B_{\mathbb{Z}_{\geq 0}}^{(1)}$, $A_{2,e>1}^{(2)}$ and $D_{e>1+1}^{(2)}$ in [MT24] and [MT23].

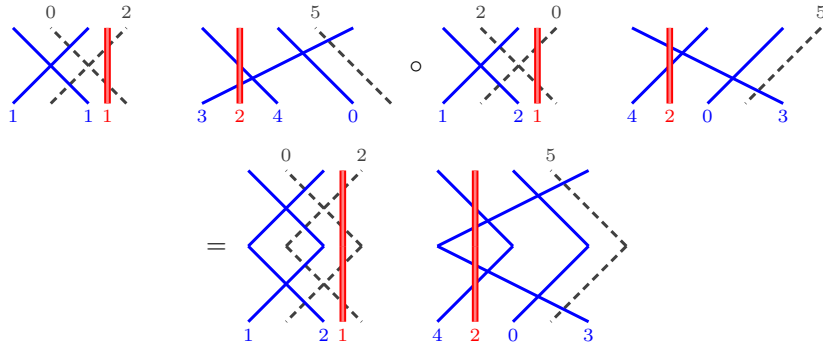
In this paper we apply the KLRW machinery to construct, in principle, explicit bases for the cyclotomic KLR and weighted KLRW algebras for quivers of finite type. To construct bases for these algebras we use the general approach that we developed in [MT24, MT23]. In these papers we described these bases using explicit tableau combinatorics, which partially existed in the literature for describing Fock spaces for the corresponding highest weight modules. Similar combinatorics exists for the KLR algebras of simply laced types, but in this paper we take a different approach and use the crystal graphs to construct bases for these algebras. By using the crystal graphs, we have a uniform combinatorics for describing bases of the cyclotomic KLR and weighted KLRW algebras for all quivers of finite type. This is very natural because Lauda–Vazirani [LV11] and Varagnolo–Vasserot [VV11] have shown that the cyclotomic KLR algebras of finite type categorify the highest weight modules and their crystal graphs. In this way we are able to directly link the crystal theory and the weighted KLRW algebras. To do this we consider a special family of weighted KLRW algebras, which are closely related to the KLR algebras.

1B. A layperson’s summary. One way to organize a complicated algebra is to give it a good set of building blocks and a recipe for how the blocks multiply. For matrix algebras, Gaussian elimination plays this role; for symmetric groups, Young diagrams and tableaux do. This paper shows that a much larger and more modern family of diagrammatic algebras, those arising from the Khovanov–Lauda–Rouquier (KLR) [KL09, KL11, Rou08] framework and their (weighted) variants [Web17a, Web19, Web17b], also admit such an organizing principle in finite type. In plain terms: we prove that in the finite-type setting there are bases and a compatible structure that let you “triangularize” the algebra and read off its representations in a controlled and combinatorial way. (Finite type here refers to the case controlled by classical Dynkin diagrams, the regime where the underlying combinatorics is sharpest and well-understood.)

Why do people care about KLR algebras? Well, KLR algebras sit at a busy crossroads. We summarized part of their history in [Section 1A](#), with the focus on the LLT conjecture part. Additionally, they categorify quantum groups, turning the combinatorics of canonical/crystal bases into concrete, computable objects; they provide a diagrammatic home for link-homology theories in low-dimensional topology (via braid and tangle actions); and they connect to geometric representation theory through quiver varieties and sheaf-theoretic models. On the algebra/combinatorics side, they unify and extend familiar diagram algebras (Hecke, Temperley–Lieb, Brauer, Schur-like quotients) and inform questions about decomposition numbers and modular phenomena. In short: understanding KLR algebras pays dividends across topology, geometry, and algebra, and having a cellular/triangular organization turns these conceptual links into practical tools. Since their inception in the mid-2000s there has been enormous progress, yet basic structural features, most notably “nice” bases that behave well under multiplication, have remained elusive. Providing such bases in finite type is the starting point and main contribution of this paper.

Let us now explain the results of this paper in more detail while keeping the details under the rug. First, we use a slightly enhanced algebra that we call wKLRW algebra. The difference between these algebras, for our purpose, is mostly cosmetic: the combinatorics is easier to see in the wKLRW picture. Readers unfamiliar

with KLR-style algebras can think of them as algebras presented by pictures: one draws colored labeled strings in a strip, allowed to cross or carry dots, and composes pictures by stacking. An example is:



Familiar older cousins are Temperley–Lieb and Brauer algebras, where noncrossing matchings or pairings govern multiplication. The power of a diagram algebra comes from having a basis of diagrams for which multiplying and simplifying is predictable. Our contribution is to show that, for finite type, the relevant KLR algebras admit exactly this kind of predictable organization, a sandwich cellular structure as e.g. in [Tub22], and that the indexing data are supplied by the crystal graphs from Lie theory.

Without technicalities this means the following. A cellular algebra (in the sense of Graham–Lehrer [GL96] and generalizations) is one that comes with: (i) a poset indexing of basis pieces (“cells”), (ii) standard modules attached to these indices, and (iii) a multiplication rule that is upper-triangular with respect to the poset. Practically, this yields a clean bookkeeping device for simple modules and decomposition numbers, and it behaves well under standard operations (duality, quotients, specializations). We work in a slightly more flexible setting, so-called sandwich cellularity, which isolates a straightforward piece in the middle of a diagram but keeps the same spirit: multiplication respects a transparent order, so representation-theoretic information can be read off in stages.

Before giving more details for the experts, here is what we prove informally.

- *Cellularity from crystals.* wKLRW algebras of finite type admit sandwich cellular structures with bases built from crystal paths. (More on crystals momentarily.)
- *Same representation theory, different models.* wKLRW and KLR algebras in finite type are Morita equivalent; their module categories are the same up to equivalence.
- *Structural corollaries.* We record criteria for when these algebras are nonzero, semisimple, quasi-hereditary, or indecomposable, and we point out situations where cellularity fails, clarifying the boundary of our results.

Although we were surprised by the deep connection between crystals and sandwich cellularity, there are conceptual reasons why crystals appear: Crystals are the combinatorial “skeletons” of representations of semisimple Lie algebras: directed graphs whose vertices label basis elements and whose arrows record how simple raising/lowering operations move you around. In finite type, it is a guiding principle that the representation theory of KLR algebras mirrors these crystal graphs [LV11, VV11]. Our results make this principle concrete for bases and cellularity: basis elements are built by following paths in the crystal and drawing the corresponding diagrams; triangularity reflects a certain partial order coming from the crystal; and the standard modules one expects in a cellular setting line up with crystal data in a hands-on way.

Takeaway. Diagrams, crystals, and sandwich cellularity fit together in finite type to provide a concrete, diagrammatic blueprint for the representation theory of KLR/wKLRW algebras. The results put the combinatorics of crystals to work as an organizing spine for bases, modules, and decomposition numbers in a broad class of modern diagrammatic algebras.

1C. More details. Using this framework, our main results are:

- (A) [Theorem 6I.1](#) shows that the weighted KLRW algebras, and their cyclotomic quotients, are graded sandwich cellular algebras. This implies the corresponding results for the KLR algebras.
- (B) In [Proposition 8B.5](#) we prove that the cyclotomic wKLRW algebras and the cyclotomic KLR algebras of finite type are graded Morita equivalent.
- (C) In [Proposition 8B.2](#) we prove that simple modules of these algebras are indexed by the vertices of the corresponding crystal graph.
- (D) In level one, under certain technical assumptions, we give a basis for the projective indecomposable modules of the cyclotomic wKLRW algebras and compute the graded decomposition numbers of the cell modules in [Section 8D](#). Except in type F_4 , [Theorem 8D.5](#) shows that the projective indecomposable

modules categorify the canonical basis of the highest weight module. In this case, we construct the simple modules explicitly and determine their dimensions in [Proposition 8E.1](#).

- (E) In [Section 8](#) we list several more consequences of sandwich cellularity, including results on when these algebras are nonzero, semisimple, quasi-hereditary and indecomposable.
- (F) We also talk about the limitations of our results, see [Proposition 8F.2](#).

All of these results are independent of the characteristic.

We briefly outline the contents of this paper. [Section 2](#) recalls the basic machinery of sandwich cellular algebras. [Section 3](#) contains the definition of wKLRW algebras and gives the basic rewriting results from [\[MT24\]](#) that we use to pull strings and jump dots to the right that underpins our basis theorems and hence all of the results in this paper. To explain (almost all) of the combinatorics used in this paper, [Section 4](#) is an extended running example of our construction of cellular bases for the wKLRW algebras. [Section 5](#) starts with some reminders from the theory of crystal graphs, which is then extended and applied to the wKLRW algebras in [Section 6](#). It is striking that our crystal basis is built from idempotent diagrams, which correspond to paths in the crystal, together with permutations of the labels along these paths. [Section 7](#) proves our sandwich cellular basis theorems and [Section 8](#) contains the applications of these results to the representation theory of the KLR and wKLRW algebras.

Remark 1C.1. Many of the results in this paper were inspired by extensive calculations with crystals using SageMath [\[Sag23\]](#) and some results for exceptional type rely on these calculations. The code that we used can be found at [\[MT22\]](#), which also includes some additional features, such as code for drawing some of the wKLRW diagrams used in this paper.

Acknowledgments. We thank Anton Evseev and Sasha Kleshchev for sharing a sketch of a proof that the affine type D cyclotomic KLR algebras are not cellular; Robert Muth for helpful discussions that gave birth to [Remark 8F.4](#); and Travis Scrimshaw for invaluable discussions about SageMath and crystals. We also thank Chris Bowman, Joe Chuang, Dinushi Munasinghe, Tao Qin, the referee, Liron Speyer and Ben Webster for helpful discussions about (weighted) KLR(W) algebras and cellularity. All of this is very much appreciated.

Both authors were supported, in part, by the Australian Research Council. D.T. thanks additionally their depression, burnout and usage of outdated ideas for long-term support.

2. SANDWICH CELLULARITY

The main results of this paper show that the wKLRW algebras of finite type are sandwich cellular algebra. This section defines sandwich cellular algebras and sets our notation.

2A. Sandwich cellular algebras.

Notation 2A.1.

- (a) A grading will always mean a \mathbb{Z} grading.
- (b) Throughout we will work with diagram algebras and left actions and left modules, which are given by acting from the top:

$$E \circ D = \begin{array}{c} E \\ \otimes \\ D \end{array}.$$

Modules will always be left modules.

- (c) Let R be an integral domain, such as $R = \mathbb{Z}$ or a field, which is our ground ring throughout. ([Section 2A](#) works in more generality but this is not important for this paper.)
- (d) In this paper all R -modules are R -free, ranks are always considered over R and we will use v to indicate the grading. More precisely, if V is a graded R -module, then the **graded rank** $\text{rk}_R^v(V) = \sum_{i \in \mathbb{Z}} \text{rk} V_i v^i \in \mathbb{Z}_{\geq 0}[v, v^{-1}]$ of V is defined by the property that there is a homogeneous degree 0 isomorphism $V \cong \bigoplus_{i \in \mathbb{Z}} R\langle i \rangle^{\oplus a_i}$, where $R\langle i \rangle$ is concentrated in degree i . Specializing $v \rightarrow 1$ recovers the usual (ungraded) rank $\text{rk}_R^1(V)$ of V .

The following is copied, almost verbatim, from [\[MT23, Definition 2A.2\]](#) and this, in turn, is a mild reformulation of [\[TV23, Definition 2.2\]](#) and [\[Tub22, Definition 2A.3\]](#):

Definition 2A.2. Let A be a locally unital graded R -algebra. A **graded sandwich cell datum** for A is a tuple $(\mathcal{P}, (S, T), (\mathcal{H}, B^{\mathcal{H}}), C, \deg)$, where:

- $\mathcal{P} = (\mathcal{P}, <)$ is a poset (the **middle poset** with **sandwich order** $< \leq <_{\mathcal{P}}$),
- $S = \coprod_{\lambda \in \mathcal{P}} S(\lambda)$ and $T = \coprod_{\lambda \in \mathcal{P}} T(\lambda)$ are collections of finite sets (the **bottom/top sets**),

- $\mathcal{H} = \bigoplus_{\lambda \in \mathcal{P}} \mathcal{H}_\lambda$ is a direct sum of graded (not necessarily unital) algebras \mathcal{H}_λ (the **sandwiched algebras**) and $B^\mathcal{H} = \coprod_{\lambda \in \mathcal{P}} B_\lambda^\mathcal{H}$ (the **sandwiched basis**) such that $B_\lambda^\mathcal{H}$ is a homogeneous basis of \mathcal{H}_λ (we write \deg for the degree function on \mathcal{H}_λ),
- $C: \coprod_{\lambda \in \mathcal{P}} S(\lambda) \times B_\lambda^\mathcal{H} \times T(\lambda) \rightarrow A; (S, b, T) \mapsto C_{ST}^b$ is an injective map (the **basis**),
- $\deg: \coprod_{\lambda \in \mathcal{P}} S(\lambda) \cup T(\lambda) \rightarrow \mathbb{Z}$ is a function (the **degree**),

such that:

- (AC₁) For $S \in S(\lambda)$, $T \in T(\lambda)$ and $b \in B_\lambda^\mathcal{H}$, $\lambda \in \mathcal{P}$ the element C_{ST}^b is homogeneous of degree $\deg(S) + \deg(b) + \deg(T)$.
- (AC₂) The set $\{C_{ST}^b \mid \lambda \in \mathcal{P}, S \in S(\lambda), T \in T(\lambda), b \in B_\lambda^\mathcal{H}\}$ is an R -basis of A .
- (AC₃) For all $x \in A$ there exist scalars $r_{SU} = r_{SU}(x) \in R$ that do not depend on T or on b , such that

$$xC_{ST}^b \equiv \sum_{U \in T(\lambda), c \in B_\lambda^\mathcal{H}} r_{SU} C_{UT}^c \pmod{A^{>\lambda}},$$

where $A^{>\lambda} = \bigcup_{\mu > \lambda} A^{\geq \mu}$ and $A^{\geq \mu}$ is the R -submodule of A spanned by $\{C_{UV}^c \mid \nu \in \mathcal{P}, \nu \geq \mu, U \in S(\nu), V \in T(\nu), c \in B_\nu^\mathcal{H}\}$.

- (AC₄) Let $A(\lambda) = A^{\geq \lambda}/A^{>\lambda}$. Then there exist free graded right and left \mathcal{H}_λ -modules $\Delta(\lambda)$ and $\nabla(\lambda)$, respectively, such that $A(\lambda) \cong \Delta(\lambda) \otimes_{\mathcal{H}_\lambda} \nabla(\lambda)$ for all $\lambda \in \mathcal{P}$.

The algebra A is a graded **sandwich cellular algebra** if it has a graded sandwich cell datum.

Assume that $S(\lambda) = T(\lambda)$ for all $\lambda \in \mathcal{P}$, and that there is a antiinvolution $(-)^*: A \rightarrow A$ and a homogeneous bijection $(-)^*: B_\lambda^\mathcal{H} \rightarrow B_\lambda^\mathcal{H}$ of order two such that:

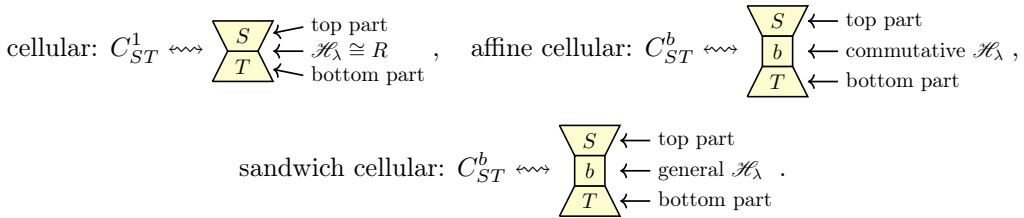
- (AC₅) We have $(C_{ST}^b)^* \equiv C_{TS}^{b^*} \pmod{A^{>\lambda}}$, for all $S, T \in T(\lambda)$ and $b \in B_\lambda^\mathcal{H}$.

In this case, we write $(\mathcal{P}, S = T, (\mathcal{H}, B^\mathcal{H}), C, \deg, (-)^*)$ and call this datum **involutive**.

We omit the brackets around $\mathcal{H}, B^\mathcal{H}$ for readability. We do not distinguish $(-)^*: A \rightarrow A$ and the map $(-)^*: B_\lambda^\mathcal{H} \rightarrow B_\lambda^\mathcal{H}$.

Remark 2A.3. Sandwich cellularity is a common generalization of cellular algebras as in [GL96] and affine cellular algebras as in [KX12]. (Strictly speaking we use a weakened condition on the antiinvolution as in [GG11, Definition 2.3] and we always use this definition when we refer to cellular or affine algebras.) The notion of sandwiched cellularity originates in work of Brown [Bro55] on the Brauer algebra, see also [Tub22] for more historical comments.

For reader familiar with diagram algebras (as in the main body of this paper), the diagrammatic incarnation of sandwich cellularity is:



In the first two pictures, the (affine) cellular algebras have involutive cell data with $\mathcal{H}_\lambda \cong R$, for $\lambda \in \mathcal{P}$.

Notation 2A.4. We usually abuse language and simply say that an algebra **is** sandwich cellular. We also use **affine sandwich cellular** to highlight that the sandwiched algebras are polynomial rings, even though affine sandwich cellular algebras are just special cases of sandwich cellular algebras.

2B. Some statements, including H -reduction. Sandwich cellularity essentially generalizes the machinery of cellular algebras to a larger class of algebras, see e.g. [TV23, Section 2] and [Tub22] for details. Moreover, incorporating a grading generalizes [HM10, Section 2] to this larger class of algebras.

Instead of filling the next few pages with definitions, all of which are not very different from the cellular case and can be found in [Tub22], we stress the statements that we will actually use.

Theorem 2B.1. *Let A be a (graded) sandwich cellular algebra.*

- (a) *Let $e \in A$ be a (homogeneous) idempotent. Then eAe is a (graded) sandwich cellular algebra.*

Assume now that R is a field.

- (b) *All (graded) simple A -modules are uniquely associated to a $\lambda \in \mathcal{P}$, called their **apex**. Denote the set of apexes by $\mathcal{P}^{\neq 0} \subset \mathcal{P}$ and assume that \mathcal{H}_λ is unital Artinian or unital commutative. Then there exist 1:1-correspondences*

$$\{(graded) simple A\text{-modules with apex } \lambda\} / \cong \xleftrightarrow{1:1} \{(graded) simple \mathcal{H}_\lambda\text{-modules}\} / \cong.$$

- (c) Assume that $\text{rk}_R(A) < \infty$. If A is involutive, $\mathcal{H}_\lambda \cong R$ for $\lambda \in \mathcal{P}$ and all cell modules are simple, then A is semisimple. Conversely, if at least one \mathcal{H}_λ is not semisimple, then A is not semisimple.

Proof. (a). This has not appeared in the literature, but is an easy adaption of the standard arguments in this setting, see e.g. [KX98, Proposition 4.3] or [ET21, Proposition 2.8.(a)]. Details are omitted.

(b)+(c). See [TV23, Theorem 2.16 and Proposition 2.9] and [Tub22, Proposition 2B.23]. \square

Remark 2B.2.

- (a) Part (b) of [Theorem 2B.1](#) is the celebrated *Clifford–Munn–Ponizovskii* theorem or *H-reduction*. The assumption that \mathcal{H}_λ is unital Artinian or unital commutative can be relaxed, see [TV23, Section 2], but these conditions are automatically satisfied in this paper.
- (b) [Theorem 2B.1](#)(b) can be strengthened at the cost of requiring more notation. The above formulation is sufficient for this paper and we refer the reader to [Tub22, Proposition 2B.23] for a stronger statement.

3. wKLRW ALGEBRAS

We now recall the main algebras considered in this paper, following [MT24]. These algebras, the *wKLRW algebras* or *wKLRW algebras* for short, were originally introduced in [Web19], [Web17b]. The wKLRW algebras are diagram algebras, but not in the traditional sense. At first sight, their definition looks more complicated than it actually is. We have tried to give a self-contained account but we encourage the reader to consult these three papers for more details.

3A. Kac–Moody datum. In this paper, a *symmetrizable Kac–Moody datum* is a set $I = \{1, \dots, e\}$ together with a bilinear form $(_, _)$ on $\mathbb{Z}[I]$ such that $(i, i) = 2$ and $(i, j) \in \{0, -1, -2, -3\}$ for all $i \neq j$. Let $a_{ij} = (i, j)$. Then $\mathbf{A} = (a_{ij})_{i,j=1}^e$ is the *Cartan matrix* of a symmetrizable Kac–Moody algebra. The Cartan matrix has an associated symmetrizer $\mathbf{d} = (d_1, \dots, d_e) \in \mathbb{Z}_{\geq 0}^e$, which is the minimal tuple such that $(d_i a_{ij})_{i,j=1}^e$ is symmetric and positive definite. We also associate a quiver $\Gamma = (I, E)$, with vertices $I = \{1, \dots, e\}$ and edges E . We fix an orientation on the simply laced edges, which will not affect the wKLRW algebras up to isomorphism (see [MT24, Proposition 3A.1] for a precise statement). Following [Kac90, Sections 1.1, 1.2 and 1.3], we have simple roots $\Pi = \{\alpha_1, \dots, \alpha_e\}$, coroots $\{h_1, \dots, h_e\}$, fundamental weights $\Lambda = \{\Lambda_1, \dots, \Lambda_d\}$, the *positive root lattice* $Q^+ = \bigoplus_{i \in I} \mathbb{Z}_{\geq 0} \alpha_i$, the *dominant weight lattice* $P^+ = \bigoplus_{i \in I} \mathbb{Z}_{\geq 0} \Lambda_i$, etc. that we will use throughout.

Notation 3A.1. We write $i \rightsquigarrow j$ if there is an edge from i to j . If we need to specify the multiplicity, then we will write $i \rightarrow j$, $i \Rightarrow j$ or $i \Rrightarrow j$ for $d_i a_{ij} = -1$, $d_i a_{ij} = -2$ and $d_i a_{ij} = -3$, respectively. In particular, if $d_i a_{ij} = -1$, then we fix an orientation $i \rightarrow j$ and, by convention, there is no edge from j to i .

We will eventually focus on quivers of finite type, with the conventions specified in [Section 5A](#) below. For now we allow arbitrary symmetrizable Kac–Moody data because we will need this for [Section 8](#).

3B. wKLRW algebras. This section defines the *wKLRW algebras* $\mathcal{W}_n^\rho(X)$, and their finite dimensional *cyclotomic* quotients $\mathcal{R}_n^\rho(X)$.

The definition of the wKLRW algebras involves two crucial ingredients:

- (a) The wKLRW algebras are graded diagram algebras. That is, they are defined using isotopy equivalence classes of *string diagrams* in \mathbb{R}^2 . These diagrams have a degree, which is determined by the Cartan datum, and they are subject to certain diagrammatic relations, which we recall in [Section 3D](#) and [Section 3E](#) below. The strings in wKLRW diagrams are of three types: *solid*, *ghost* and *red*. In [Section 6A](#), we introduce *affine red* strings, but these strings are used only as a notational convenience and are not part of the wKLRW diagrams. These strings are illustrated as:

$$\text{solid string : } \begin{array}{c} | \\ i \end{array}, \quad \text{ghost string : } \begin{array}{c} | \\ i \end{array}, \quad \text{red string : } \begin{array}{c} \textcolor{red}{|} \\ i \end{array}, \quad \text{affine red string : } \begin{array}{c} \textcolor{brown}{|} \\ i \end{array}.$$

These strings are labeled by *residues* $i \in I$, which are written under the solid and (affine) red strings and over the ghost strings. Solid and ghost strings are also allowed to carry finitely many *dots*. We list all possible local configurations in [\(3E.1\)](#), where we also define the degrees of these configurations.

- (b) The various strings, their labels and positions are determined as follows.
- (i) We fix $n \in \mathbb{Z}_{\geq 0}$, the number of solid strings, the *level* $\ell \in \mathbb{Z}_{>0}$, which is the number of red strings, and $\rho \in I^\ell$. The n solid strings are labeled by residues in I , and the ℓ red strings are labeled by the fixed choices ρ_1, \dots, ρ_ℓ .

For example, taking $n = 3$, $\ell = 2$ and $\rho = (1, 0)$:

$$(3B.1) \quad \begin{array}{c} \text{Quiver } \Gamma: \text{Three nodes } 1, 2, 3 \text{ with edges } 1 \xrightarrow{0.75} 2, 2 \xrightarrow{1.25} 3. \\ \rightsquigarrow \text{wKLRW diagram: Two solid strings (blue) and two ghost strings (red). Node } 1 \text{ has ghost shift } 0.75, \text{ node } 3 \text{ has ghost shift } 1.25. \end{array}$$

On the left-hand side, we have drawn an example quiver Γ . For the wKLRW diagram on the right-hand side we could use any quiver with no edges leaving 1 and 3, and two edges leaving 2.

- (ii) The number of ghost strings and their labels is determined as follows. Every edge $\epsilon: i \rightsquigarrow j$ is given a positive real number $\sigma_\epsilon > 0$ called its *ghost shift*. (More general constructions are allowed in see [MT24, Section 2], but we do not need the most general setting here.) Then each solid i -string has a ghost i -string that is shifted σ_ϵ units to the right. The ghost string mimics its solid string. In particular, for each dot on the solid string there is a corresponding dot on the ghost string that is shifted σ_ϵ units to the right.

An example is:

$$\begin{array}{c} \text{Quiver } \Gamma: \text{Three nodes } 1, 2, 3 \text{ with edges } 1 \xleftarrow{0.75} 2, 2 \xrightarrow{1.25} 3. \\ \rightsquigarrow \text{wKLRW diagram: Two solid strings (blue) and two ghost strings (red). Node } 1 \text{ has ghost shift } 0.75, \text{ node } 3 \text{ has ghost shift } 1.25. \end{array}$$

- (iii) To position the solid and ghost strings we fix a *solid positioning* $\mathbf{x} = (x_1, \dots, x_n) \in \mathbb{R}^n$, and a *ghost shift* $\sigma = (\sigma_\epsilon \in \mathbb{R}_{>0})_{\epsilon \in E}$, which is graph theoretic *weighting* of the quiver Γ . The solid positioning gives the *coordinates* of the solid strings on the real line, with the corresponding ghost strings shifted σ_ϵ units to the right. The positions of the red strings are determined by a *charge* $\kappa = (\kappa_1, \dots, \kappa_\ell) \in \mathbb{R}^\ell$ with $\kappa_1 < \dots < \kappa_\ell$. The solid positioning, ghost shifts and charge are chosen so that no two strings have the same endpoints. All diagrams use the same ghost shifts and charge but we allow different diagrams to have different solid positionings.

For example, in (3B.1) we have $\mathbf{x} = (0, 1.2, 2)$ and $\kappa = (-0.5, 1)$. In this diagram, the solid 2-string has two ghost strings, with ghost shifts 0.75 and 1.25, because the corresponding quiver has two edges starting at 2.

Notation 3B.2.

- (a) For clarity, we often omit strings from diagrams if they are not relevant to the features of the diagram that we are describing.
- (b) Care needs to be taken when drawing diagrams because they are very sensitive with respect to the positions of the strings. However, we can rescale diagrams without harm by [MT24, Section 5], so we often do this to improve our exposition.

3C. **Q-polynomials.** Except in Section 8F, we only consider quivers Γ with $a_{ij}a_{ji} \leq 3$. This includes all quivers of finite and affine type except $A_2^{(2)}$. We will always use the following choice of Q -polynomials (although the relations in Section 3D work in greater generality):

$$Q_{ij}(u, v) = \begin{cases} u - v & \text{if } i \rightarrow j, \\ u - v^2 & \text{if } i \Rightarrow j, \\ u - v^3 & \text{if } i \Leftarrow j, \\ 0 & \text{if } i = j, \end{cases} \quad \begin{cases} v - u & \text{if } i \leftarrow j, \\ v - u^2 & \text{if } i \Leftarrow j, \\ v - u^3 & \text{if } i \Rightarrow j, \\ 1 & \text{otherwise.} \end{cases}$$

With these choices the values for $Q_{i,j,i}(u, v, w) = \frac{Q_{ij}(u, v) - Q_{ij}(u, w)}{w - v}$ are

$$Q_{i,j,i}(u, v, w) = \begin{cases} 1 & \text{if } i \rightarrow j, \\ v + w & \text{if } i \Rightarrow j, \\ v^2 + vw + w^2 & \text{if } i \Leftarrow j, \\ 0 & \text{if } i = j, \end{cases} \quad \begin{cases} -1 & \text{if } i \leftarrow j, \\ -v - w & \text{if } i \Rightarrow j, \\ -v^2 - vw - w^2 & \text{if } i \Leftarrow j, \\ 0 & \text{otherwise.} \end{cases}$$

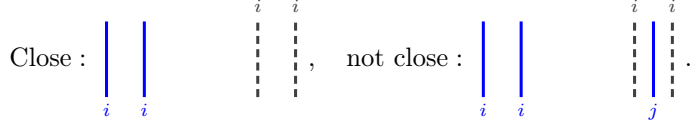
To use these polynomials in relations we make the following definition. Let $\mathbf{u} = (u_1, \dots, u_n)$ and let D be a diagram with n solid strings. For a monomial $f(\mathbf{u}) = u_1^{a_1} \dots u_n^{a_n} \in \mathbb{Z}_{\geq 0}[u_1, \dots, u_n]$ the diagram $f(\mathbf{u})D$ is the diagram obtained from D by putting a_k dots at the top of the k th solid string, and a_k dots on all of its ghosts. Here we number the solid strings from left to right along the top of the diagram so that the k th solid string is the k th string from the left. (From Notation 6E.3 onwards, we use a different numbering.) More generally, given an arbitrary polynomial $f(\mathbf{u}) \in \mathbb{Z}_{\geq 0}[u_1, \dots, u_n]$ let $f(\mathbf{u})D$ be the corresponding linear combination of diagrams.

3D. The relations of wKLRW algebras. We repeat the multilocal relations of wKLRW algebras from [MT24, Definition 2C.7]. The reader may consult that paper for examples and general results about the wKLRW algebras.

Definition 3D.1. Two strings are *close* if, using isotopies, they can be pulled arbitrarily close together in a neighborhood that does not contain any other strings.

It is often necessary to pull strings close together in order to apply the relations below.

Example 3D.2. Let $i, j \in I$ and consider the following two diagrams:



The two solid (and ghost) i -strings on the left are close, but the two solid i -strings on the right are not because the solid j -string prevents the ghost i -strings from being close. This implies that the relation (3D.6) below can be applied to the left-hand diagram. In contrast, (3D.6) cannot be applied to the right-hand diagram even though it appears that it can be applied if we look only in a local neighborhood of the two solid i -strings. \diamond

Following [MT24], a *multilocal* relation is a relation that needs to be applied simultaneously in two or more local neighborhoods. We use multilocal relations because we want to simultaneously apply relations to the solid strings and their ghosts. For simplicity, we often only illustrate one of the local neighborhoods where the relations are applied. Multilocal relations can only be applied if the strings in all relevant neighborhoods are close.

Recall from Section 3B.(b).(iii) that we have fixed a charge $\kappa = (\kappa_1, \dots, \kappa_\ell) \in \mathbb{R}^\ell$. Fix $\varepsilon \ll 1$ such that

$$(3D.3) \quad 0 < \varepsilon < \frac{1}{n^2} \min\left\{\frac{1}{4n(\ell+ne)}, \kappa_{l+1} - \kappa_l \mid 1 \leq i < \ell\right\},$$

and define the set X of *positions* to be

$$(3D.4) \quad X = X_n = \{\kappa_1 - m\varepsilon - m \mid 1 \leq m \leq n\}.$$

The set X gives the possible solid positionings for the solid strings. That is, the top and bottom coordinates of strings are given by the n coordinates in X . The definition of ε in (3D.3) ensures that there will always be enough parking positions for our strings, in the sense of Definition 6B.3 below. The positions in X ensure that the endpoints solid strings are always to the left of the red strings, which implies that the wKLRW algebras defined below are isomorphic to KLR algebras.

Recall that we fixed $\rho \in I^\ell$ in Section 3B. The red strings in the wKLRW diagrams have residues ρ_1, \dots, ρ_ℓ , when read from left to right.

Definition 3D.5. The *affine level* is $\underline{\ell} = \ell + ne$. Define the *affine charge* $\underline{\kappa} = (\underline{\kappa}_1, \dots, \underline{\kappa}_\ell) \in \mathbb{Z}^\ell$ and the *affine red labels* $\underline{\rho} = (\underline{\rho}_1, \dots, \underline{\rho}_\ell) \in I^\ell$ by

$$\underline{\kappa}_m = \begin{cases} \kappa_m & \text{if } 1 \leq m \leq \ell, \\ \kappa_\ell + (2n+1)(m-\ell) & \text{otherwise,} \end{cases} \quad \text{and} \quad \underline{\rho}_m = \begin{cases} \rho_m & \text{if } 1 \leq m \leq \ell, \\ \lfloor \frac{m-\ell-1}{n} \rfloor + e\mathbb{Z} & \text{otherwise,} \end{cases}$$

and set

$$\underline{\Lambda} = (\Lambda_{\underline{\rho}_1}, \dots, \Lambda_{\underline{\rho}_\ell}) = (\Lambda_{\rho_1}, \dots, \Lambda_{\rho_\ell}, \underbrace{\Lambda_1, \dots, \Lambda_1}_{n \text{ times}}, \dots, \underbrace{\Lambda_e, \dots, \Lambda_e}_{n \text{ times}}).$$

The *affine wKLRW algebra* $\mathcal{W}_n^{\underline{\rho}} = \mathcal{W}_n^{\underline{\rho}}(X)$ is the graded unital associative R -algebra spanned by these string diagrams, with *isotopy relations* in \mathbb{R}^2 and subject to the multilocal relations:

- (a) The *(honest) dot sliding relations* hold (that is, solid and ghost dots can pass through any crossing) except in the following cases:

$$(3D.6) \quad \text{Diagram showing two crossing relations: } \text{Diagram with dot on top} - \text{Diagram with dot on bottom} = \text{Diagram with dot on top} = \text{Diagram with dot on bottom} - \text{Diagram with dot on top}.$$

(b) The *(honest) Reidemeister II relations* hold except in the following cases:

$$(3D.7) \quad \begin{array}{c} \text{Diagram: } \text{X} \\ \text{Labels: } i, i \end{array} = 0, \quad \begin{array}{c} \text{Diagram: } \text{X} \\ \text{Labels: } i, j \end{array} = Q_{ij}(\mathbf{u}) \quad \begin{array}{c} \text{Diagram: } \text{X} \\ \text{Labels: } j, j \end{array} \quad \text{or} \quad \begin{array}{c} \text{Diagram: } \text{X} \\ \text{Labels: } j, j \end{array} = Q_{ji}(\mathbf{u}) \quad \begin{array}{c} \text{Diagram: } \text{X} \\ \text{Labels: } j, j \end{array} \quad \text{if } i \rightsquigarrow j, \\ \begin{array}{c} \text{Diagram: } \text{X} \\ \text{Labels: } i, i \end{array} = \begin{array}{c} \text{Diagram: } \text{X} \\ \text{Labels: } i, i \end{array}, \quad \begin{array}{c} \text{Diagram: } \text{X} \\ \text{Labels: } i, i \end{array} = \begin{array}{c} \text{Diagram: } \text{X} \\ \text{Labels: } i, i \end{array}.$$

(c) The *(honest) Reidemeister III relations* hold except in the following cases:

$$(3D.8) \quad \begin{array}{c} \text{Diagram: } \text{X} \\ \text{Labels: } i, i \end{array} = \begin{array}{c} \text{Diagram: } \text{X} \\ \text{Labels: } j, j \end{array} - Q_{iji}(\mathbf{u}) \quad \begin{array}{c} \text{Diagram: } \text{X} \\ \text{Labels: } j, j \end{array} \quad \text{or} \quad \begin{array}{c} \text{Diagram: } \text{X} \\ \text{Labels: } j, j \end{array} = \begin{array}{c} \text{Diagram: } \text{X} \\ \text{Labels: } j, j \end{array} + Q_{ijj}(\mathbf{u}) \quad \begin{array}{c} \text{Diagram: } \text{X} \\ \text{Labels: } j, j \end{array} \quad \text{if } i \rightsquigarrow j, \\ \begin{array}{c} \text{Diagram: } \text{X} \\ \text{Labels: } i, i, i \end{array} = \begin{array}{c} \text{Diagram: } \text{X} \\ \text{Labels: } i, i, i \end{array} - \begin{array}{c} \text{Diagram: } \text{X} \\ \text{Labels: } i, i, i \end{array}.$$

The algebra \mathcal{W}_n^ρ is graded because all of the relations are homogeneous with respect to the degree function given in (3E.1) below.

As in Section 3C, the right-hand side of relations (3D.7) and (3D.8) carry dots determined by the fixed choices of Q -polynomials. We emphasize that in these relations we have drawn only a solid string or its ghost, but the other string is still implicitly part of the relation. The relations can only be applied if they can be simultaneously applied in local neighborhoods around both the solid and ghost strings in the relation.

Example 3D.9. Note that the relations (3D.7) and (3D.8) are not symmetric with respect to the solid and ghost strings. For example, take the quiver $\bullet \rightarrow \bullet \rightarrow \bullet$ of type A_3 numbered and oriented left to right. On the one hand, (3D.7) gives a nontrivial relation between the ghost 1-string and the solid 2-string. On the other hand, the ghost 2-string and the solid 1-string satisfy an honest Reidemeister II relation. That is, we have:

$$\begin{array}{c} \text{Diagram: } \text{X} \\ \text{Labels: } 1, 2 \end{array} = Q_{ij}(\mathbf{u}) \quad \begin{array}{c} \text{Diagram: } \text{X} \\ \text{Labels: } 2, 1 \end{array} \quad \text{and} \quad \begin{array}{c} \text{Diagram: } \text{X} \\ \text{Labels: } 2, 1 \end{array} = \begin{array}{c} \text{Diagram: } \text{X} \\ \text{Labels: } 1, 2 \end{array}.$$

This asymmetry is an important feature of the wKLRW algebras. \diamond

3E. Degrees of diagrams. Diagrams are given a grading by using the following local rules (not multilocal). The *degree* of a fixed diagram is the sum of its local degrees. The local degrees are:

$$(3E.1) \quad \begin{array}{c} \text{Diagram: } \text{X} \\ \text{Labels: } i \end{array} = 2d_i, \quad \begin{array}{c} \text{Diagram: } \text{X} \\ \text{Labels: } i \end{array} = 0, \quad \begin{array}{c} \text{Diagram: } \text{X} \\ \text{Labels: } i, j \end{array} = -\delta_{i,j}2d_i, \quad \begin{array}{c} \text{Diagram: } \text{X} \\ \text{Labels: } j, i \end{array} = \deg \begin{array}{c} \text{Diagram: } \text{X} \\ \text{Labels: } i, j \end{array} = \begin{cases} -(i, j) & \text{if } i \rightsquigarrow j, \\ 0 & \text{else,} \end{cases} \\ \begin{array}{c} \text{Diagram: } \text{X} \\ \text{Labels: } j, i \end{array} = 0, \quad \begin{array}{c} \text{Diagram: } \text{X} \\ \text{Labels: } i, j \end{array} = \deg \begin{array}{c} \text{Diagram: } \text{X} \\ \text{Labels: } j, i \end{array} = \frac{1}{2}\delta_{i,j}(i, i), \quad \begin{array}{c} \text{Diagram: } \text{X} \\ \text{Labels: } i, i \end{array} = \deg \begin{array}{c} \text{Diagram: } \text{X} \\ \text{Labels: } i, i \end{array} = 0.$$

Here, $(-, -)$ is the Cartan pairing associated to Γ , which gives the entries of the Cartan matrix, and (d_1, \dots, d_e) is the symmetrizer. It is straightforward to check that the relations of $\mathcal{W}_n^\rho(X)$ are homogeneous with respect to these local rules, so $\mathcal{W}_n^\rho(X)$ is a graded algebra with degree function \deg .

3F. Cyclotomic quotients. We now define of the finite dimensional quotients of $\mathcal{W}_n^\rho(X)$ that play a key role in this paper.

Example 3F.1. All diagrams in this paper are defined up to isotopy, so isotopy relations play a crucial role when working with wKLRW algebras. Let us give an example and a nonexample of isotopy:

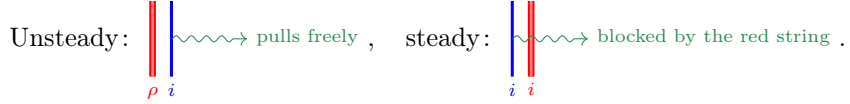
$$\begin{array}{c} \text{Diagram: } \text{X} \\ \text{Labels: } \rho, i \end{array} \xrightarrow{\text{isotopy}} \begin{array}{c} \text{Diagram: } \text{X} \\ \text{Labels: } \rho, i \end{array}, \quad \text{not an isotopy of the left-hand diagram : } \begin{array}{c} \text{Diagram: } \text{X} \\ \text{Labels: } \rho, i \end{array}.$$

Any move that changes the topological nature of a diagram is not an isotopy. All isotopies need to deform solid strings and their ghosts in the same way and dots must move with the strings that they are on. Isotopies never introduce new crossings between strings. \diamond

A solid string is **unsteady** if it can be pulled, using isotopies, arbitrarily far to the right while the red strings stay inside a bounded region. A diagram is **unsteady** if it contains an unsteady string. A string or diagram is **steady** if it is not unsteady.

Note that being unsteady is biased towards the right-hand side. A unsteady diagram can contain solid strings that are steady.

Example 3F.2. The following diagrams are examples of an unsteady and a steady diagram.



The relations imply that the solid i -string cannot be pulled through the red i -string, so the right-hand diagram is steady. Note that the assumption that the red strings stay inside a bounded region is necessary because otherwise the solid i -string and the red i -string in the right-hand diagram can be simultaneously pulled arbitrarily far to the right under isotopy. \diamond

The **cyclotomic wKLRW algebra** $\mathcal{R}_n^p(X)$ is the quotient of $\mathcal{W}_n^p(X)$ by the two-sided ideal \mathcal{U} generated by the unsteady diagrams. As the unsteady ideal is homogeneous, the cyclotomic wKLRW algebra $\mathcal{R}_n^p(X)$ is also graded.

By [MT24, Proposition 3B.12], the affine wKLRW algebras are infinite dimensional and by [MT24, Proposition 3D.4] the cyclotomic wKLRW algebras are finite dimensional algebras.

Remark 3F.3. One of the key features of the homogeneous affine sandwich cellular bases constructed in [MT24] and [MT23] is that they restrict to give homogeneous sandwich cellular bases of $\mathcal{R}_n^p(X)$. We will see that the same is true in this paper.

3G. Pulling strings and jumping dots. Note that the relations (3D.6)–(3D.8) come in mirrored pairs, where the roles of the solid and ghost strings. We use this as follows:

Notation 3G.1. Up to scalars, the set of relations is invariant under reflecting diagrams in their vertical axis and, in some circumstances, swapping the roles of solid and ghost strings (in the sense of (3G.3) below). Many of the relations we will use have this type of duality, which we call **partner relations**.

Related diagrams appearing in a pair of partner relations can have different scalars. Nevertheless, as we will see, we use the symmetry in the partner relations to reduce the number of relations that we need to consider.

Example 3G.2. Let $i \rightsquigarrow j$. Then

$$(3G.3) \quad \text{Diagram showing partner relations: } \text{Diagram with } i \text{ and } j \text{ (solid and dashed)} = \text{Diagram with } i \text{ and } j \text{ (solid and dashed)} - Q_{iji}(\mathbf{u}) \xleftarrow{\text{partner relations}} \text{Diagram with } i \text{ and } j \text{ (solid and dashed)} = \text{Diagram with } i \text{ and } j \text{ (solid and dashed)} + Q_{jij}(\mathbf{u}) \text{,}$$

is an example of partner relations. Note that the scalar in front of the identity diagram changes from $-Q_{iji}(\mathbf{u})$ in the left-hand relation to $+Q_{jij}(\mathbf{u})$ in the right-hand relation. \diamond

Remark 3G.4. One of the key diagrammatic techniques in this paper is **pulling strings** and **jumping dots to the right**. As the next lemma shows, this allows us to rewrite some diagrams as a linear combination of diagrams with certain strings or dots moved further to the right. To make it clearer which strings or dots are moving, we mark the string that is being pulled, or the string that carries a jumping dot, in green.

In all the relations listed below, the diagrams on the right-hand side of each relation are obtained from the diagram on the left-hand side by pulling a (green) string, or the dot on a string, further to the right. In **Definition 6G.4** below, we introduce a total order $<_{\mathbb{R}}$ that keeps track of how far strings are placed to the right. **Lemma 3G.5** can be viewed as saying that diagrams become bigger when strings are pulled to the right. To give our (homogeneous affine) sandwich cellular bases we also want to jump dots as far to the right as possible.

As in **Definition 3D.1**, all of the multilocal relations in **Lemma 3G.5**, and **Lemma 3G.6**, are close configurations. The relations in **Lemma 3G.5.(a)** hold for any quiver and they give a stronger form of the failure of the honest Reidemeister II relations. The relations in **Lemma 3G.5.(b)** depend on the quiver (and our choice of Q -polynomials).

Recall that partner relations are defined in **Notation 3G.1**.

Lemma 3G.5. Suppose that $i, j \in I$.

(a) The following relations, and their partner relations, hold:

(b) The following relations, and their partner relations, hold:

Proof. The first relation in (a), and all of part (b), follows immediately from the defining relations. The second relation in (a) is proved in [MT24, Lemma 6D.1], and the other two relations follow by using this relation, together with (3D.6) and (3D.7), and then cancelling some terms. \square

Lemma 3G.5 is really just a reformulation of some of the defining relations in $\mathcal{W}_n^{\rho}(X)$. As in [MT24] and [MT23], this result should be viewed as a mechanism for pulling strings and jumping dots to the right, which is crucial for this paper.

The following relations are inspired by [Bow22, Equation (5.2)]. We call them *plactic relations* for the reasons explained in Remark 3G.7 below.

Lemma 3G.6. The following relations hold, together with their partner relations:

The dotted plactic relations, and their partner relations,

hold as well.

Proof. We only prove one of these identities, namely the plactic relation for a doubly laced edge. All of the other relations can be proven similarly. Using Lemma 3G.5 we compute

Now, the Reidemeister III relation, i.e. (3D.8), for $i \Rightarrow j$ and our choice of Q -polynomials gives the following left-hand equation, while (3D.6) gives the right-hand relation, again including their partner relations:

Using these two relations to rewrite the relation in the preceding displayed equation completes the proof. \square

Remark 3G.7. In Lie theory, the plactic relations are the image of the Serre relations in the crystals, and the relations in Lemma 3G.6 mimic these as follows. Cutting the pictures in Lemma 3G.6 along their equator gives linear relations between different words in the residues I . More precisely, we obtain relations between the following words:

$$i \not\sim j : \underline{ij}, ji, \quad i \rightarrow j : \overline{ij}, \underline{ij}, jii, \quad i \Rightarrow j : \overline{iii}j, \underline{iji}, ijii, jiii, \quad i \Rrightarrow j : \overline{iiij}, \underline{iji}, ijii, ijiii, jiiii.$$

These relations express the underlined words in terms of the other words, all of which have i -strings further to the right. It is clear that the i -strings are further to the right in all of these words, except for the overlined words for which we can use Lemma 3G.5 to create dots. The extra dots again allow us to pull an i -string further to the right.

4. MAIN EXAMPLE

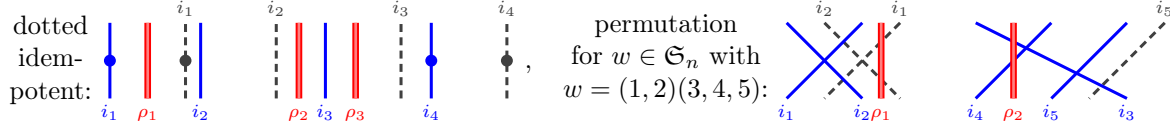
We now give an example that emphasizes the ideas underpinning our construction of the sandwich cellular bases. Some of the terms we use have not been defined yet but, hopefully, the meaning will be clear. We encourage the reader to come back to this example while reading the definitions in Section 5.

4A. Strategic interlude. Similarly to [MT24] and [MT23], and also Remark 2A.3, the picture to keep in mind for the sandwich cellular basis elements $D_{ST}^{a,f}$ that we construct is:

$$(4A.1) \quad D_{ST}^{a,f} \rightsquigarrow \begin{array}{c} S \\ \hbar_{\lambda}^{a,f} \\ T \end{array} = \begin{array}{c} S \\ y^a \\ y^f \\ 1_{\lambda}^y \\ T \end{array}, \quad \text{where} \quad \begin{array}{ll} \begin{array}{c} S \\ \hbar_{\lambda}^{a,f} \\ T \end{array} & \text{a permutation diagram,} \\ \begin{array}{c} y^a \\ y^f \\ 1_{\lambda}^y \\ T \end{array} & \text{an "affine/unsteady" dot placement,} \\ \begin{array}{c} y^f \\ 1_{\lambda}^y \\ T \end{array} & \text{a "finite/steady" dot placement,} \\ \begin{array}{c} 1_{\lambda}^y \\ T \end{array} & \text{a dotted idempotent,} \\ \begin{array}{c} T \end{array} & \text{a permutation diagram.} \end{array}$$

As our terminology suggests, the steady and unsteady dot placements will correspond to steady and unsteady diagrams. The middle of the diagram is given by a **(dotted) idempotent diagram**, possibly with sandwiched

dots $y^a y^f$, and the bottom and top are given by *permutation diagrams*. Examples of these types of diagrams are:



Here, and throughout, we let $\mathfrak{S}_n = \text{Aut}(\{1, \dots, n\})$ be the symmetric group on $\{1, \dots, n\}$, where we use the cycle notation for its elements.

As we have said, our basic strategy is to *pull strings and jump dots to the right* using the results of Section 3G.

As in [MT24] and [MT23], an important observation is that certain Reidemeister II relations do not hold, which stops us from pulling strings to the right. For example, assume that $i \Rightarrow j$. Then Lemma 3G.5.(b) tells us that we can pull a ghost i -string with one dot to the right, or jump the dot on a ghost i -string to the right. However, none of the relations allow us to pull a ghost i -string without dot, or a solid j -string with one dot, to the right, so these strings are *blocked*. It is possible that some of the other relations allow us to pull these strings further to the right but we eventually see that it is not possible to pull these strings further to right.

Generalizing the simple observation from the last paragraph to all residues leads us to our main strategy for constructing idempotents: we place the solid strings and their ghosts inductively by putting the new strings on the left of the diagram and then pull them to the right until they are blocked by another string for which there is no Reidemeister II relation. Using categorification, we show that the residue sequences for the idempotent diagrams are given by paths in the corresponding crystal graph, so the idempotent diagrams are naturally indexed by vertices of the crystal graph. We will see that the idempotent diagrams in our sandwich cellular basis are maximal with respect to a total order $<_{\mathbb{R}}$, which measures how far strings are placed to the right.

The inductive process used to construct idempotent diagrams can be thought of as follows. For the idempotent diagram that we are constructing, we assume that the first $(k-1)$ solid strings, and their ghosts, have already been placed. We then put the k th solid string, and any ghosts, on the far left of the diagram and pull these strings to the right using isotopies and honest Reidemeister II moves. We emphasize that the solid strings and their ghosts have to be pulled at the same time, because the ghost strings are shifts of the solid string. These strings will eventually become blocked, by either an affine red string or by a previously placed solid or ghost string, which becomes the final position of these strings. This process ensures that idempotents in the cellular basis are maximal with respect to $<_{\mathbb{R}}$. Pulling strings to the right in this way also allows us to argue by induction by working modulo higher order terms with respect to $<_{\mathbb{R}}$.

After the idempotent diagram is constructed we need to decorate the idempotent with dots whenever there are close strings with repeated residues. This is necessary because we want to flank diagrams with crossings, cf. (4A.1), but (3D.7) annihilates two close solid i -strings whenever they are flanked with crossings.

In addition, it is sometimes possible to add more dots to a dotted idempotent diagram in such a way that the strings are still blocked. For example, the partner relations of the relations in Lemma 3G.5.(b) only allow strings to be pulled to the right when they have enough dots. This means that these strings are blocked if we add one or two dots, with the number of allowed dots depending on the quiver. These additional dot placements define the middle, or the sandwiched part, of our basis. In contrast, for the strings in the unsteady part of these diagrams we allow arbitrarily many dots, which corresponds to the sandwich algebra being a polynomial algebra.

Permutations diagrams can then be added to the bottom and top of diagrams, as it is very common in the KLR and wKLRW world.

4B. The main example.

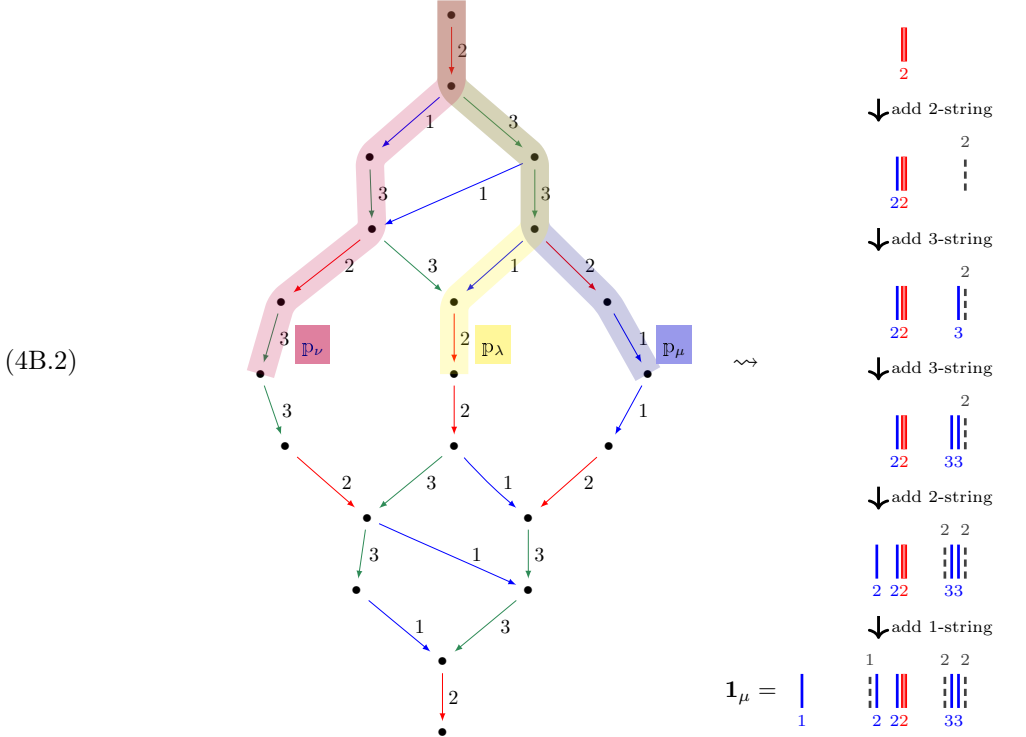
Example 4B.1. We will now combine all of the ingredients above in one example. In this example we take a quiver Γ of type B_3 , that is $\bullet \rightarrow \bullet \rightarrow \bullet$ with vertices 1, 2 and 3, read left to right, with the additional orientation $1 \rightarrow 2$. The symmetrizer for this quiver is $\mathbf{d} = (2, 2, 1)$. We take the crystal graph $\mathcal{G}(\Lambda_2)$ for the second fundamental weight. Fix $n = 5$, $\ell = 1$, $\kappa = (0)$ and $\rho = (2)$, and set all ghost shifts to be 1. We will describe how we will construct a homogeneous sandwich cellular basis for $\mathcal{R}_n^{\rho}(X)$.

(a) **Residue sequences and idempotents.** The root of the crystal graph $\mathcal{G}(\Lambda_2)$ is the highest weight vertex of weight Λ_2 . The graph on the left-hand side of (4B.2) below is the crystal graph of Λ_2 .

For each vertex σ of distance n in $\mathcal{G}(\Lambda_2)$ we fix a rooted path p_{σ} from Λ_2 to σ . The residue sequence $\text{res}(p_{\sigma}) = (i_1, \dots, i_n) \in I^n$ of such a path p_{σ} is the sequence of colors on the edges of the path. By standard properties of crystal graphs, a path is uniquely determined by its residue sequence. To each vertex σ we associate an idempotent diagram $\mathbf{1}_{\sigma}$ using $\text{res}(p_{\sigma})$ by pulling the strings to the right, by the inductive procedure outlined in Section 4A.

For this example, we have chosen the highlighted paths p_λ , p_μ and p_ν as our *preferred paths*. Therefore, $\text{res}(p_\lambda) = 23312$, which is shorthand notation for $\text{res}(p_\lambda) = (2, 3, 3, 1, 2)$, $\text{res}(p_\mu) = 23321$ and $\text{res}(p_\nu) = 21323$, as illustrated in (4B.2) below. Note that there are several paths in the crystal to each of these vertices and, for our purposes it does not matter which paths we choose.

Let us consider μ first. We order the five solid strings, from left to right, using $\text{res}(p_\mu)$. That is, in order, we have a solid 2-string, two solid 3-strings, a solid 2-string and a solid 1-string. Our strategy from Section 4A for placing these strings in order, and then pulling them to the right, gives the following sequence of diagrams:



The final picture on the right-hand side is the idempotent diagram 1_μ . Note that the first placed solid 2-string is blocked by the red 2-string, since in this case the Reidemeister II move (3D.7) can only be applied if there a dot. Moreover, the second string that we place is a solid 3-string, which is blocked by the ghost 2-string, again by (3D.7). The second solid 3-string is blocked similarly whereas the second solid 2-string, and the solid 1-string, have their ghost strings blocked by the solid strings on their right. That is, each string in 1_μ is blocked in the sense that none of the defining relations allow any string to be pulled the string further to the right. A priori, it is possible that there is a some cunning way to apply the relations to pull strings further to the right but we will eventually see that this is not the case.

In the same way, we construct the idempotent diagrams for λ and ν , using the residue sequences $\text{res}(p_\lambda) = 23312$ and $\text{res}(p_\nu) = 21323$. This gives the three idempotent diagrams:

(4B.3)

$$\begin{aligned} 1_\lambda &= \begin{array}{c|c|c} & 1 & 2 \ 2 \\ \hline 1 & 2 \ 22 & 33 \end{array}, \\ 1_\mu &= \begin{array}{c|c|c} & 1 & 2 \ 2 \\ \hline 1 & 2 \ 22 & 33 \end{array}, \\ 1_\nu &= \begin{array}{c|c|c} & 1 & 2 \ 2 \\ \hline 1 & 222 & 33 \end{array}. \end{aligned}$$

Reading left to right, the sequences of coordinates of the solid strings in these idempotent diagrams are $(-1.3, -0.4, -0.1, 0.7, 0.8)$ for λ , $(-1.5, -0.4, -0.1, 0.7, 0.8)$ for μ and $(-1.2, -0.3, -0.1, 0.6, 0.8)$ for ν . Reading these coordinate sequences lexicographically defines an order $<_{\mathbb{R}}$ on the vertices. In this case, $\nu <_{\mathbb{R}} \mu <_{\mathbb{R}} \lambda$. Note that the order of the strings, from left to right, in the idempotent diagrams is, in general, different from the order coming from reading along the residue sequences.

By definition, the idempotent diagrams 1_λ , 1_μ and 1_ν do not belong to the algebra $\mathcal{R}_5^\rho(X)$ because not all of the x -coordinates of the strings in these diagrams belong to X . However, we will see that we

can use these diagrams to give a basis for $\mathcal{R}_5^\rho(X)$ because the steady diagrams in this algebra factor through these idempotents.

- (b) **Dots on idempotents.** Note the two close solid 3-strings in $\mathbf{1}_\lambda$ and $\mathbf{1}_\mu$. We want to flank these two strings with crossings, however, doing this annihilates these diagrams by (3D.7). To avoid this we put a dot on the right-hand solid 3-string in each diagram, which gives the dotted idempotents $\mathbf{1}_\lambda^y$ and $\mathbf{1}_\mu^y$, associated to λ and μ , respectively. The diagram for ν does not need any extra dots because it has no repeated residues. Let y_k be the operation of putting a dot on the k th solid string when reading along the residue sequence. Then:

$$\mathbf{1}_\lambda^y = y_2 \mathbf{1}_\lambda = \begin{array}{c} 1 \\ | \\ 1 \\ 2 \ 22 \\ 33 \end{array}, \quad \mathbf{1}_\mu^y = y_2 \mathbf{1}_\mu = \begin{array}{c} 1 \\ | \\ 1 \\ 2 \ 22 \\ 33 \end{array} \quad \text{and} \quad \mathbf{1}_\nu^y = \mathbf{1}_\nu.$$

Note that our convention for multiplying idempotent diagrams by polynomials $f(\mathbf{u}) \in \mathbb{Z}_{\geq 0}[\mathbf{u}]$ is based on the residue sequence, which is different to the initial convention that we used in Section 3C but more convenient for what follows. These dotted idempotents have positive degree if they carry dots. For example, above $\deg(\mathbf{1}_\lambda^y) = \deg(\mathbf{1}_\mu^y) = 2$ and $\deg(\mathbf{1}_\nu^y) = 0$.

- (c) **Sandwiched dots.** Our basis will require sandwich dots on some dotted idempotents $\mathbf{1}_\lambda^y$, which will give the basis $B_\lambda^{\mathcal{H}}$ for the corresponding sandwich algebra \mathcal{H}_λ . If there are no sandwich dots then, up to shift, $\mathcal{H}_\lambda = R$. The idempotent $\mathbf{1}_\nu^y$ has two solid 3-strings that are each blocked by a ghost 2-string. By Lemma 3G.5.(b) they are still blocked when we put a dot on them, so we allow putting a dot on either these strings. We will see that $B_\nu^{\mathcal{H}} = \{\mathbf{1}_\nu^y, y_3 \mathbf{1}_\nu^y, y_5 \mathbf{1}_\nu^y, y_3 y_5 \mathbf{1}_\nu^y\}$ is a homogeneous basis of the sandwich algebra \mathcal{H}_ν . The other two sandwiched bases are trivial, so $B_\lambda^{\mathcal{H}} = \{\mathbf{1}_\lambda^y\}$, $B_\mu^{\mathcal{H}} = \{\mathbf{1}_\mu^y\}$ and $\mathcal{H}_\lambda \cong \mathcal{H}_\mu \cong R$. Hence, the graded ranks of the sandwiched algebras are $\text{rk}_R^v(\mathcal{H}_\lambda) = \text{rk}_R^v(\mathcal{H}_\mu) = v^2$ and $\text{rk}_R^v(\mathcal{H}_\nu) = (1 + v^2)^2$.
- (d) **Face permutations.** A permutation $\sigma \in \mathfrak{S}_5$ acts on a residue sequence of length 5 by permuting entries. Let D_w be the associated permutation diagram that permutes the solid strings and their ghosts. We want to find all permutations of the residue sequences that are compatible with the dotted idempotent diagrams for the rooted paths in $\mathcal{G}(\Lambda_i)$. We consider those permutations for which composition of diagrams $\mathbf{1}_{\lambda_1}^y D_w \mathbf{1}_{\lambda_2}^y$ is nonzero. As we will see later, these permutations are precisely the **face permutations**, which permute the paths in the crystal around faces.

Note that there are three paths in the crystal graph to λ , which have residue sequences 23321, 231323 and 21332. It turns out that these three paths correspond to the same wKLRW idempotent diagram, so we do not need to consider them. The point is that these paths differ only by the direction in which we travel around a square with edges labeled by 1 and 3, and these strings commute in the wKLRW algebra (as do the corresponding generators of the quantum group). Similarly, the different paths to μ and ν in the crystal graph correspond to the same wKLRW diagrams.

The complete list of face permutations is given by the following table:

λ_1	λ_2	$\{\sigma\}$
λ	λ	$\{1, (2, 3)\}$
λ	μ	$\{(2, 3)(4, 5)\}$
λ	ν	$\{(2, 5, 4)\}$
μ	μ	$\{1, (2, 3)\}$
ν	ν	$\{1\}$

- (e) **The basis.** The basis we construct starts with the smallest idempotent diagram $\mathbf{1}_\nu^y$ and its sandwiched basis $B_\nu^{\mathcal{H}}$, which is flanked with

- $D_{(2,4,5)} = D_{(2,5,4)^{-1}}$ going from ν to λ ;
- $D_{(2,3)}$ going from ν to ν_2 .

The next biggest is μ and its sandwiched basis $B_\mu^{\mathcal{H}}$ is flanked with

- $D_{(2,3)}$ going from μ to μ itself;
- $D_{(2,3)(4,5)}$ going from μ to ν .

Finally, the sandwiched basis $B_\lambda^{\mathcal{H}}$ is flanked with

- $D_{(2,3)}$ going from λ to λ itself;
- $D_{(2,4,3)}$ and $D_{(2,4)}$ going from λ to λ_2 and λ_3 , respectively.

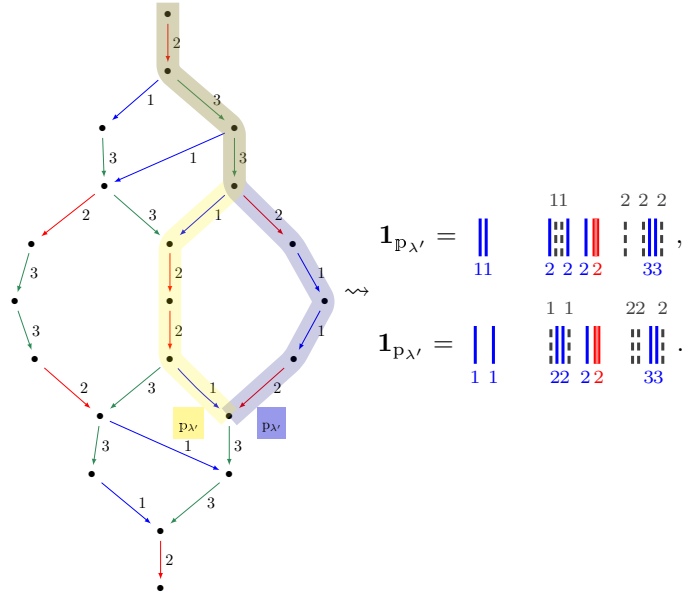
Hence, the graded rank is $\text{rk}_R^v(\mathcal{R}_n^\rho) = 6v^{-2} + 19 + 26v^2 + 19v^4 + 6v^6$, so that $\text{rk}_R^1(\mathcal{R}_n^\rho) = 76$. These numbers are obtained by computing the degrees of the basis elements listed above. More explicitly,

the nonzero ranks $\text{rk}_R^v(\mathbf{1}_{\lambda_1} \mathcal{R}_n^\rho \mathbf{1}_{\lambda_2}) = \text{rk}_R^v(\mathbf{1}_{\lambda_2} \mathcal{R}_n^\rho \mathbf{1}_{\lambda_1})$ are given by:

λ_1	λ_2	$\text{rk}_R^v(\mathbf{1}_{\lambda_1} \mathcal{R}_n^v \mathbf{1}_{\lambda_2})$
λ	λ	$(v^4 + 1)(v^2 + 1)^2 v^{-2}$
λ	μ	$(v^2 + 1)^2$
λ	ν	$(v^2 + 1)^2$
μ	μ	$(v^4 + 1)(v^2 + 1)^2 v^{-2}$
ν	ν	$(v^2 + 1)^2$

These numbers agree with the general formula for the graded ranks of the cyclotomic KLR algebras given by Hu–Shi [HS24, Theorem 1.1]. Note that the graded rank is palindromic up to a shift, which is expected since the cyclotomic KLR algebras are graded symmetric algebras by [Web17a, Remark 3.19].

- (f) **Detour permutations.** Finally, consider the two paths $p_{\lambda'}$ and $p_{\lambda'}$ below, which end at the same vertex λ' of the crystal:



The paths $p_{\lambda'}$ and $p_{\lambda'}$ differ by the direction in which they travel around the octagon, which has edges labeled by noncommuting residues 1 and 2. As a result, these paths correspond to different idempotent diagrams in the wKLRW algebra, so both of them need to be considered. For our basis, we fix the path that is minimal with respect to the total order $\leq_{\mathbb{R}}$, which in this case is $p_{\lambda'}$. We also need to include the face permutation $(4, 6)(5, 7)$ from $p_{\lambda'}$ to $p_{\lambda'}$. We call such permutations ***detour permutations*** because they give different paths to the same vertex in the crystal graph.

- (g) **Sandwich cellularity.** By Theorem 6H.4.(b) below, this basis is a sandwich cellular basis of $\mathcal{R}_n^p(X)$. As the sandwich algebra \mathcal{H}_ν is nontrivial, it turns out that this basis cannot be refined to a cellular basis. In fact, by results of Robert Muth, $\mathcal{R}_n^p(X)$ is not cellular, cf. Remark 8F.4.

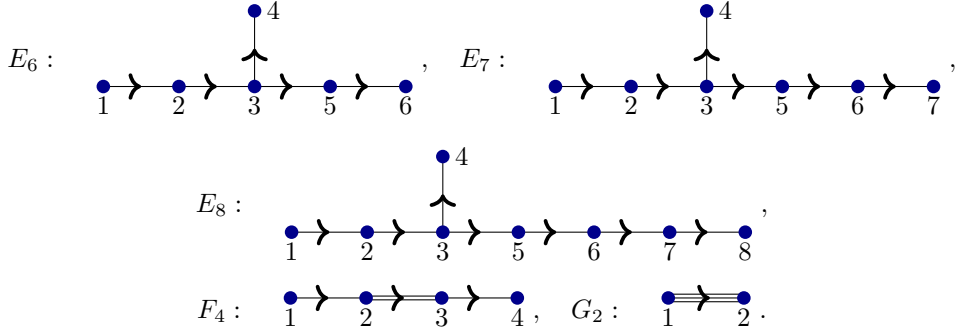
We use this example as a running example throughout the paper

5. FINITE TYPES AND CRYSTAL GRAPHS

We now specify the combinatorial notions we use.

5A. **Finite type combinatorics.** We use the following conventions for the *finite types*. Let $e \in \mathbb{Z}_{\geq 1}$.

$$\begin{array}{c}
A_e : \quad \begin{array}{ccccccccc} \bullet & \nearrow & \bullet & \nearrow & \bullet & \cdots & \bullet & \nearrow & \bullet \\ 1 & & 2 & & 3 & & e-2 & & e-1 & \nearrow & e \end{array}, \quad B_{e>1} : \quad \begin{array}{ccccccccc} \bullet & \nearrow & \bullet & \nearrow & \bullet & \cdots & \bullet & \nearrow & \bullet & \nearrow & \bullet \\ 1 & & 2 & & 3 & & e-2 & & e-1 & \nearrow & e \end{array}, \\
C_{e>2} : \quad \begin{array}{ccccccccc} \bullet & \nearrow & \bullet & \nearrow & \bullet & \cdots & \bullet & \nearrow & \bullet & \nearrow & \bullet \\ 1 & & 2 & & 3 & & e-2 & & e-1 & \nearrow & e \end{array}, \quad D_{e>3} : \quad \begin{array}{ccccccccc} & & & & & & & & \bullet \\ & & & & & & & & e-1 \\ & & & & & & & & \nearrow \\ & & & & & & & & \begin{array}{ccccccccc} \bullet & \nearrow & \bullet & \nearrow & \bullet & \cdots & \bullet & \nearrow & \bullet \\ 1 & & 2 & & 3 & & e-3 & & e-2 & \nearrow & e \end{array} \end{array},
\end{array}$$



The types A_e , D_e and E_i are *simply laced*, and their symmetrizers are $\mathbf{d} = (1, \dots, 1)$. The *doubly laced* types are B_e (symmetrizer $\mathbf{d} = (2, \dots, 2, 1)$), C_e (symmetrizer $\mathbf{d} = (2, 1, \dots, 1)$) and F_4 (symmetrizer $\mathbf{d} = (2, 2, 1, 1)$). The types A_e , B_e , C_e and D_e are the *classical types*, while E_i , F_4 and G_2 (symmetrizer $\mathbf{d} = (3, 1)$) are the *exceptional types*. The number of vertices in Γ is the *rank*.

The vertices $e - 1$ and e in type D_e , and the vertices 4 and 5 in types E_i are *fishtail vertices*. We call $i, j \in I$ *adjacent* if there is an edge between them in Γ , otherwise they are *nonadjacent*.

Remark 5A.1. Our labeling conventions are almost the same as [Bou02, Pages 265–290, plates I–IX] and SageMath [Sag23] but differs from both. Specifically, compared with SageMath we have reflected the diagrams in type $C_{e>2}$ and G_2 and renumbered the vertices in type E_i . We have chosen this labeling because it leads to slightly better combinatorics for the ghost strings.

5B. Crystal graphs. We explain the combinatorial background on crystal graphs that is needed for this paper. Everything below is well-known and can be found, for example, in [BS17]. We also fix our notation for paths in the crystal, which is not standard but is necessary in what follows because we need to keep track of the different paths in the crystal.

Let \mathcal{B} be a (Lusztig–Kashiwara) crystal, as defined in [BS17, Definition 2.13]. As usual, we associate to \mathcal{B} a labeled directed graph $\mathcal{G}(\mathcal{B})$, called the **crystal graph**. The vertices in \mathcal{B} are labeled by weights and the edges labeled by residues $i \in I$. More explicitly, $x, y \in \mathcal{B}$ the graph $\mathcal{G}(\mathcal{B})$ has an edge $x \rightarrow y$ labeled $i \in I$ if and only if $f_i(x) = y$ in \mathcal{B} or, equivalently, $e_i(y) = x$, where e_i and f_i are the Kashiwara operators. In addition, for each $i \in I$ the crystal \mathcal{B} comes equipped with maps $\varepsilon_i, \varphi_i: \mathcal{B} \rightarrow \mathbb{Z}_{\geq 0} \cup \{-\infty\}$ such that if $\varepsilon_i(x) \neq -\infty$ then $\varepsilon_i(x) = \max\{k \geq 0 \mid e_i^k(x) \neq 0\}$ and if $\varphi_i(x) \neq -\infty$ then $\varphi_i(x) = \max\{k \geq 0 \mid f_i^k(x) \neq 0\}$.

In this paper we only consider crystal graphs $\mathcal{G}(\Lambda_i)$ associated to fundamental weights Λ_i in finite types, for $i \in I$.

The following well-known result will be used silently throughout.

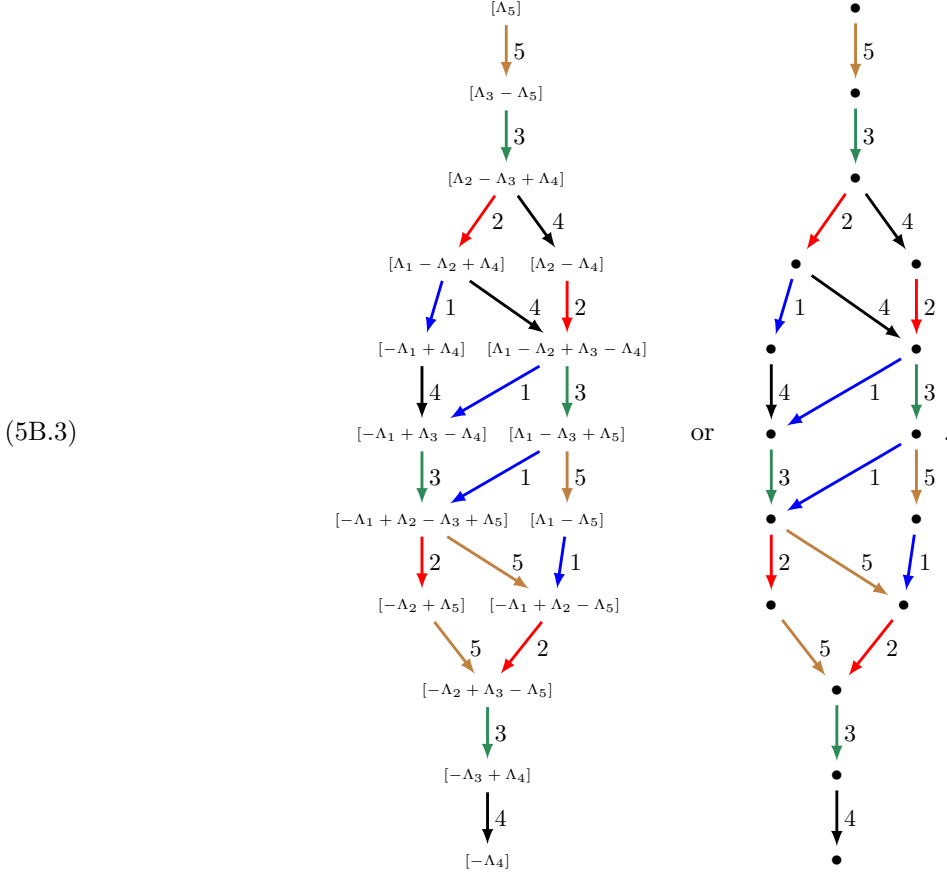
Lemma 5B.1. *Suppose that Γ is a quiver of finite type and let $\Lambda \in P^+$. There exists a unique crystal graph $\mathcal{G}(\Lambda)$ for the highest weight module $L(\Lambda)$ of the quantum Lie algebra for Γ . The crystal graph $\mathcal{G}(\Lambda)$ has a unique source, the highest weight, and sink, the lowest weight. In the crystal limit, the action of the Kashiwara operations e_i and f_i on $\mathcal{G}(\Lambda)$ correspond to the action of the Chevalley generators E_i and F_i on $L(\Lambda)$, for $i \in I$.*

Proof. See, for example, [Jan96, Theorem 9.25] for an explicit construction. \square

We identify the vertices of $\mathcal{G}(\Lambda)$ with the weights in the associated highest weight module, written in terms of the fundamental weight, with the source vertex of $\mathcal{G}(\Lambda)$ labeled by Λ . This said, as on the right-hand side of (5B.3) below, the vertex labels do not play an important role in what follows, so we often replace the labels with a \bullet to increase readability.

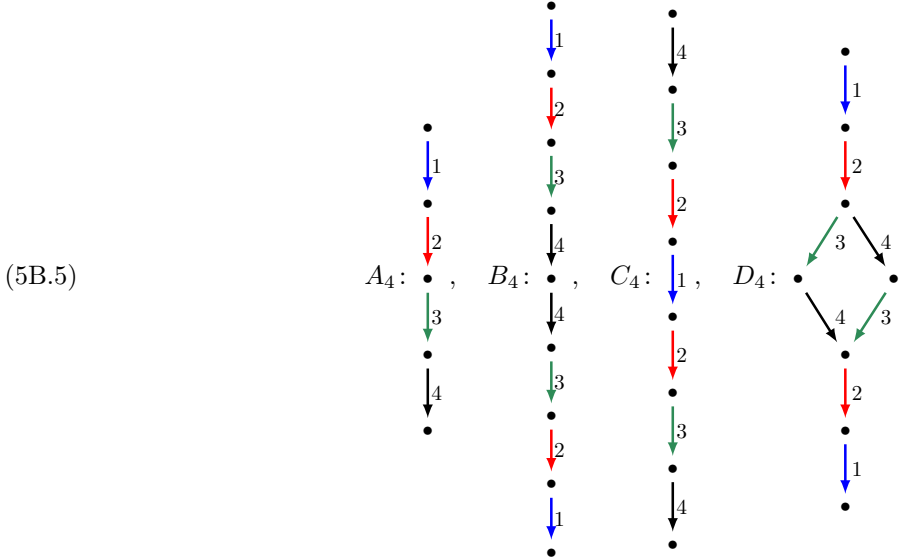
Example 5B.2. One can use SageMath [Sag23] to draw crystal graphs. The code below generated the L^AT_EX TikZ code for the crystal graph below:

```
sage: R = RootSystem(['D',5])
sage: La = R.weight_space().basis()
sage: LS = crystals.LSPaths(La[5])
sage: C = LS.subcrystal()
sage: G = LS.digraph(subset = C)
sage: latex(G)
```



This is the crystal graph $\mathcal{G}(\Lambda_5)$ in type D_5 . \diamond

Example 5B.4. The crystal graphs $\mathcal{G}(\Lambda_1)$ in types A_4 , B_4 and D_4 , and the crystal graph $\mathcal{G}(\Lambda_4)$ in type C_4 , are:



The associated representations are the vector representations. For the classical types, these examples for the crystals of the vector representations generalize in the obvious way to all ranks. \diamond

The crystal graph $\mathcal{G}(\Lambda)$ is a directed graph. A **path** in $\mathcal{G}(\Lambda)$ is a directed path. A path in $\mathcal{G}(\Lambda)$ is **rooted** if it starts at the highest weight vector. The **distance** $d(\lambda) \in \mathbb{Z}_{\geq 0}$ of a vertex $\lambda \in \mathcal{G}(\Lambda)$ from the highest weight is the length of any rooted path to λ , which is the same for all paths. The vertices with $d(\lambda) = n$ form the ***n*th layer** of $\mathcal{G}(\Lambda)$. For example, the source vertex forms the 0th layer.

Definition 5B.6. For $\lambda \in \mathcal{G}(\Lambda)$, a **path to λ** is a rooted path p_λ in $\mathcal{G}(\Lambda)$ that ends in λ . A **path of length n** is a rooted path to some $\lambda \in \mathcal{G}(\Lambda)$ with $d(\lambda) = n$. Let P_n^Λ be the set of all paths in $\mathcal{G}(\Lambda)$ of length n . For every $p_\lambda \in P_n^\Lambda$ its **residue sequence** $\text{res}(p_\lambda)$ is the ordered tuple of the labels of the edges in λ .

Remark 5B.7. We will see that rooted paths play the same role in the representation theory of wKLRW algebras as partitions do in the representation theory of the symmetric groups. We use p_λ for a generic path to the vertex λ . Later we will fix a *preferred path* p_λ for each vertex.

We let \mathfrak{S}_n act on residue sequences of length n by place permutations. Crystal theory implies that a rooted path \mathbf{p} in $\mathcal{G}(\Lambda)$ is uniquely determined by its residue sequence $\text{res}(\mathbf{p})$. Hence, we identify a path with its residue sequence. Note that not every sequence in I^n corresponds to a path in $\mathcal{G}(\Lambda)$.

Lemma 5B.8. *Let $\lambda \in \mathcal{G}(\Lambda)$ be a vertex with $d(\lambda) = n$. Then any two paths to λ are in the same \mathfrak{S}_n -orbit. That is, their residue sequences are the same up to permutation.*

Proof. This follows directly from the definitions, see [BS17, Definition 2.13, Axiom A2]. \square

As in [Example 4B.1](#), the permutations appearing in [Lemma 5B.8](#) play an important role in this paper, so we give them a special name.

Definition 5B.9. Let \mathbf{p} and \mathbf{q} be two paths of length n in $\mathcal{G}(\Lambda)$ to the same vertex. Then $w \in \mathfrak{S}_n$ is a *detour permutation* if $\mathbf{p} = w\mathbf{q}$.

Remark 5B.10. Strictly speaking w is a detour permutation for the pair of paths (\mathbf{p}, \mathbf{q}) to the same vertex. As we have already seen in [Example 4B.1](#), it also happens that $p_\lambda = wp_\mu$, for some $w \in \mathfrak{S}_n$, where p_λ and p_μ to are paths in $\mathcal{G}(\Lambda)$ to different vertices $\lambda \neq \mu$. Such permutations are not detour permutations. See also [Example 5B.12](#) for another example.

Example 5B.11. We again consider the crystal graph as in [Example 5B.2](#). There are three paths to $\lambda = [-\Lambda_1 + \Lambda_3 - \Lambda_4]$, giving three different residue sequences 53214, 53241 and 53421. These residue sequences are all permutations of each other by detour permutations. The crystal graph $\mathcal{G}(\Lambda_5)$ has ten layers. \diamond

Example 5B.12. In the main example in [Section 4](#) there are three vertices λ, μ and ν in $P_5^{\Lambda_2}$ and the crystal graph $\mathcal{G}(\Lambda_2)$ has ten layers. [Example 4B.1](#) considers three paths of length five: p_λ, p_μ and p_ν for the vertices λ, μ and ν , respectively. These paths are related by the permutations that are explicitly listed in [Example 4B.1](#). As these paths correspond to distinct vertices of $\mathcal{G}(\Lambda_2)$, none of the permutations between distinct paths are detour permutations. [Example 4B.1.\(f\)](#) also describes a detour permutation from $p_{\lambda'}$ to $p_{\lambda''}$. \diamond

Recall that every Dynkin diagram of finite type admits a Dynkin diagram automorphism $(-)^{w_0}$ of order at most two induced by $\alpha_i \mapsto -w_0\alpha_i$, for $i \in I$, where w_0 is the longest element of the associated Weyl group.

Example 5B.13. The automorphism $(-)^{w_0}$ in classical types is as follows:

Quiver	$(-)^{w_0}$
A_e	flip $i \leftrightarrow e - i$
$B_{e>1}, C_{e>2}$	identity
$D_{e>3}$	flip $(e - 1) \leftrightarrow e$

Note $(-)^{w_0}$ induces a relabeling of I . \diamond

Lemma 5B.14. *The graph $\mathcal{G}(\Lambda)$ has a symmetry given by changing the residues using $(-)^{w_0}$, reversing the orientation of the arrows, and multiplying the labels (=weights) of the vertices by -1 .*

Proof. This follows because the associated highest weight module $L(\Lambda)$ has this symmetry. \square

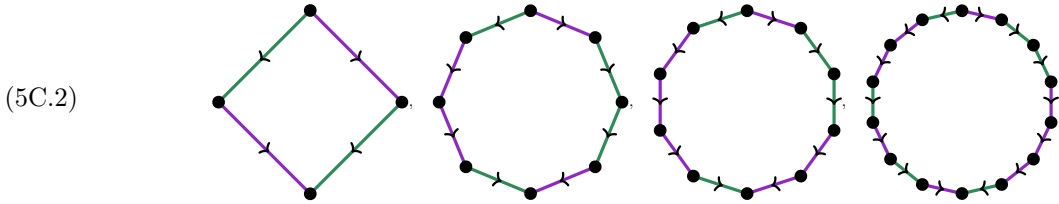
Example 5B.15. For example, in (5B.3), $(-)^{w_0}$ swaps the residues 4 and 5, rotates around the middle of the crystal graph, which is $\{[-\Lambda_1 + \Lambda_3 - \Lambda_4], [\Lambda_1 - \Lambda_3 + \Lambda_5]\}$, reverses the orientation of the arrows and finally multiplies the vertex labels by -1 . \diamond

5C. Stembridge–Sternberg relations. We need to identify certain faces in crystal graphs, where *faces* are defined respect to any embedding of the graph into a surface of high enough genus. Combinatorially:

Definition 5C.1. A *two color face* in a crystal graph \mathcal{G} is an equation $a = b$ between two (not necessarily rooted) paths a, b that are of minimal length such that they have the same end points and their residue sequences only contain the symbols $i, j \in I$ with $i \neq j$. The *source* and *sink* of a two color face are the vertices of minimal and maximal distance, respectively, from the highest weight vector in \mathcal{G} .

As we will see in [Proposition 5C.4](#) below, the only two color faces that appear in the fundamental crystals are *squares*, *octagons*, *decagons* and *tetradecagon*. Hence, keeping the face picture in mind, some examples

of two color faces are:



Other colorings of the edges around a two color face are allowed, with the two colors appearing in different orders. The crystal graph machinery ensures that the same number of edges of color i and color j appear in the two paths from the source to the sink.

Example 5C.3. In (5B.3) the two color faces are $24 = 42$, $14 = 41$, $13 = 31$, $15 = 51$ and $25 = 52$. (4B.2)(f) contains the two octagons $2332 = 3223$ and $1221 = 2112$, in addition to four squares. \diamond

The next result is motivated by [Ste03] and [Ste07]. In Section 6D below, we will impose additional constraints on the adjacent squares in types E_i and F_4 .

Proposition 5C.4. Fix a crystal graph $\mathcal{G}(\Lambda_i)$, for some fundamental weight Λ_i .

- (a) For type A_e , the only two color faces are $ij = ji$ for nonadjacent $i, j \in I$ (a nonadjacent square).
- (b) For types B_e, C_e, D_e , the only two color faces are:
 - (i) $ij = ji$ for nonadjacent $i, j \in I$ (a nonadjacent square), or $ij = ji$ for adjacent $i, j \in I$ (an adjacent square) with $i \neq j$ and $i \neq j$ and there is a preceding i or j , up to nonadjacent permutations.
 - (ii) $ijji = jiji$ for adjacent $i, j \in I$ (an octagon).
- (c) For type E_i , the only two color faces are:
 - (i) $ij = ji$ for nonadjacent $i, j \in I$ (a nonadjacent square), or $ij = ji$ for adjacent $i, j \in I$ (an adjacent square). We do not necessarily have a preceding i or j , up to nonadjacent permutations.
 - (ii) $ijji = jiji$ for adjacent $i, j \in I$ (an octagon).
- (d) For type F_4 , the only two color faces are:
 - (i) $ij = ji$ for nonadjacent $i, j \in I$ (a nonadjacent square), or $ij = ji$ for adjacent $i, j \in I$ (an adjacent square). We do not necessarily have a preceding i or j , up to nonadjacent permutations.
 - (ii) $ijji = jiji$ for adjacent $i, j \in I$ (an octagon).
 - (iii) $23332 = 32233 = 32323$ (a decagon).
 - (iv) $2332323 = 3223332 = 3232332 = 2333223$ (a tetradecagon).
- (e) For type G_2 , the only two color face is $1221 = 2112$ (an octagon).

Proof. Classical types. For minuscule weights the statement is clear by their construction in, for example, [BS17, Section 5.4]. So we only discuss the other fundamental weights.

We will use the Young diagrams combinatorics as in e.g. [BS17, Section 6.2]. The combinatorics works as follows. (We do not need to consider type A_e , since all weights are minuscule, but we list it for completeness.) We fix the partially ordered *filling sets*

$$\begin{aligned} A_e: \{1 < \dots < e\}, \quad B_{e>1}: \{1 < \dots < e < \bar{e} < \dots < \bar{1}\}, \\ C_{e>2}: \{e < \dots < 1 < \bar{1} < \dots < \bar{e}\}, \quad D_{e>3}: \{1 < \dots < e, \bar{e} < \dots < \bar{1}\}, \end{aligned}$$

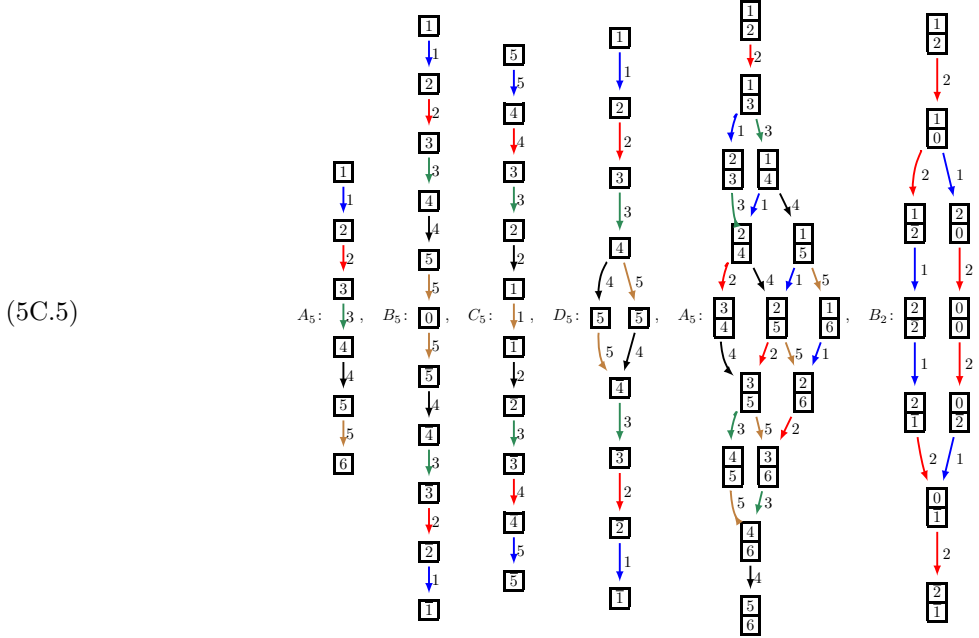
which we use to fill tableaux. Note that e and \bar{e} are not comparable in type $D_{e>3}$. A Young diagram of shape (1^k) is a column of height k , and we fill these with numbers from the filling sets such that:

- (i) The entries are strictly increasing from top to bottom with the exception that the letter 0 in $B_{e>1}$ can be repeated once, and the letters e and \bar{e} in type $D_{e>3}$ can alternate once.
- (ii) If both letters i and \bar{i} appear, and i is in the a th node and \bar{i} is in the b th node from the top $a + b \leq i$.

See [BS17, Section 6.2] for several examples (but note that our labeling of the Dynkin diagrams of type $C_{e>2}$ is different).

The Young diagrams of shape (1^k) with the above fillings correspond to the vertices of $\mathcal{G}(\Lambda_k)$, except in type $C_{e>2}$ where this corresponds to $\mathcal{G}(\Lambda_{e-k+1})$. The arrows in these graphs are determined by the following

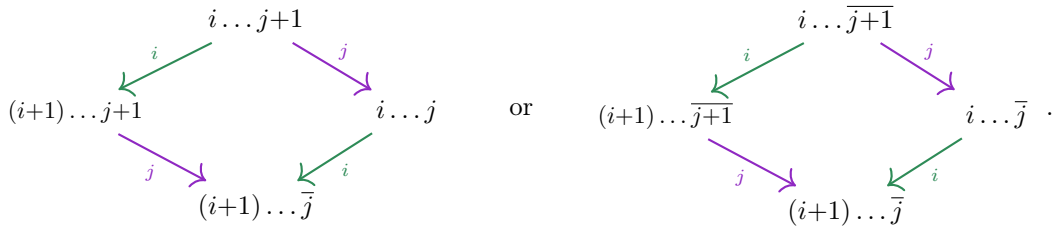
replacement rules, which generalize to larger e accordingly):



These also exemplify the tableaux realizations for $k = 1$, which should be compared to [Example 5B.4](#), and also gives the cases A_5 and B_2 with $\Lambda_i = 2$. In type B_e we write $0 = e + 1$ for typographical reasons.

We only discuss type B_e , the other cases are similar and are omitted. Note that it suffices to concentrate on the column words obtained by reading a tableau from top to bottom. If $w = w_1 \dots w_k$ is a column word, then the edge $w \xrightarrow{i} w'$ is given by replacing i with $i + 1$, or $\overline{i+1}$ with \overline{i} .

Assume first that we have a square $ij = ji$, with $i < j \neq e$. Locally, the column words vertices in the square must be of the form:

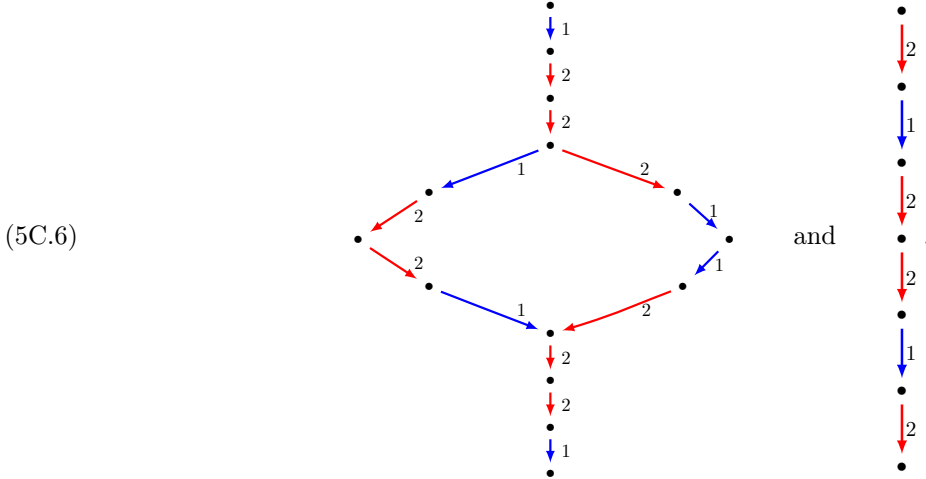


or an overlined version of the first diagram. In the first case $i + 1$ and $j + 1$ do not appear in the initial word and in the second case $i + 1$ and $\overline{j + 1}$ do not appear. If i and j are adjacent, then the first case does not arise and in order to get from the highest weight vertex $12 \dots k$ to the vertex $i \dots j + 1$ there must be previous edge labeled j since only this edge could have erased to entry j . The edge labeled j must come right before the top vertex $i \dots j + 1$ in the diagram above since otherwise the order condition would not be satisfied. Thus, we get the desired conditions when j precedes i .

The other cases with $j < i \neq e$ are similar. To conclude the square case, for $i = e - 1$ and $j = e$ there is no possible square since e needs to appear in the column word directly before or after $e - 1$, and similarly for $i = e$ and $j = e - 1$.

A minimal octagon can only appear for adjacent i and j since i and j must be applied twice because of the column word combinatorics. Hence, by [\[Ste07, Theorem 1\]](#), it remains to look at decagons and tetradecagons as in loc. cit. However, these cannot appear because they must involve three consecutive applications of, say, i which is impossible by the column word combinatorics.

Exceptional types. As there are only finitely many fundamental crystal graphs of exceptional type, this can be verified directly by inspection. For type G_2 , these crystal graphs are:



These are the two relevant fundamental crystals in type G_2 . In type E_i the statements follow from [Ste03] and [Ste07]. All other types were checked using the code available at [MT22]. \square

As we will see, all cases in [Proposition 5C.4](#) correspond to relations in the wKLRW algebra.

Recall from [Section 3A](#) that P^+ is the set of dominant weights for Γ . For the rest of this section, fix a dominant weight $\Lambda \in P^+$ and let $\mathcal{G}(\Lambda)$ be the crystal graph of highest weight Λ . A **rooted path** in $\mathcal{G}(\Lambda)$ is a path with source the highest weight vector in $\mathcal{G}(\Lambda)$. Let P_n^Λ be the set of rooted paths in $\mathcal{G}(\Lambda)$. If $\mathbf{p} \in P_n^\Lambda$. The **residue sequence** of \mathbf{p} is the sequence $\text{res}(\mathbf{p}) \in I^n$ of edges labels for \mathbf{p} . As before, the path \mathbf{p} is uniquely determined by its residue sequence. The **sink** $\omega(\mathbf{p})$ of \mathbf{p} is the final vertex in the path \mathbf{p} .

We want to associate an idempotent diagram to each path \mathbf{p} in $\mathcal{G}(\Lambda)$. Before we can do this we need to introduce red strings and affine red strings, which we postpone to [Section 6](#).

5D. Face permutations. One of the basic building blocks for our cellular basis are the permutations of the residue sequences of paths in the crystal, which we now introduce.

Definition 5D.1. Let λ and μ be vertices of $\mathcal{G}(\Lambda)$. A **basic face permutation** between paths $\mathbf{p}, \mathbf{q} \in P_n^\Lambda$ is the equivalence classes of permutations that act on the residue sequences around a two color face as follows:

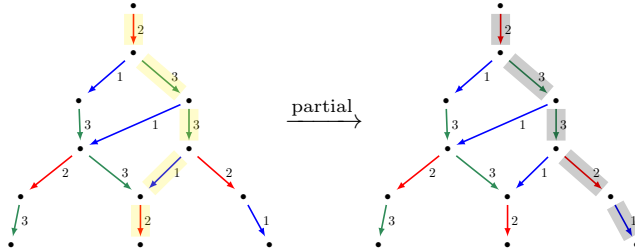
$$\begin{aligned} \text{square: } ij &\rightarrow ji, \quad \text{octagon: } ijji \rightarrow jiji \text{ or } ij \rightarrow ji, \\ \text{decagon: } &\begin{cases} 23332 \rightarrow 32233, 23332 \rightarrow 32323, 32233 \rightarrow 32323, \\ 23 \rightarrow 32, 32 \rightarrow 23, 233 \rightarrow 323, 323 \rightarrow 233, 3223 \rightarrow 3232, 3232 \rightarrow 3223, \\ \text{tetradecagon: all permutations of } 2332323, 3223332, 3232332, 2333223. \end{cases} \end{aligned}$$

A **partial face permutation** is a (residue preserving) basic face permutation that is applied only partially around a face starting from the top of the face. A **face permutation** of two paths \mathbf{p} and \mathbf{q} is a composition of basic and partial face permutations. Let $\text{Face}_\Lambda(\mathbf{p}, \mathbf{q})$ be the set of face permutations from \mathbf{p} to \mathbf{q} .

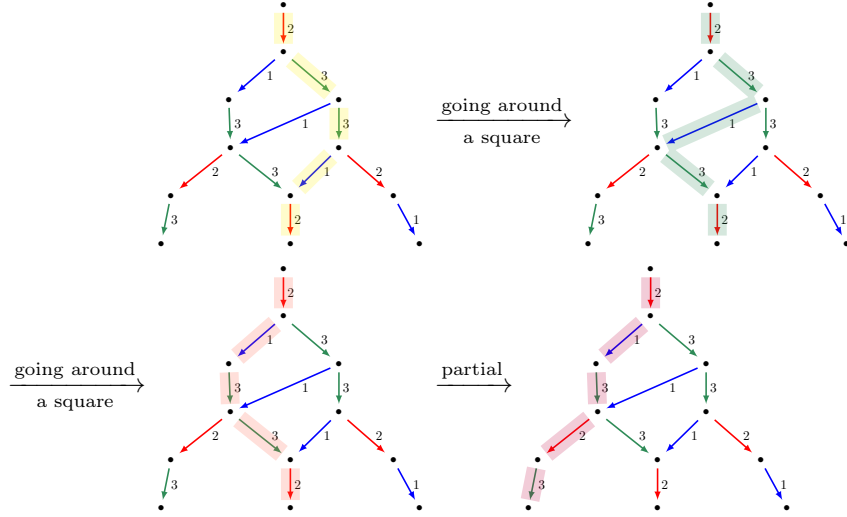
For fundamental weight, decagons and tetradecagons appear only in type F_4 precisely for the faces listed in [Proposition 5C.4](#), for the residues 2 and 3.

Remark 5D.2. A face permutation from \mathbf{p} to \mathbf{q} is determined by its action on the residue sequences. For squares, there is a unique permutation that sends ij to ji , but for each of the other basic face permutations there is more than one permutation in the equivalence class. For example, $(1, 3)(2, 4)$ and $(1, 2)(3, 4)$ both send $ijji$ to $jiji$. In [Definition 6G.9](#) below we fix a representative for each equivalence class of face permutations. In what follows we abuse terminology and call a face permutation any permutation in the corresponding equivalence class.

Example 5D.3. In (4B.2), the path p_λ is related to p_μ by using a partial face permutation around the $1221 = 2112$ octagon. This can be pictured as:



Applying basic face permutations to go from λ to ν needs three steps:



So, the face permutation from p_λ to p_μ is the composition of two basic face permutations and a partial face permutation. \diamond

Lemma 5D.4. Let \mathbf{p} and \mathbf{q} be two paths in $\mathcal{G}(\Lambda)$ ending at the vertex $\omega(\mathbf{p}) = \omega(\mathbf{q})$. Then $\text{res}(\mathbf{p}) = w\text{res}(\mathbf{q})$, for some face permutation w .

Proof. For simply laced quivers this is [HL17, Theorem 4.2] and the remaining types follow by [HL17, Remark 4.3(2)]. Note that even though this remark only mentions doubly laced quivers it also applies to G_2 because the conditions required by this remark always hold in finite type. \square

Recall from Section 3A that $Q^+ = \bigoplus_{i \in I} \mathbb{Z}_{\geq 0} \alpha_i$ is the positive root lattice of Γ .

Definition 5D.5. Let \mathbf{p} be a rooted path in a crystal graph \mathcal{B} . Let $\alpha_{\mathbf{p}} = \sum_{k=1}^n \alpha_{i_k} \in Q^+$, where $\text{res}(\mathbf{p}) = (i_1, \dots, i_n)$. If λ is any vertex of \mathcal{B} let $\alpha_\lambda = \alpha_{\mathbf{p}}$, where \mathbf{p} is any path in \mathcal{B} with sink $\omega(\mathbf{p}) = \lambda$. Two paths \mathbf{p} and \mathbf{q} in \mathcal{B} are in the same **block** if $\alpha_{\mathbf{p}} = \alpha_{\mathbf{q}}$. Similarly, two vertices λ and μ of \mathcal{B} are in the same block if $\alpha_\lambda = \alpha_\mu$.

If λ is a vertex of \mathcal{B} , then the root $\alpha_\lambda = \alpha_{\mathbf{p}}$ is independent of the choice of path \mathbf{p} with $\omega(\mathbf{p}) = \lambda$ by Lemma 5D.4.

Proposition 5D.6. Two paths \mathbf{p} and \mathbf{q} in the crystal \mathcal{B} are in the same block if and only if $\text{res}(\mathbf{p}) = w\text{res}(\mathbf{q})$, for some face permutation w .

Proof. It is enough to consider the case when $\mathcal{B} = \mathcal{G}(\Lambda)$, for some dominant weight $\Lambda \in P^+$.

(\Leftarrow). The condition $\text{res}(\mathbf{p}) = w\text{res}(\mathbf{q})$ implies that $\alpha_{\mathbf{p}} = \alpha_{\mathbf{q}}$, so they are in the same block.

(\Rightarrow). Since Γ is of finite type, the crystal graph $\mathcal{G}(\Lambda)$ has unique lowest weight vertex ζ of weight $-\Lambda_i$. Let \mathbf{p}_ζ and \mathbf{q}_ζ be extensions of \mathbf{p} and \mathbf{q} , respectively, to paths to ζ . By Lemma 5D.4, there exists a face permutation w_ζ such that $\text{res}(\mathbf{p}_\zeta) = w_\zeta \text{res}(\mathbf{q}_\zeta)$. Since w_ζ is a face permutation, we can restrict w_ζ to \mathbf{q} give the result. \square

5E. Tensor product crystals. This section attaches crystal graphs to the tuples $\underline{\Lambda} = (\Lambda_{\rho_1}, \dots, \Lambda_{\rho_\ell})$ and $\Lambda = (\Lambda_{\rho_1}, \dots, \Lambda_{\rho_\ell})$ from Definition 3D.5. By definition, $\rho_i = \rho_i$, for $1 \leq i \leq \ell$.

By [Kas91], if \mathcal{G} and \mathcal{H} are crystals then their tensor product $\mathcal{G} \otimes \mathcal{H}$ is also a crystal. More explicitly, the vertices of $\mathcal{G} \otimes \mathcal{H}$ are tensor products of the vertices of \mathcal{G} and \mathcal{H} and the edges are given by the following

variant of Kashiwara's tensor product rule [Kas91, Proposition 6]:

$$(5E.1) \quad e_i(a \otimes x) = \begin{cases} e_i(a) \otimes x & \text{if } \varphi_i(a) < \varepsilon_i(x), \\ a \otimes e_i(x) & \text{if } \varphi_i(a) \geq \varepsilon_i(x), \end{cases} \quad \text{and} \quad f_i(a \otimes x) = \begin{cases} f_i(a) \otimes x & \text{if } \varphi_i(a) \geq \varepsilon_i(x), \\ a \otimes f_i(x) & \text{if } \varphi_i(a) < \varepsilon_i(x). \end{cases}$$

Let $\mathcal{G}_\otimes(\underline{\Lambda}) = \mathcal{G}(\Lambda_{\rho_1}) \otimes \cdots \otimes \mathcal{G}(\Lambda_{\rho_\ell})$ be the tensor product of the crystal graphs $\mathcal{G}(\Lambda_{\rho_1}), \dots, \mathcal{G}(\Lambda_{\rho_\ell})$. By classical results, $\mathcal{G}_\otimes(\underline{\Lambda})$ is a direct sum of highest weight crystals. In view of (5E.1), the vertices of $\mathcal{G}_\otimes(\underline{\Lambda})$ are tensor products $\lambda_1 \otimes \cdots \otimes \lambda_\ell$, where λ_k is a vertex of $\mathcal{G}(\Lambda_{\rho_k})$, and the labeled edges of $\mathcal{G}_\otimes(\underline{\Lambda})$ are of the form $\lambda_1 \otimes \cdots \otimes \lambda_\ell \xrightarrow{i} \lambda'_1 \otimes \cdots \otimes \lambda'_\ell$ such that there exists an m such that $\lambda_k = \lambda'_k$ for $k \neq m$ and $\lambda_m \xrightarrow{i} \lambda'_m$ is an edge in $\mathcal{G}(\Lambda_{\rho_m})$. Similarly, let $\mathcal{G}_\otimes(\underline{\Lambda}) = \mathcal{G}(\Lambda_{\rho_1}) \otimes \cdots \otimes \mathcal{G}(\Lambda_{\rho_\ell})$.

Our choice of tensor product rule in (5E.1) prefers using edges coming from the left-hand tensor factors before edges in the right-hand tensor factors. In terms of KLRW diagrams, this corresponds to preferring to put solid strings to the left of as many red strings as possible.

Lemma 5E.2. *There is an injective map $\tau: \mathcal{G}_\otimes(\underline{\Lambda}) \rightarrow \mathcal{G}_\otimes(\underline{\Lambda})$ such that $\tau(f_i(x)) = f_i(\tau(x))$, whenever $f_i(x) \neq 0$ for $x \in \mathcal{G}_\otimes(\underline{\Lambda})$ and $i \in I$.*

Proof. For $1 \leq r \leq \ell$ let v_{ρ_r} be the highest weight vector of weight Λ_{ρ_r} in $\mathcal{G}(\Lambda_{\rho_r})$. The vertices of $\mathcal{G}_\otimes(\underline{\Lambda})$ are of the form $x = x_1 \otimes \cdots \otimes x_\ell$, for $x_r \in \mathcal{G}(\Lambda_{\rho_r})$. Define $\tau(x) = x_1 \otimes \cdots \otimes x_\ell \otimes v_{\rho_{\ell+1}} \otimes \cdots \otimes v_{\rho_\ell}$, a vertex of $\mathcal{G}_\otimes(\underline{\Lambda})$. By (5E.1), if $f_i(x) \neq 0$ then $\tau(f_i(x)) = f_i(\tau(x))$, for $i \in I$ since $\varepsilon_i(v_{\rho_r}) = 0$ for $\ell < r \leq \ell$. This completes the proof. \square

The map τ of Lemma 5E.2 is not a crystal embedding because the image of τ is not necessarily a connected component of $\mathcal{G}_\otimes(\underline{\Lambda})$. This will not matter for the results that follow.

Recall that $\mathcal{G}(\Lambda_i)$ is the crystal graph of highest weight Λ_i . Abusing notation, let $\mathcal{G}(\underline{\Lambda})$ and $\mathcal{G}(\Lambda)$ be the crystal graphs of highest weights $\sum_{k=1}^\ell \Lambda_{\rho_k}$ and $\sum_{k=1}^\ell \Lambda_{\rho_k}$, respectively.

Lemma 5E.3. *There are injective maps $\mathcal{G}(\Lambda) \hookrightarrow \mathcal{G}_\otimes(\underline{\Lambda})$ and $\mathcal{G}(\underline{\Lambda}) \hookrightarrow \mathcal{G}_\otimes(\underline{\Lambda})$ that commute with the Kashiwara operators whenever they are nonzero.*

Proof. The existence of a crystal embedding $\tau: \mathcal{G}(\Lambda) \hookrightarrow \mathcal{G}_\otimes(\underline{\Lambda})$ is a well-known consequence of Kashiwara's tensor product rule (5E.1). It can be proved by repeating the arguments of Lemma 5E.4. \square

Recall from Definition 5B.6 that $P_n^{\Lambda_i}$ is the set of rooted paths of length n in $\mathcal{G}(\Lambda_i)$. Similarly, let P_n^Λ and $P_n^{\underline{\Lambda}}$ be the sets of rooted paths of length n in $\mathcal{G}(\underline{\Lambda})$ and $\mathcal{G}(\Lambda)$, respectively. We consider P_n^Λ and $P_n^{\underline{\Lambda}}$ as subcrystals of $\mathcal{G}_\otimes(\underline{\Lambda})$ and $\mathcal{G}_\otimes(\Lambda)$, respectively.

As the paths in $\mathcal{G}_\otimes(\underline{\Lambda})$ are given by applying the Kashiwara operators f_i , for $i \in I$, the map τ of Lemma 5E.2 induces an injective, residue sequence preserving, map from P_n^Λ to $P_n^{\underline{\Lambda}}$. Hereafter, we identify the rooted paths in P_n^Λ and $P_n^{\underline{\Lambda}}$ with the corresponding paths in $\mathcal{G}_\otimes(\underline{\Lambda})$ under the map τ of Lemma 5E.2. Similarly, we identify the crystals $\mathcal{G}(\Lambda)$, $\mathcal{G}_\otimes(\Lambda)$, and $\mathcal{G}(\underline{\Lambda})$ with their images in $\mathcal{G}_\otimes(\underline{\Lambda})$. In particular, we always think of the crystal graphs $\mathcal{G}(\Lambda)$ and $\mathcal{G}(\underline{\Lambda})$ as being embedded in $\mathcal{G}_\otimes(\underline{\Lambda})$. These embeddings are the crystal graph analog of the difference between $\Lambda = \sum_{k=1}^\ell \Lambda_{\rho_k} \in P^+$ and the ordered sequence $\rho \in I^\ell$, which corresponds to the order of the residues on the red strings.

Let \mathbf{p} be a path in $\mathcal{G}_\otimes(\underline{\Lambda})$. Recall from the end of Section 5D that the *sink* $\omega(\mathbf{p})$ of \mathbf{p} is the final vertex $\lambda_1 \otimes \cdots \otimes \lambda_\ell$ in the path \mathbf{p} . As described above, each edge in \mathbf{p} corresponds to a unique edge in one of the tensor factors, $\mathcal{G}(\Lambda_{\rho_k})$. Let \mathbf{p}_k be the (connected) path in $\mathcal{G}(\Lambda_{\rho_k})$ consisting of all of the edges that come from $\mathcal{G}(\Lambda_{\rho_k})$, for $1 \leq k \leq \ell$. We write $\mathbf{p} = (\mathbf{p}_1, \dots, \mathbf{p}_\ell)$.

As above, if \mathbf{p} is a path in $\mathcal{G}_\otimes(\Lambda)$ let $\omega(\mathbf{p})$ be its *sink* and write $\mathbf{p} = (\mathbf{p}_1, \dots, \mathbf{p}_\ell)$, where \mathbf{p}_k is the component path in $\mathcal{G}(\Lambda_{\rho_k})$.

We warn the reader that writing $\mathbf{p} = (\mathbf{p}_1, \dots, \mathbf{p}_\ell)$ is a slight abuse of notation because we have not shown that the path \mathbf{p} is uniquely determined by the paths $\mathbf{p}_1, \dots, \mathbf{p}_\ell$. For example, suppose that $\Lambda = (\Lambda_i, \Lambda_j)$, where $i, j \in I$ are nonadjacent, and let \mathbf{p}_i and \mathbf{p}_j be the rooted paths of length 1 in $\mathcal{G}(\Lambda_i)$ and $\mathcal{G}(\Lambda_j)$, respectively. Then there are, potentially, two paths in $\mathcal{G}_\otimes(\Lambda)$ such that $\mathbf{p} = (\mathbf{p}_1, \mathbf{p}_2)$, which have residue sequences (i, j) and (j, i) , respectively.

Lemma 5E.4. *Suppose that $\mathbf{p} = (\mathbf{p}_1, \dots, \mathbf{p}_\ell) \in P_n^\Lambda$. Then \mathbf{p}_k is a rooted path in $\mathcal{G}(\Lambda_{\rho_k})$, for $1 \leq k \leq \ell$.*

Proof. Let λ_k be the source of \mathbf{p}_k , corresponding to a vertex $\lambda = \lambda_1 \otimes \cdots \otimes \lambda_\ell$ in $\mathcal{G}_\otimes(\underline{\Lambda})$. By way of contradiction, suppose that λ_k is not the highest weight vector in $\mathcal{G}(\Lambda_{\rho_k})$. Then $\varepsilon_j(\lambda_k) > 0$ for some $j \in I$. By (5E.1), we can find $N = n_1 + \cdots + n_{k-1} + 1$ such that $e_j^N \lambda = e_j^{n_1} \lambda_1 \otimes \cdots \otimes e_j^{n_{k-1}} \lambda_1 \otimes e_j \lambda_k \otimes \cdots \otimes \lambda_\ell$ is nonzero, so λ_k is not the source of \mathbf{p}_k , which is a contradiction. Hence, λ_k is the highest weight vector in $\mathcal{G}(\Lambda_{\rho_k})$, so \mathbf{p}_k is a rooted path. \square

To give a partial converse to [Lemma 5E.4](#), a *rooted path* in $\mathcal{G}_\otimes(\underline{\Lambda})$, or in $\mathcal{G}_\otimes(\Lambda)$, is a path with sink the highest weight vector of weight $\underline{\Lambda}$, or Λ , respectively. If \mathbf{q} is a path in a crystal graph, let $|\mathbf{q}|$ be its the *length*.

Lemma 5E.5. *For $1 \leq m \leq \underline{\ell}$, suppose that \mathbf{p}_m is a rooted path in $\mathcal{G}(\Lambda_{\rho_m})$. Then there is a rooted path $\mathbf{p} \in P_n^\Lambda$ such that $\mathbf{p} = (\mathbf{p}_1, \dots, \mathbf{p}_{\underline{\ell}})$. Moreover, if $|\mathbf{p}_m| = 0$ for $\ell < m \leq \underline{\ell}$ then $\mathbf{p} \in P_n^\Lambda$.*

Proof. We argue by induction on the total length $|\mathbf{p}_1| + \dots + |\mathbf{p}_{\underline{\ell}}|$ of the paths. If they all have length zero then there is nothing to prove. Suppose that the total length of these paths is positive and fix $i \in I$ so that at least one of the paths $\mathbf{p}_1, \dots, \mathbf{p}_{\underline{\ell}}$ ends in a path of residue i . Let λ_m be the source of \mathbf{p}_m , for $1 \leq m \leq \underline{\ell}$, and set $\lambda = \lambda_1 \otimes \dots \otimes \lambda_{\underline{\ell}} \in \mathcal{G}_\otimes(\underline{\Lambda})$. Let m be minimal such that

$$\varepsilon_i(\lambda_m) + \sum_{1 \leq l < m} (\varepsilon_i(\lambda_l) - \varphi_i(\lambda_l)) \geq \varepsilon_i(\lambda_k) + \sum_{1 \leq l < k} (\varepsilon_i(\lambda_l) - \varphi_i(\lambda_l))$$

for $k < m$. Allowing for our different conventions for the tensor product of crystals [\(5E.1\)](#), [\[BS17, Lemma 2.33\]](#) implies that $e_i \lambda = \lambda_1 \otimes \dots \otimes e_i \lambda_m \otimes \dots \otimes \lambda_{\underline{\ell}}$ in $\mathcal{G}_\otimes(\underline{\Lambda})$. Let $\mathbf{p}' = \mathbf{p}_k$ if $k \neq m$ and let \mathbf{p}'_m be the path obtained from \mathbf{p}_m by removing the last edge, which has residue i . By induction, there exists a path \mathbf{p}' in $\mathcal{G}_\otimes(\Lambda)$ such that $\mathbf{p}' = (\mathbf{p}'_1, \dots, \mathbf{p}'_{\underline{\ell}})$. By what we have just said, $f_i \omega(\mathbf{p}') = \lambda$ in $\mathcal{G}_\otimes(\underline{\Lambda})$. Therefore, $\mathbf{p} = (\mathbf{p}_1, \dots, \mathbf{p}_{\underline{\ell}})$ where \mathbf{p} is obtained from \mathbf{p}' by adding an edge from $\omega(\mathbf{p}')$ to $\lambda = \omega(\mathbf{p})$. The final claim that $\mathbf{p} \in P_n^\Lambda$ if \mathbf{p}_m is empty for $\ell < m \leq \underline{\ell}$ is immediate from the construction. \square

We emphasize that [Lemma 5E.5](#) only claims that there exists at least one path \mathbf{p} in P_n^Λ such that $\mathbf{p} = (\mathbf{p}_1, \dots, \mathbf{p}_{\underline{\ell}})$, where \mathbf{p}_m is a path in $P_n^{\Lambda_{\rho_m}}$ for $1 \leq m \leq \underline{\ell}$. As shown in [Example 7C.8](#) below, there may be more than one path \mathbf{p} such that $\mathbf{p} = (\mathbf{p}_1, \dots, \mathbf{p}_{\underline{\ell}})$.

6. SANDWICH CELLULAR BASES

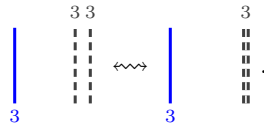
We are almost ready to describe homogeneous (affine) sandwich cellular bases for $\mathcal{W}_n^\rho(X)$ and $\mathcal{R}_n^\rho(X)$.

6A. Affine red strings.

Notation 6A.1. Until [Section 8F](#), unless otherwise stated, we fix a finite type Dynkin diagram $\Gamma = (I, E)$ and set $e = \#I$. We also fix $n, \ell \in \mathbb{Z}_{\geq 0}$, the number of solid and red strings, $\kappa \in \mathbb{R}^\ell$ with $\kappa_1 < \dots < \kappa_\ell$ and $\rho \in I^\ell$, giving the positions and the residues of the red strings, respectively.

Recall from [Definition 3D.5](#) that we fixed $\Lambda = (\Lambda_{\rho_1}, \dots, \Lambda_{\rho_\ell})$, an ℓ tuple of fundamental weights. As described in the next paragraph, we also fix ghost shifts for our choice of ε in [\(3D.3\)](#).

We will use a ghost shift of 1 for all edges except for the fishtail edges (the ones pointing into fishtail vertices) in types $D_{e>3}$, E_6 , E_7 or E_8 . For the fishtail edges we chose a ghost shift of 1 for the edge pointing to the right in [Section 5A](#) and a ghost shift of $1 - \varepsilon^2$ for the other edge. The resulting ghost strings for these two edges are very close and in what follows it does not matter which of these strings is on the left because these strings satisfy an honest Reidemeister II relation. We draw these strings as a doubled line and do not distinguish between them. For example, in type E_6 we write:



For convenience, we only draw one ghost dot on the doubled ghost string rather than a dot on each ghost string, as required by the definitions.

Recall from [Section 3F](#) that steady and unsteady diagrams are nonzero in the infinite dimensional affine wKLRW algebra $\mathcal{W}_n^\rho(X)$, while only the steady diagrams are nonzero in their finite dimension cyclotomic quotient $\mathcal{R}_n^\rho(X)$, since this algebra is defined by quotienting out by the ideal generated by the unsteady diagrams.

In order to distinguish between steady and unsteady diagrams, we now introduce affine red strings. The notation that we use to describe these is taken, mutatis mutandis, from [\[MT24\]](#) and [\[MT23\]](#). For everything affine, or unsteady, we use an underline as part of the notation.

In [Definition 3D.5](#) we fixed an affine charge $\kappa = (\kappa_1, \dots, \kappa_\ell) \in \mathbb{Z}^\ell$ and affine red labels $\rho = (\rho_1, \dots, \rho_\ell) \in I^\ell$, which we use to control the unsteady diagrams in $\mathcal{W}_n^\rho(X)$. More precisely, as in [Definition 3D.5](#), we place *red strings* at positions $\kappa_1, \dots, \kappa_\ell$, with residues ρ_1, \dots, ρ_ℓ . In addition, we imagine that there are *affine red strings* at positions $\kappa_{\ell+1}, \dots, \kappa_{\underline{\ell}}$, with residues $\rho_{\ell+1}, \dots, \rho_{\underline{\ell}}$, that are illustrated as:

$$\text{genuine red string : } \begin{array}{c} \textcolor{red}{||} \\ i \end{array}, \quad \text{affine red string : } \begin{array}{c} \textcolor{yellow}{||} \\ i \end{array}.$$

The affine red strings are not part of the wKLRW diagrams: they do not exist and are included only as a visual aid to mark the positions of the unsteady parts of the diagrams. By definition, unsteady strings can be pulled arbitrarily far to the right, but we think of them as being blocked by the affine red strings as in [Example 3F.2](#). By [\(3D.7\)](#), a dotted i -string is not blocked by a red i -string. In contrast, we think of an i -string that is immediately to the left of an affine i -string, with arbitrarily many dots, as being blocked. On the other hand, when two solid i -strings are immediately adjacent to an affine i string, as in [Notation 3G.1.\(a\)](#), then the left-hand i string can be pulled past the affine i -string. Like red strings, an affine i -string does not block ghost strings or j -strings, for $j \neq i$. That is, we have:

$$\begin{array}{c} \text{blue dot} \\ \text{blue line} \\ \text{yellow line} \end{array} \text{, } \quad \begin{array}{c} \text{blue line} \\ \text{blue line} \\ \text{yellow line} \end{array} = \begin{array}{c} \text{blue line} \\ \text{blue line} \\ \text{yellow line} \end{array} - \begin{array}{c} \text{blue line} \\ \text{blue line} \\ \text{yellow line} \end{array}.$$

The number of affine red strings is $\underline{\ell} = \ell + ne$. This depends on n because, as we will see, this ensures that there are enough affine red strings to block every solid string in any undotted diagram with residue sequence $i \in I^n$.

Example 6A.2. For $n = 2$, $\ell = 1$ and $e = 2$ we have $\underline{\ell} = 1 + 2 \cdot 2 = 5$. For $\kappa = (0)$ and $\rho = (1)$ we have $\kappa = (0, 3, 6, 9, 12)$ and $\rho = (1, 1, 1, 2, 2)$. Every diagram in this case has one red string and four affine red strings positioned as (the number above each string is its position):

$$\begin{array}{ccccc} 0 & & 3 & & 6 & & 9 & & 12 \\ \text{red} & & \text{yellow} & & \text{yellow} & & \text{yellow} & & \text{yellow} \\ 1 & & 1 & & 1 & & 2 & & 2 \end{array} \rightarrow \mathbb{R}.$$

Finally, if $\Lambda = (\Lambda_1)$, then $\underline{\Lambda} = (\Lambda_1, \Lambda_1, \Lambda_1, \Lambda_2, \Lambda_2)$. Note that we have enough affine red strings to block all solid strings (for all possible residues of these strings). For example, the relations in [Lemma 3G.5](#) give

$$\begin{array}{c} \text{blue line} \\ \text{red line} \end{array} = \begin{array}{c} \text{blue line} \\ \text{red line} \end{array}, \quad \begin{array}{c} \text{blue line} \\ \text{yellow line} \end{array} = \begin{array}{c} \text{blue line} \\ \text{yellow line} \end{array}, \quad \begin{array}{c} \text{blue line} \\ \text{blue line} \\ \text{yellow line} \end{array} = \begin{array}{c} \text{blue line} \\ \text{blue line} \\ \text{yellow line} \end{array} - \begin{array}{c} \text{blue line} \\ \text{blue line} \\ \text{yellow line} \end{array}.$$

Unlike with red strings, a dotted solid i -string does not lose its dot when it is pushed through an affine i -string (after all, the affine strings are not really there). These identities imply that we can pull two solid 2-strings all the way to the right, so that the right-hand diagram factors through the diagram:

$$\begin{array}{ccccc} 0 & & 3 & & 6 & & 9 & & 12 \\ \text{red} & & \text{yellow} & & \text{yellow} & & \text{yellow} & & \text{yellow} \\ 1 & & 1 & & 1 & & 2 & & 2 \end{array} \rightarrow \mathbb{R}.$$

Hence, the two affine red 2-strings are needed to block the two solid 2-strings. \diamond

As in [Example 6A.2](#), in general there are n affine red strings of any possible residue, which are placed far enough to the right so that they do not interfere with the steady strings in the diagram.

6B. Blocking strings. The string s in the next definition corresponds to the rightmost string on the left-hand side of the identities in [Lemma 3G.5.\(b\)](#).

Definition 6B.1. For $i \in I$, assume there is a solid, ghost or red j -string s in one of the following situations:

$$s = \begin{array}{c} j \\ \text{red} \end{array} \text{ and } i = j, \quad s = \begin{array}{c} j \\ \text{blue} \end{array} \text{ and } i = j, \quad s = \begin{array}{c} j \\ \text{yellow} \end{array} \text{ and } i \rightsquigarrow j, \quad \text{or} \quad s = \begin{array}{c} j \\ \text{blue} \end{array} \text{ and } i \rightsquigarrow j.$$

In the first three cases from the left, we say s **blocks solid i -strings**, and in the rightmost case s **blocks ghost i -strings**. We allow affine red strings to block strings in the same way that red strings do, as in the leftmost case above.

Similarly, solid i -strings are blocked by affine i -strings. Unlike red strings, which satisfy [\(3D.7\)](#), we think of a dotted solid i -string as being blocked by an affine i -string.

Solid and ghost strings can block as many strings with different residues as they have neighbors in Γ . In particular, if j corresponds to a fishtail vertex in Γ , then it will block i -strings corresponding to its two neighbors.

Notation 6B.2. There will always be two cases depending on whether the string s in [Definition 6B.1](#) blocks solid or ghost i -strings. All notions involving these two cases run in parallel and we say s **blocks i -strings** to cover both cases, allowing us to treat both cases mutatis mutandis.

Given a positioning \mathbf{x} and $\mathbf{j} \in I^n$, the **idempotent diagram** $\mathbf{1}_{(\mathbf{x}, \mathbf{j})}$ is the diagram with vertical solid j_k -strings at position x_k , for $1 \leq k \leq n$, together with their ghost strings. The idempotent diagrams described in [Example 4B.1](#) are all of this form.

Definition 6B.3. Fix an idempotent diagram $\mathbf{1}_{(\mathbf{x}, \mathbf{j})}$. Let s be the j_k -string of $\mathbf{1}_{(\mathbf{x}, \mathbf{j})}$ positioned at $x_j \in \mathbb{R}$ and suppose that s blocks i -strings. Then the coordinates $x_k - m\varepsilon$ for $m \in \{1, \dots, n\}$ are the **i -parking positions**, or **parking positions** if i is not specified. The position $x_k - m\varepsilon$ is **occupied** if $x_k - m\varepsilon \in \{x_1, \dots, x_n\}$ and otherwise it is **free**.

Example 6B.4. Let $i \rightsquigarrow j$. The illustration



shows a solid j -string that blocks i -strings. The first few free i -parking positions are illustrated by dotted and colored strings. The third parking position $x_1 - 3\varepsilon$ is occupied by a ghost k -string, and the tenth position is occupied by a red ρ -string. All other positions are free. \diamond

Definition 6B.5. If a j -string blocks i -strings, then an i -parking position for a j -string is **admissible** if it is the rightmost free parking position such that if an i -string is placed in this position, then the i and j strings can be pulled arbitrarily close to one another, in some neighborhood containing no other strings, using only isotopies and honest Reidemeister II relations.

If an i -string is in an admissible parking position for a j -string, then the i -string is **blocked** by the j -string. More generally, a i -string is blocked by a j -string if its solid or ghost string is blocked by the j -string. We extend being blocked transitively, so that if an i_{k+1} -string is blocked by an i_k -string, for $1 \leq k < m$, then the i_m -string is blocked by the i_1 -string.

Note that if an i -string is in an admissible parking position for j -string, then the i -string is blocked by the j -string. In particular, an honest Reidemeister II relation cannot be applied to pull the i -string past the j -string. Importantly, if the j -string is in position x_k , then the admissible parking position is not necessarily at $x_k - \varepsilon$ because, for example, the associated ghost and solid strings might be blocked and so prevent the i -string from reaching this position.

Example 6B.6. An i -string being blocked by a j -string is not the same as the i -string being close to the j -string. For example, if Γ is a quiver of type D_e , then both the ghost $(e-1)$ and e -strings are blocked by the solid $(e-2)$ -string in the diagram:



Note that the ghost $(e-1)$ and e -strings do not block each other. \diamond

Note that if a string is placed in an admissible i -parking position, then it can be blocked by a j -string that is placed in an admissible j -parking position. If the j string is not an (affine) red string, then, in turn, it can be blocked by a k -string that sits in an admissible parking position. As there are only finitely many parking positions, continuing in this way we can associate an (affine) red string to every admissible parking position, which we call its **anchor**.

Lemma 6B.7. *Every admissible parking position is associated to a unique red string, its anchor.*

Proof. By [\(3D.3\)](#), ε is very small with respect to the charge κ , so the admissible parking position belongs to $\kappa_m - \{1, \dots, n\}\varepsilon + \mathbb{Z}$ for a unique m . By the paragraph above, the (affine) red string at position κ_m is the anchor associated with this parking position. \square

We use [Lemma 6B.7](#) to associate (affine) red strings as anchors for parking positions. Anchors block strings in the following sense: if an i -string is placed in an admissible parking position, then this i -string will be blocked by its anchor if we inductively add strings using the process described before [Lemma 6B.7](#).

As in [Section 3B](#), the steady strings of the diagrams are blocked by the (genuine) red strings and the unsteady strings are blocked by the affine red strings. We will see that a string in an admissible parking possible is steady if and only if it is anchored by a red string and it is unsteady if and only if it is anchored by an affine red string. If D is a diagram, then its **steady part** consists of those strings that are anchored on the red strings, corresponding to $(\Lambda_{\rho_1}, \dots, \Lambda_{\rho_\ell})$, and its **unsteady part** consists of the strings anchored on the affine red strings, corresponding to $(\Lambda_{\rho_{\ell+1}}, \dots, \Lambda_{\rho_\ell})$.

6C. Idempotent diagrams. We now describe how to construct idempotent diagrams $\mathbf{1}_{\mathbf{p}}$ such that every string in $\mathbf{1}_{\mathbf{p}}$ is in an admissible parking position. To define the indexing set for these diagrams if $\mathbf{i} = (i_1, \dots, i_a) \in I^a$ and $\mathbf{j} = (j_1, \dots, j_b) \in I^b$ let $\mathbf{ij} = (i_1, \dots, i_a, j_1, \dots, j_b) \in I^{a+b}$ be the concatenation of these two sequences. Define

$$I^{n,\ell} = \{\mathbf{p} = (\mathbf{p}_1, \dots, \mathbf{p}_\ell) \mid \mathbf{p}_1 \dots \mathbf{p}_\ell \in I^n\}.$$

We will eventually see that the elements of $I^{n,\ell}$ are the residue sequences of paths in an ℓ -tuple of crystal graphs. As before, we call the elements of $I^{n,\ell}$ **residue sequences** and $\mathbf{p}_1, \dots, \mathbf{p}_\ell$ are the **components** of \mathbf{p} . For convenience, if $\mathbf{p} \in I^{n,\ell}$ we write $\mathbf{p} = (i_{11} \dots i_{1n_1}, \dots, i_{\ell 1} \dots i_{\ell n_\ell})$ if $\mathbf{p} = ((i_{1,1}, \dots, i_{1,n_1}), \dots, (i_{\ell,1}, \dots, i_{\ell,n_\ell}))$. If $1 \leq a \leq n$, then the a th residue in \mathbf{p} is $i_{k,m}$, where $a = k + \sum_{l < m} n_l$.

Definition 6C.1. Let $\mathbf{p} \in I^{n,\ell}$. We inductively construct the idempotent diagram $\mathbf{1}_{\mathbf{p}}$ as follows.

- (a) Let $\mathbf{1}_{\mathbf{p}}^0$ be the diagram with no solid or ghost strings and ℓ red strings, of residues ρ_m , placed at κ_m in the steady part for $m \in \{1, \dots, \ell\}$. We imagine that there are $\underline{\ell} - \ell$ affine red string of residues ρ_m at positions κ_m , in the unsteady part, for $m \in \{\ell + 1, \dots, \underline{\ell}\}$.
- (b) Assume that $\mathbf{1}_{\mathbf{p}}^{a-1}$ is constructed for $a \in \{1, \dots, n\}$, and suppose that $i_{k,m}$ is the a th residue in \mathbf{p} . Then $\mathbf{1}_{\mathbf{p}}^a$ is the diagram obtained from $\mathbf{1}_{\mathbf{p}}^{a-1}$ by adding a solid $i_{k,m}$ -string, and its ghosts, in the leftmost admissible parking position for an $i_{k,m}$ -string in component l , where $l \leq \underline{\ell}$ is minimal such that $l \geq m$.

We set $\mathbf{1}_{\mathbf{p}} = \mathbf{1}_{\mathbf{p}}^n$. Let $\mathbf{x}_{\mathbf{p}} = (x_1 < \dots < x_n)$ be the coordinates of the solid strings of $\mathbf{1}_{\mathbf{p}}$, read from left to right.

It is not clear that this construction is well-defined because, a priori, the diagram $\mathbf{1}_{\mathbf{p}}^{a-1}$ may not have an admissible parking position for an $i_{k,m}$ -string. We prove this below. We also note that, in general, $\mathbf{x}_{\mathbf{p}} \notin X$, so $\mathbf{1}_{\mathbf{p}}$ is not an element of $\mathcal{W}_n^{\rho}(X)$. Nonetheless, we will show that every element of $\mathcal{W}_n^{\rho}(X)$ **factors through** these idempotents in the sense that every element of $\mathcal{W}_n^{\rho}(X)$ is a linear combination of diagrams of the form $D\mathbf{1}_{\mathbf{p}}E$, for some diagrams D and E and $\mathbf{p} \in I^{n,\ell}$.

We will eventually see that it is enough to consider idempotent diagrams associated to paths in crystal graphs. If $\mathbf{p} = (\mathbf{p}_1, \dots, \mathbf{p}_\ell)$ is a path in the crystal graph $\mathcal{G}(\Delta)$, let $\mathbf{1}_{\mathbf{p}}$ be the idempotent diagram for the residue sequence $\text{res}(\mathbf{p}) = (\text{res}(\mathbf{p}_1), \dots, \text{res}(\mathbf{p}_\ell)) \in I^{n,\ell}$. Similarly, if $\mathbf{p} = (\mathbf{p}_1, \dots, \mathbf{p}_\ell)$ is a path in $\mathcal{G}(\Delta)$ define the idempotent diagram $\mathbf{1}_{\mathbf{p}}$ using the residue sequence $\text{res}(\mathbf{p}) = (\text{res}(\mathbf{p}_1), \dots, \text{res}(\mathbf{p}_\ell)) \in I^{n,\ell}$.

Remark 6C.2. The conditions in [Definition 6C.1\(b\)](#) are not as convoluted as they appear. One should think of placing an $i_{k,m}$ -string on the left of component m , and then pulling it to the right until it is blocked. The definition chooses the leftmost admissible parking position for the solid $i_{k,m}$ -string in the l th component where l is minimal such that $m \leq l \leq \underline{\ell}$.

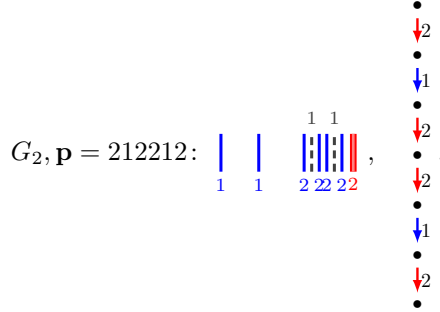
Example 6C.3. In this example, let $\ell = 1$, $\kappa = (0)$, $\rho = (1)$, and assume that ghost shifts are 1. Below, we describe a path \mathbf{p} in the crystal graph by giving its residue sequence $\text{res}(\mathbf{p})$.

- (a) The main example [\(4B.2\)](#) shows how to construct the idempotent diagram $\mathbf{1}_{\mu}$ by adding one string at a time.
- (b) For the crystal graphs in [\(5B.5\)](#),

$$\begin{aligned}
 A_4, \mathbf{p} = 1234: & \quad \begin{array}{c} 1 \\ \text{11} \\ 2 \\ \text{2} \end{array} \quad \begin{array}{c} 2 \\ \text{3} \end{array} \quad \begin{array}{c} 3 \\ \text{4} \end{array} \quad \begin{array}{c} 4 \end{array}, \quad B_4, \mathbf{p} = 12344321: \quad \begin{array}{c} 1 \\ \text{11} \\ 2 \\ \text{2} \\ \text{3} \\ \text{3} \\ \text{44} \end{array}, \\
 C_4, \mathbf{p} = 4321234: & \quad \begin{array}{c} 1 \\ \text{1} \\ \text{22} \\ \text{22} \\ \text{33} \\ \text{33} \end{array} \quad \begin{array}{c} 22 \\ \text{4} \\ \text{44} \end{array}, \quad D_4, \begin{cases} \mathbf{p} = 123421: \quad \begin{array}{c} 1 \\ \text{11} \\ 2 \\ \text{2} \\ \text{2} \\ \text{43} \end{array}, \\ \mathbf{p} = 124321: \quad \begin{array}{c} 1 \\ \text{11} \\ 2 \\ \text{2} \\ \text{2} \\ \text{34} \end{array}, \end{cases}
 \end{aligned}$$

are the associated idempotent diagrams. The two idempotent diagrams in type D_4 are almost exactly the same except that the solid 3 and 4-strings are swapped. These two residue sequences correspond to different paths to the same vertex in the crystal graph $\mathcal{G}(\Delta_1)$, see [\(5B.5\)](#) for this graph.

(c) In type G_2 and $\mathbf{p} = 212212$ the idempotent diagram and crystal graph $\mathcal{G}(\Lambda_2)$ are:



The reader should compare the examples in (b) with the crystal graphs in [Example 5B.4](#). \diamond

Example 6C.4. Suppose we are in type A_e , and set $n = 2$, $\ell = 2$, for $e > 2$, $\kappa = (0, 3)$, and $\rho = (1, 2)$. Consider the residue sequences $(1, 2)$ and $(12, \emptyset)$ in $I^{2,2}$. The associated idempotent diagrams are:

$$\mathbf{1}_{(1,2)} = \begin{array}{c} \text{1} \\ \text{1 1} \end{array} \quad \begin{array}{c} \text{2} \\ \text{2 2} \end{array} \quad \text{and} \quad \mathbf{1}_{(12,\emptyset)} = \begin{array}{c} \text{1} \\ \text{1 1} \end{array} \quad \begin{array}{c} \text{2} \\ \text{2} \end{array} .$$

Note that in $\mathbf{1}_{(1,2)}$ the solid 2-string is anchored on the red 2-string even though there is an admissible 2-parking position to the left of the ghost 1-string.

In contrast, when placing strings in the unsteady part of the diagram we will always require that the leftmost admissible parking positions in the steady and unsteady part of the diagram are occupied first. In particular, applying our definitions gives the diagram

$$\mathbf{1}_{(\emptyset,12)} = \begin{array}{c} \text{1} \\ \text{1} \end{array} \quad \begin{array}{c} \text{2} \\ \text{2 2} \end{array} \quad \begin{array}{c} \text{1} \\ \text{1 1} \end{array} \quad \begin{array}{c} \text{1} \\ \text{2} \end{array} .$$

This distinction between placing strings in the steady and unsteady parts of the diagram is necessary because the affine red strings are a notational sleight of hand, which requires slightly different combinatorics, because we want every string to be blocked by either a red string or an affine red string. In this example, the solid 1-string is unsteady and is blocked by the first affine 1-string, whereas the solid 2-string is blocked by the red 2-string. \diamond

Example 6C.5. In the setting of [Example 6A.2](#), consider a special case of relation [Lemma 3G.5](#):

$$(6C.6) \quad \begin{array}{c} \text{1 1 1} \end{array} = \begin{array}{c} \text{1 1 1} \\ \text{1 1 1} \end{array} - \begin{array}{c} \text{1 1 1} \\ \text{1 1 1} \end{array} = \begin{array}{c} \text{1 1 1} \\ \text{1 1 1} \end{array} - \begin{array}{c} \text{1 1 1} \\ \text{1 1 1} \end{array} ,$$

where we have ignored the ghost strings. The left-hand side of this relation has a diagram with two consecutive solid 1-strings. The crystal graph $\mathcal{G}(\Lambda_1)$ does not contain a path with residue sequence 11. On the other hand, if $\mathbf{p} = (11) \in I^{2,1}$, then [Definition 6C.1](#) gives:

$$\mathbf{1}_{\mathbf{p}} = \begin{array}{c} \text{1 1} \\ \text{1 1} \end{array} \quad \begin{array}{c} \text{1 1} \\ \text{1 1} \end{array} \quad \begin{array}{c} \text{1} \\ \text{1} \end{array} \quad \begin{array}{c} \text{2} \\ \text{2} \end{array} .$$

Note that this diagram is unsteady. We think of $\mathbf{1}_{\mathbf{p}}$ as being obtained from the relation above by pulling the solid 1-string through the red string until it is close to the affine red string. Observe that $\mathbf{1}_{\mathbf{p}}$ appears as the equator of the diagrams on the right-hand side of (6C.6) above. We emphasize that the affine strings are not really part of the diagram $\mathbf{1}_{\mathbf{p}}$, however, the first affine 1-string serves as a good visual aid because it appears to block the rightmost solid 1-string, which could otherwise be pulled arbitrarily far to the right. In general, the affine strings give parking positions for the unsteady strings. \diamond

Lemma 6C.7. *Let $\mathbf{p} \in I^{n,\ell}$. The construction of $\mathbf{1}_{\mathbf{p}}$ in [Definition 6C.1](#) is well-defined.*

Proof. The definition of the affine charge in [Section 6A](#) ensures that there are n affine red strings for each $i \in I$. The inductive construction of [Definition 6C.1](#) places the $i_{k,m}$ -string from component m to the left of the m th red string and then pulls it to the right into component l , where $l \geq m$. In particular, unsteady strings are placed, from left to right, into components $\ell + 1, \dots, \underline{\ell}$. As each $\mathbf{p} \in I^{n,\ell}$ has n solid strings, this implies the claim because there are enough admissible parking positions anchored on the affine red strings so that every string in \mathbf{p} becomes anchored on either a red string or an affine string when it is pulled to the right. \square

Let \perp be the equivalence relation on I that is trivial except that $(e-1)\perp e$ in $D_{e>3}$ and $4\perp 5$ in types E_e , for $e \in \{6, 7, 8\}$, where we use the labeling of the Dynkin diagrams given in [Section 5A](#). Note that \perp is only concerned with fishtail vertices.

Lemma 6C.8. *Let s be a solid string in $\mathbf{1}_{\mathbf{p}}$, for $\mathbf{p} \in I^{n,\ell}$. Then the coordinate of s is uniquely determined by its components and its residue, up to \perp -equivalence.*

Proof. This follows directly from the definitions. That is, the component can be read off from the position of the anchor as in [Lemma 6B.7](#), which is given by the κ_m , and the residue can be read off from the parking positions, up to \perp -equivalence. \square

6D. Plastic crystals. This section introduces a condition on idempotent diagrams that can be checked on the crystal graph $\mathcal{G}(\Lambda)$, for $\Lambda \in P^+$. We use this condition to control the detour permutations in $\mathcal{W}_n^{\rho}(X)$.

A **weighted plastic monoid move** is a multilocal change of strings of the form

$$(6D.1) \quad i \not\sim j: \begin{array}{c} i \\ \vdash \\ j \end{array} \rightarrow \begin{array}{c} i \\ \vdash \\ j \end{array}, \quad i \rightarrow j: \begin{array}{c} i & i \\ \vdash & \vdash \\ j & \end{array} \rightarrow \begin{array}{c} i & i \\ \vdash & \vdash \\ j & \end{array}, \quad i \Rightarrow j: \begin{array}{c} i & i & i \\ \vdash & \vdash & \vdash \\ j & & \end{array} \rightarrow \begin{array}{c} i & i & i \\ \vdash & \vdash & \vdash \\ j & & \end{array},$$

and a similar relation in case $i \Rightarrow j$ (we do not need this one explicitly), or any of their partner moves. Two diagrams are **plactic equivalent** if they related by a sequence of weighted plastic monoid moves.

Remark 6D.2. This nomenclature comes from a special case of the **Knuth relations** in the plactic monoid (see, for example, [\[BS17, Chapter 8\]](#)), which are the relations $iji = iij$ and $iji = jii$.

The **plactic moves on residues sequences** are:

$$(6D.3) \quad i \not\sim j: ij \rightarrow ji, \quad i \rightarrow j: iij \rightarrow iji, \quad i \Rightarrow j: iiij \rightarrow iiji, \quad i \Rightarrow j: iiiij \rightarrow iiiji.$$

In practise, the weighted plastic monoid moves on idempotent diagrams can be detected by looking at the residue sequences:

Lemma 6D.4. *If two residue sequences are related by plactic moves, then the corresponding idempotent diagrams are related by weighted plastic moves.*

Proof. By comparing [\(6D.1\)](#) with [\(6D.3\)](#), this follows by the construction of the idempotent diagram $\mathbf{1}_{\mathbf{p}}$ from its residue sequences, for $\mathbf{p} \in I^{n,\ell}$. \square

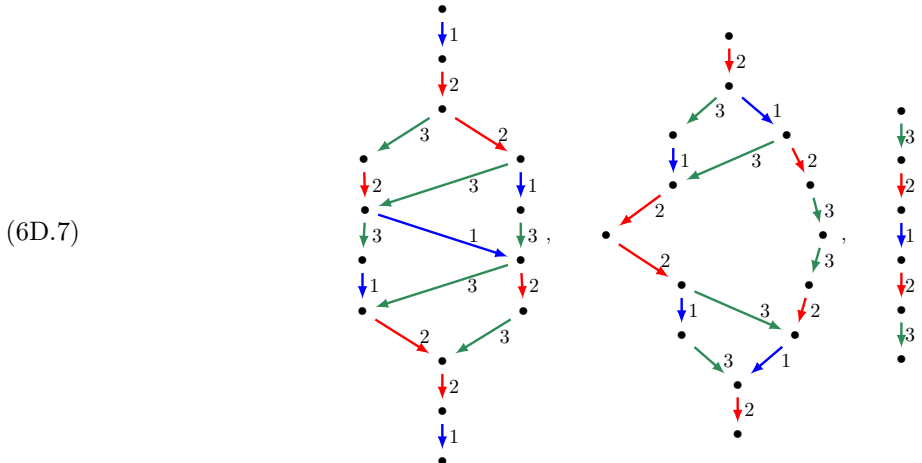
Recall the definition of adjacent squares $ij = ji$, for $i \rightsquigarrow j$, in the crystal graph $\mathcal{G}(\Lambda_k)$ from [Section 5C](#). By [Definition 5C.1](#), the source of a square is its unique vertex λ of minimal distance $d(\lambda)$ from Λ_k .

Definition 6D.5. A crystal graph \mathcal{B} is **plactic** if whenever λ is the source of an adjacent square $ij = ji$ in \mathcal{B} then one of the following holds:

- (a) There exists a path \mathbf{p} to λ that ends in an edge labeled i or j .
- (b) There exists a path \mathbf{p} to λ and an idempotent diagram $\mathbf{1}_{(\mathbf{x}, i)}$ with $i = \text{res}(\mathbf{p})$ that ends with an edge labeled i or j such that $\mathbf{1}_{\mathbf{p}}$ and $\mathbf{1}_{(\mathbf{x}, i)}$ are plactic equivalent.

In particular, crystal graphs without adjacent squares are plactic, which includes all fundamental crystals for quivers of type $A_{e \geq 1}$ by [Proposition 5C.4](#).

Example 6D.6. Let us list the three fundamental crystal graphs in type C_3 :



All of these are plactic: for the two graphs on the right this is clear, because they do not have any adjacent squares. As predicted by [Proposition 5C.4](#), the left-hand graph contains two adjacent squares $23 = 32$ one of which has an incoming edge labeled 2 and the other has an incoming edge labeled by 3. In both cases, these squares are preceded by an edge that also appears in the square itself. Hence, all of these crystals satisfy [Definition 6D.5.\(a\)](#) and so are plactic

An example of a crystal that satisfies [Definition 6D.5.\(b\)](#) is the crystal graph $\mathcal{G}(\Lambda_2)$ of type F_4 , which contains the path 231233241432 to the source λ of a $34 = 43$ square. (With 1274 vertices, this crystal graph is too large to display but can be viewed using SageMath [[Sag23](#)].) No path to λ ends in an edge labeled 3 or 4, however, one can check that the following is a sequence of plactic moves on this residue sequence:

$$2312332 \text{ (green box)} 41 \text{ (green box)} 432 \xrightarrow{41 \rightarrow 14} 23123321 \text{ (red box)} 443 \text{ (red box)} 2 \xrightarrow{443 \rightarrow 434} 2312332143 \text{ (purple box)} 42 \xrightarrow{42 \rightarrow 24} 231233214324,$$

where we use [Lemma 6D.4](#). The plactic moves allow us to move the residue 4 to the end of the sequence. \diamond

Lemma 6D.8. *We have the following.*

- (a) *All fundamental crystal graphs of classical type and of type G_2 are plactic.*
- (b) *All fundamental crystal graphs of types E_6 and F_4 are plactic.*
- (c) *In type E_7 the fundamental crystal graphs $\mathcal{G}(\Lambda_k)$ for $k \in \{1, 2, 3, 6, 7\}$ are plactic.*
- (d) *In type E_8 the fundamental crystal graphs $\mathcal{G}(\Lambda_k)$ for $k \in \{1, 8\}$ are plactic.*

Proof. Part (a) follows from [Proposition 5C.4](#) for classical types and from [\(5C.6\)](#) for type G_2 . Parts (b)–(d) were verified with the code from [[MT22](#)], which uses [Lemma 6D.4](#). \square

For types E_7 and E_8 we are only claiming that the fundamental crystals listed above are plactic, and not that the missing fundamental crystals are not plactic. It turns out that knowing that the crystals listed are plactic is enough to show that all crystals are plactic (and computationally, the remaining cases take a long time to check).

Lemma 6D.9. *Suppose that \mathcal{G} and \mathcal{H} are plactic crystal graphs. Then $\mathcal{G} \otimes \mathcal{H}$ is plactic.*

Proof. The vertices of the crystal graph $\mathcal{G} \otimes \mathcal{H}$ are tensor products of the vertices of \mathcal{G} and \mathcal{H} and the Kashiwara operator f_i , for $i \in I$, acts via [\(5E.1\)](#). Therefore, any ij -square in $\mathcal{G} \otimes \mathcal{H}$ either comes from an ij -square in \mathcal{G} or \mathcal{H} or it comes from the tensor product of subgraphs:

$$a \xrightarrow{i} b \otimes x \xrightarrow{j} y = b \otimes x \xrightarrow{j} a \otimes y = b \otimes y \xrightarrow{i} a \otimes x$$

By [Definition 6D.5\(a\)](#), to prove that this square is plactic it is enough to show that there is an edge labeled by i or j coming into the vertex $a \otimes x$. That is, it is enough to show that $\varepsilon_i(a \otimes x) > 0$ or $\varepsilon_j(a \otimes x) > 0$. By [\(5E.1\)](#), if $\varepsilon_i(a) > 0$ then there is an i -edge coming into $a \otimes x$. Similarly, if $\varepsilon_i(x) > 0$ there is a j -edge coming into $a \otimes x$. Hence, the ij -square is plactic in both of these cases, so it remains to consider the case when $\varepsilon_j(a) = 0 = \varepsilon_i(x)$.

We first assume that the quiver Γ is simply laced. By the Stembridge axioms (see [[Ste03](#), Theorem 2.4] or [[BS17](#), Proposition 4.5]), we are in one of the following four mutually exclusive cases:

- $\varphi_j(a) = \varphi_j(b)$ and $\varepsilon_j(a) = \varepsilon_j(b) + 1$, and $\varphi_i(x) = \varphi_i(y)$ and $\varepsilon_i(x) = \varepsilon_i(y) + 1$,
- $\varphi_j(a) = \varphi_j(b)$ and $\varepsilon_j(a) = \varepsilon_j(b) + 1$, and $\varphi_i(x) = \varphi_i(y) + 1$ and $\varepsilon_i(x) = \varepsilon_i(y)$,
- $\varphi_j(a) = \varphi_j(b) + 1$ and $\varepsilon_j(a) = \varepsilon_j(b)$, and $\varphi_i(x) = \varphi_i(y)$ and $\varepsilon_i(x) = \varepsilon_i(y) + 1$,
- $\varphi_j(a) = \varphi_j(b) + 1$ and $\varepsilon_j(a) = \varepsilon_j(b)$, and $\varphi_i(x) = \varphi_i(y) + 1$ and $\varepsilon_i(x) = \varepsilon_i(y)$.

Since $\varepsilon_j(a) = 0 = \varepsilon_i(x)$, the Stembridge axioms imply that $\varphi_j(a) = \varphi_j(b) + 1$ and $\varphi_i(x) = \varphi_i(y) + 1$. However, this gives a contradiction because [\(5E.1\)](#) now implies that $\mathcal{G} \otimes \mathcal{H}$ contains the edge $a \otimes x \xrightarrow{j} f_j a \otimes x$ and so, in particular, the ij -square above cannot appear in the crystal $\mathcal{G} \otimes \mathcal{H}$.

Now suppose that Γ is doubly laced. By assumption, $\varepsilon_j(a) = 0 = \varepsilon_i(x)$ in the displayed ij -square above. If i and j are both simply laced edges then the argument of the last paragraph using the Stembridge axioms shows that this ij -square cannot appear in $\mathcal{G} \otimes \mathcal{H}$. If one of i or j is a doubly laced edge then Sternberg [[Ste07](#), Theorem 1] shows that $a_{ij} = 0$ since $\varepsilon_j(a) = 0 = \varepsilon_i(x)$. Hence, $\mathcal{G} \otimes \mathcal{H}$ is plactic.

Finally, it remains to consider the quiver of type G_2 . This follows easily from the definitions because crystal graphs for G_2 only have two colors. \square

Proposition 6D.10. *Let $\Lambda \in P^+$ be a dominant weight. Then $\mathcal{G}(\Lambda)$ is plactic.*

Proof. Write $\Lambda = \sum_{i \in I} l_i \Lambda_i$. By Kashiwara's tensor product theorem [Kas91], $\mathcal{G}(\Lambda)$ is a connected subgraph of the tensor product crystal $\bigotimes_{i \in I} \mathcal{G}(\Lambda_i)^{\otimes l_i}$. Therefore, by Lemma 6D.9, it is enough to show that the fundamental crystals are plactic. By [BS17, Section 5], all of the fundamental crystals appear in tensor products of the fundamental crystals considered in Lemma 6D.8, so another application of Lemma 6D.9 completes the proof. \square

Applying Lemma 6D.9 to Proposition 6D.10 we obtain:

Corollary 6D.11. *The two crystal graphs $\mathcal{G}_\otimes(\mathbf{A})$ and $\mathcal{G}_\otimes(\underline{\mathbf{A}})$ are plactic.* \square

6E. Dots on idempotents. Following the recipe of Section 4B, the next step is to put dots on the path idempotents $\mathbf{1}_\mathbf{p}$, for $\mathbf{p} \in I^{n,\ell}$. This is necessary because flanking two adjacent solid i -strings with crossings annihilates them by (3D.7). The next definition allows us to avoid this problem.

Recall from Section 3E that $(a_{ij})_{i,j=1}^e$ is the Cartan matrix of Γ .

Definition 6E.1. Let $\mathbf{p} \in I^{n,\ell}$ and $i \in I$. Write $\text{res}(\mathbf{p}) = (i_1, \dots, i_n)$. Fix $1 \leq m \leq n$. The **dotted i_m -subsequence** of $\text{res}(\mathbf{p})$ is the maximal subsequence $(i_p, i_{p+1}, \dots, i_m)$ such that $1 \leq p \leq m$, i_p is in the same component of \mathbf{p} as i_m , and either $a_{i_r i_m} = 0$, or $i_r = i_m$ and the i_r -string has the same anchor as the i_m -string in $\mathbf{1}_\mathbf{p}$, for $p \leq r < m$. Define $d_m(\mathbf{p}) = \#\{p \leq r < m \mid i_r = i_m\}$.

Note that every residue $i = i_m$ of \mathbf{p} is contained in a unique dotted i_m -subsequence, so $d_m(\mathbf{p})$ is defined for $1 \leq m \leq n$. In particular, $d_m(\mathbf{p}) = 0$ if i_m appears only once in its dotted i_m -sequence. The condition $a_{i_r i_m} = 0$ implies that close i_r and i_m -strings satisfy an honest Reidemeister II relation. The condition on anchors implies that if $i_r = i_m$ then these strings are close in $\mathbf{1}_\mathbf{p}$.

Remark 6E.2. In many examples we consider below, such as in Example 6E.6, all of the dotted i -subsequences are of the form $i \dots i$. For these examples, $d_m(\mathbf{p}) + 1$ is just the length of this i -subsequence. The point of Definition 6E.1 is that, if $a_{ij} = 0$ and $i_m = i$, then $d_m(\mathbf{p}) + 1$ is equal to the number of times that i appears in the sequences $ji, iji, ijiji, \dots$.

Notation 6E.3. Let $\mathbf{p} \in I^{n,\ell}$. From now on, the **m th solid string of $\mathbf{1}_\mathbf{p}^y$** is the solid string that corresponds to the m th entry of $\text{res}(\mathbf{p})$. Note, in particular, that this changes the convention that we use for the (linear combination of) diagrams $f(\mathbf{u})D$ as in Section 3C, for $\mathbf{u} \in \mathbb{Z}_{\geq 0}[\mathbf{u}]$. This convention will also be used when we associate permutation diagrams D_w to permutations $w \in \mathfrak{S}_n$ in Section 6G.

Example 6E.4. In the second displayed equation of Example 6E.6 below, the third solid string of the (dotted) idempotent diagram in type B_4 with residue sequence 12344321 is the rightmost solid 3-string. \diamond

Definition 6E.5. Let $\mathbf{p} \in I^{n,\ell}$. The **dotted idempotent** $\mathbf{1}_\mathbf{p}^y$ is the diagram $\mathbf{1}_\mathbf{p}^y = y_1^{d_1(\mathbf{p})} \dots y_n^{d_n(\mathbf{p})} \mathbf{1}_\mathbf{p}$.

Definition 6E.5 will remind some readers of the idempotents in the nil-Hecke algebra. As the following example shows, the dotted idempotent for a residue sequence containing a substring of the form ii has only one dot on the second i -string, while the substring iii obtains three dots, and $iiii$ gets six dots etc.

Locally, the dot placement from Definition 6E.5 takes the form:

$$\begin{array}{lllll} \text{i : } & \begin{array}{|c|} \hline i \\ \hline \end{array}, & \text{ii : } & \begin{array}{|c|c|} \hline i & i \\ \hline \end{array}, & \text{iii : } & \begin{array}{|c|c|c|} \hline i & i & i \\ \hline \end{array}, & \text{iiii : } & \begin{array}{|c|c|c|c|} \hline i & i & i & i \\ \hline \end{array}, \end{array}$$

where we assume that the illustrated number of solid i -strings is maximal.

Example 6E.6. Continuing Example 6C.3:

$$\text{res}(\mathbf{p}) = 123 \begin{array}{|c|c|c|} \hline 44 & 321 \\ \hline \end{array} \Big\} : \mathbf{1}_\mathbf{p}^y = \begin{array}{|c|c|c|c|c|} \hline 1 & \begin{array}{|c|c|} \hline 1 & 1 \\ \hline 1 & 2 \\ \hline \end{array} & \begin{array}{|c|c|} \hline 1 & 2 \\ \hline 2 & 3 \\ \hline 3 & 3 \\ \hline \end{array} & \begin{array}{|c|c|} \hline 2 & 2 \\ \hline 4 & 4 \\ \hline \end{array} & \begin{array}{|c|c|c|} \hline 3 & 3 \\ \hline 44 \\ \hline \end{array} \\ \hline \end{array}, \quad \text{res}(\mathbf{p}) = 21 \begin{array}{|c|c|c|} \hline 22 & 12 \\ \hline \end{array} \Big\} : \mathbf{1}_\mathbf{p}^y = \begin{array}{|c|c|c|c|c|} \hline 1 & \begin{array}{|c|c|} \hline 1 & 1 \\ \hline 2 & 2 \\ \hline \end{array} & \begin{array}{|c|c|} \hline 1 & 1 \\ \hline 22 & 22 \\ \hline \end{array} & \begin{array}{|c|c|} \hline 1 & 1 \\ \hline 222 & 22 \\ \hline \end{array} \\ \hline \end{array}$$

as the dotted idempotent diagrams. The other idempotents in Example 6C.3 do not get extra dots. For shorter residue sequences we have

$$\text{res}(\mathbf{p}) = 1234 \Big\} : \mathbf{1}_\mathbf{p}^y = \begin{array}{|c|c|c|c|} \hline 1 & \begin{array}{|c|c|} \hline 1 & 1 \\ \hline 2 & 2 \\ \hline \end{array} & \begin{array}{|c|c|} \hline 2 & 2 \\ \hline 3 & 3 \\ \hline \end{array} & \begin{array}{|c|c|} \hline 3 & 3 \\ \hline 4 \\ \hline \end{array} \\ \hline \end{array}, \quad \text{res}(\mathbf{p}) = 212 \Big\} : \mathbf{1}_\mathbf{p}^y = \begin{array}{|c|c|c|} \hline 1 & \begin{array}{|c|c|} \hline 1 & 1 \\ \hline 2 & 2 \\ \hline \end{array} \\ \hline \end{array}.$$

The extra dots only appear when, up to commuting strings, there are close strings of the same residue. \diamond

6F. Sandwiched dots. Recall from [Definition 6E.1](#) that $d_m(\mathbf{p}) + 1$ is the length of a dotted i -sequence in $\text{res}(\mathbf{p})$. The following definition should be compared to [Lemma 3G.5](#).

Definition 6F.1. Let $\mathbf{p} \in I^{n,\ell}$ and $1 \leq m \leq n$. Assume that the m th string of $\mathbf{1}_{\mathbf{p}}^y$ is an i -string. Set $c_m(\mathbf{p}) = d_i - d_m(\mathbf{p}) - 1$. Define the sets of **finite dots** and **affine dots** to be

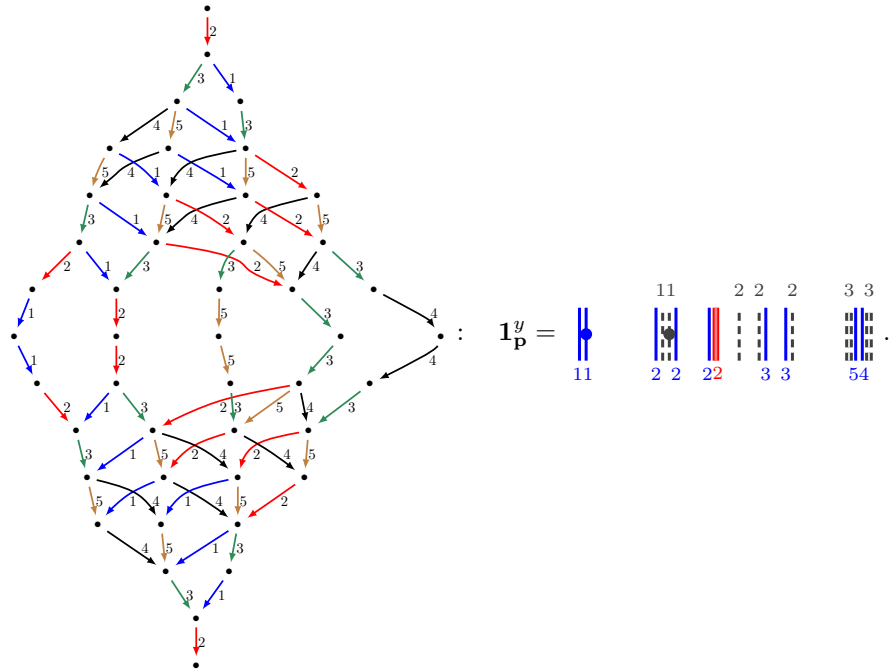
$$F^y(\mathbf{p}) = \{ \mathbf{f} = (f_1, \dots, f_n) \in \mathbb{Z}_{\geq 0}^n \mid 0 \leq f_m \leq c_m(\mathbf{p}) \},$$

$$A^y(\mathbf{p}) = \left\{ \mathbf{a} = (a_1, \dots, a_n) \in \mathbb{Z}_{\geq 0}^n \mid \begin{array}{l} a_m = 0 \text{ whenever the } m\text{th string is not immediately} \\ \text{to the left of an affine string of the same residue} \end{array} \right\}.$$

The set of **sandwiched dots** is $H^y(\mathbf{p}) = A^y(\mathbf{p}) \cup F^y(\mathbf{p})$. We set $h_{\mathbf{p}}^{\mathbf{a}, \mathbf{f}} = y^{\mathbf{a}} y^{\mathbf{f}} \mathbf{1}_{\mathbf{p}}^y$ for $\mathbf{p} \in I^{n,\ell}$, where $\mathbf{a} \in A^y(\mathbf{p})$ and $\mathbf{f} \in F^y(\mathbf{p})$. When $\mathbf{a} = (0, \dots, 0)$ we write $h_{\mathbf{p}}^{\mathbf{f}} = h_{\mathbf{p}}^{(0, \dots, 0), \mathbf{f}}$.

Again, these definitions are not as complicated as they appear because they can be checked (multi)locally in the diagrams. It follows from the proof of [Corollary 7C.4](#) below, that $c_m(\mathbf{p})$ is always non-negative. When computing $c_m(\mathbf{p})$ note that solid strings are only blocked by ghost strings, and ghost strings are only blocked by solid strings.

Example 6F.2. Let Γ be the quiver of type D_5 and consider the path $\text{res}(\mathbf{p}) = 234532112$ in the fundamental crystal $\mathcal{G}(\Lambda_2)$. Then:



In this case, $F^y(\mathbf{p}) = \{(0, 0, 0, 0, 0, 0, 0, 0, 0, 0), (0, 0, 0, 0, 0, 0, 1, 0, 0), (0, 0, 0, 0, 0, 0, 0, 0, 1), (0, 0, 0, 0, 0, 0, 1, 0, 1)\}$ and $A^y(\mathbf{p}) = \{(0, 0, 0, 0, 0, 0, 0, 0, 0)\}$. \diamond

Definition 6F.3. In the setting of [Definition 6F.1](#), the **(affine) sandwiched algebra** $\mathcal{H}_{\mathbf{p}}$ at $\mathbf{p} \in I^{n,\ell}$ is the algebra $\mathcal{W}_n^{\rho}(X)$ generated by $\underline{B}_{\mathbf{p}}^{\mathcal{H}} = \{h_{\mathbf{p}}^{\mathbf{a}, \mathbf{f}} \mid \mathbf{a} \in A^y(\mathbf{p}), \mathbf{f} \in F^y(\mathbf{p})\}$.

The **(finite) sandwiched algebra** $\mathcal{H}_{\mathbf{p}}$ at $\mathbf{p} \in I^{n,\ell}$ is the algebra generated by $B_{\mathbf{p}}^{\mathcal{H}} = \{h_{\mathbf{p}}^{\mathbf{f}} \mid \mathbf{f} \in F^y(\mathbf{p})\}$ for $\mathbf{p} \in I^{n,\ell}$.

As we will see, the sandwich bases of $\mathcal{W}_n^{\rho}(X)$ and $\mathcal{R}_n^{\rho}(X)$ that we construct in [Theorem 6H.4](#) below factor through the sandwiched algebras. This will imply that the diagrams in $\underline{B}_{\mathbf{p}}^{\mathcal{H}}$ and $B_{\mathbf{p}}^{\mathcal{H}}$ are linearly independent. Later, we will fix preferred paths \mathbf{p}_{λ} for a vertex λ in $\mathcal{G}(\Lambda_i)$ we will write $\text{res}(\lambda) = \text{res}(\mathbf{p}_{\lambda})$, $\mathbf{1}_{\lambda}^y = \mathbf{1}_{\mathbf{p}_{\lambda}}^y$, $\mathcal{H}_{\lambda} = \mathcal{H}_{\mathbf{p}_{\lambda}}$ etc. We give some examples.

Example 6F.4. The diagrams $\mathbf{1}_{\lambda}^y$, $\mathbf{1}_{\mu}^y$ and $\mathbf{1}_{\nu}^y$ in [Example 4B.1](#) have five strings, all of which are in the steady part of these diagrams. We have $c_1(\nu) = c_2(\nu) = c_4(\nu) = 0$, while $c_3(\nu) = c_5(\nu) = 1$, which we will see implies that the sandwiched algebra \mathcal{H}_{ν} is nontrivial, agreeing with [Example 4B.1\(c\)](#). The sandwich algebras \mathcal{H}_{λ} and \mathcal{H}_{μ} are both trivial. \diamond

Example 6F.5. Returning to [Example 6E.6](#), for type B_4 and $\text{res}(\mathbf{p}) = 12344321$ we have $c_k(\mathbf{p}) = 0$ for all $k \in \{1, \dots, 8\}$, so $\mathcal{H}_{\mathbf{p}} = R$ is trivial. In contrast, again in type B_4 , but with $\text{res}(\mathbf{p}) = 1234$, we have $c_k(\mathbf{p}) = 0$, for $k \in \{1, 2, 3\}$, and $c_4(\mathbf{p}) = 1$, so $\mathcal{H}_{\mathbf{p}} = R[y_4]/(y_4^2)$. Similarly, in the type G_2 example, we have a trivial sandwich algebra for $\text{res}(\mathbf{p}) = 212212$. On the other hand, $c_3(\mathbf{p}) = 2$ for $\text{res}(\mathbf{p}) = 212$, since $d_2 = 3$ because (the partner relation of) [Lemma 3G.6](#) applies, so $\mathcal{H}_{\mathbf{p}} = R[y_3]/(y_3^2)$. \diamond

Example 6F.6. Continuing Example 6C.5, the sandwiched algebra is spanned by

$$B_{\lambda}^{\mathcal{H}} = \left\{ \begin{array}{c} \text{blue vertical line} \\ \text{red vertical line} \\ \text{blue dot on blue line} \\ \text{red dot on red line} \\ \text{blue vertical line} \\ \text{red vertical line} \end{array} \mid a \in \mathbb{Z}_{\geq 0} \right\}$$

where a is the number of (affine) dots. Hence, $\mathcal{H}_{\lambda} \cong R[y]$ is a polynomial ring. \diamond

6G. Preferred paths and permutation diagrams. We are now ready to define our sandwich cellular bases. We start with defining the sets that label the cell modules in our basis.

Recall from Definition 6C.1 that each path $\mathbf{p} \in P_n^{\Lambda}$, via its residue sequence $\text{res}(\mathbf{p})$, determines an idempotent diagram $\mathbf{1}_{\mathbf{p}}$. Recall from Definition 6C.1 that $\mathbf{x}_{\mathbf{p}} = (x_1 < \dots < x_n)$ records the coordinates of the solid strings in $\mathbf{1}_{\mathbf{p}}$, for $\mathbf{p} \in P_n^{\Lambda}$.

Let $w \in \mathfrak{S}_n$. As in [MT24, Definition 3B.1], given $\mathbf{x}, \mathbf{y} \in X$ and $\mathbf{i} \in I^n$ let $D_{\mathbf{x}, \mathbf{y}, \mathbf{i}}(w)$ be the **permutation diagram** with residue sequence \mathbf{i} and with a minimal number of crossings such that has a solid i_k -string connecting $(x_k, 1)$ to $(y_{w(k)}, 0)$, for $1 \leq k \leq n$, together with the corresponding ghost and red strings. The diagram $D_{\mathbf{x}, \mathbf{y}, \mathbf{i}}(w)$ depends on the choice of crossings but by [MT24, Lemma 3B.3] different choices give diagrams that are equal modulo “bigger” terms. To simplify notation, we often write D_w instead of $D_{\mathbf{x}, \mathbf{y}, \mathbf{i}}(w)$ when \mathbf{x}, \mathbf{y} and \mathbf{i} are clear.

Definition 6G.1. Let $\mathbf{p} \in P_n^{\Lambda}$. Let $E_{\mathbf{p}}$ be the unique diagram such that $E_{\mathbf{p}} = \mathbf{1}_{\mathbf{p}} E_{\mathbf{p}} \mathbf{1}_{\mathbf{x}, \text{res}(\mathbf{p})}$ and the r th string in $\mathbf{1}_{\mathbf{x}, \text{res}(\mathbf{p})}$ is joined to the r th string in $\mathbf{1}_{\mathbf{p}}$, for $1 \leq r \leq n$. As paths in $\mathcal{G}(\Lambda)$ are uniquely determined by the residue sequences, set $E_{\text{res}(\mathbf{p})} = E_{\mathbf{p}}$.

Example 6G.2. Take $\mathbf{p} = p_{\lambda}$ in Example 4B.1. Then there are three paths \mathbf{q} in the crystal graph $\mathcal{G}(\Lambda_2)$ with sink λ , which have residue sequences 21332, 23132 and 23312.

$$\begin{aligned} E_{21332} &= \text{Diagram with residue sequence 21332, showing blue and red strings with labels 1, 2, 3, 1, 2, 2.} \\ E_{23132} &= \text{Diagram with residue sequence 23132, showing blue and red strings with labels 2, 3, 1, 3, 2, 2.} \\ E_{23312} &= \text{Diagram with residue sequence 23312, showing blue and red strings with labels 2, 1, 3, 3, 2, 2.} \end{aligned}$$

\diamond

For $\mathbf{p}, \mathbf{q} \in P_n^{\Lambda}$ let $\mathbf{1}_{\mathbf{p}}$ and $\mathbf{1}_{\mathbf{q}}$ be the idempotent diagrams constructed in Definition 6C.1. If $w \in \mathfrak{S}_n$ is a permutation such that $\text{res}(\mathbf{p}) = w \text{res}(\mathbf{q})$, then let $D_{\mathbf{p}, \mathbf{q}}(w) = D_{\mathbf{x}_{\mathbf{p}}, \mathbf{x}_{\mathbf{q}}, \text{res}(\mathbf{p})}(w)$ be the permutation diagram that connects the k th solid string of $\mathbf{1}_{\mathbf{p}}$ to the $w(k)$ th solid string of $\mathbf{1}_{\mathbf{q}}$, for $1 \leq k \leq n$. Then $D_{\mathbf{p}, \mathbf{q}}(w) = \mathbf{1}_{\mathbf{p}} D_{\mathbf{p}, \mathbf{q}}(w) \mathbf{1}_{\mathbf{q}}$. Note that the coordinates of the strings at the top and bottom of $D_{\mathbf{p}, \mathbf{q}}(w)$ are given by the parking functions for \mathbf{p} and \mathbf{q} , respectively.

Let $\mathbf{i}, \mathbf{j} \in I^n$ and write $\mathbf{i} = (i_1, \dots, i_n)$. Let \sim be the equivalence relation on I^n that is the transitive closure of the relation $\mathbf{i} \sim \mathbf{j}$ if $\mathbf{i} = (k, k+1) \mathbf{j}$ for some k such that $a_{i_k, i_{k+1}} = 0$. Write $\mathbf{p} \sim \mathbf{q}$ if $\mathbf{p}, \mathbf{q} \in P_n^{\Lambda}$ and $\text{res}(\mathbf{p}) \sim \text{res}(\mathbf{q})$.

Lemma 6G.3. Suppose that $\mathbf{p}, \mathbf{q} \in P_n^{\Lambda}$ and that $w \in \mathfrak{S}_n$ is a path permutation from \mathbf{p} to \mathbf{q} such that $\text{res}(\mathbf{p}) \sim w \text{res}(\mathbf{q})$. Then $D_{w^{-1}} D_w \mathbf{1}_{\mathbf{p}} = \mathbf{1}_{\mathbf{p}} = \mathbf{1}_{\mathbf{p}} D_{w^{-1}} D_w$. Consequently, if $\omega(\mathbf{p}) = \omega(\mathbf{q})$ then $\mathbf{1}_{\mathbf{p}} = \mathbf{1}_{\mathbf{q}}$.

Proof. By Proposition 5D.6, w is a face permutation, so it is enough to consider the case when w is a partial face permutation. By assumption, if i and j are the two colors appearing in w , then $a_{ij} = 0$. In particular, if all of the strings in $\mathbf{1}_{\mathbf{p}}$ corresponding to the edges permuted by w are in the same component, then the result follows by the honest Reidemeister II relations, as in (3D.7). If the strings are in different components, then the result still holds because the number of i and j 's appearing the two arms of the face is the same, since $\text{res}(\mathbf{p}) \sim w \text{res}(\mathbf{q})$. Hence, by Definition 6C.1, the edges allowed by the tensor product rule (5E.1) occur between

the same vertices, the corresponding strings are placed in the same components. Therefore, the strings in $\mathbf{1}_p$ and $\mathbf{1}_q$ again differ by honest Reidemeister II relations. (In particular, this shows that the idempotent diagrams $\mathbf{1}_p$ and $\mathbf{1}_q$ coincide unless i and j are nonadjacent fishtail vertices.) Hence, $D_{w^{-1}}D_w\mathbf{1}_p = \mathbf{1}_p = \mathbf{1}_pD_{w^{-1}}D_w$.

For the second statement, if $\omega(p) = \omega(q)$ then $\text{res}(p) = \text{res}(q)$. Therefore, the construction of the idempotent diagrams from [Definition 6C.1](#) ensures that $\mathbf{1}_q = D_w\mathbf{1}_pD_{w^{-1}}$, so the result follows from the first claim. \square

We can now define the indexing sets for our cellular bases.

Definition 6G.4.

- (a) Let $V_n^\Lambda = \{\omega(p) \mid p \in P_n^\Lambda\}$ and $V_n^{\underline{\Lambda}} = \{\omega(p) \mid p \in P_n^{\underline{\Lambda}}\}$ be the sets of sinks of the paths in P_n^Λ and $P_n^{\underline{\Lambda}}$, respectively. We think of V_n^Λ as being contained in $V_n^{\underline{\Lambda}}$ via [Lemma 5E.2](#).
- (b) The (*diagrammatic dominance order*), on the set of idempotent diagrams is the order $<_{\mathbb{R}}$ where $\mathbf{1}_{(x,i)}$ and $\mathbf{1}_{(y,j)}$ if there exists a k such that $x_k < y_k$ and $x_l = y_l$ for $k < l \leq n$. We use $\leq_{\mathbb{R}}$, $\geq_{\mathbb{R}}$ etc. with the evident meaning. If $p, q \in P_n^\Lambda$ write $p \leq_{\mathbb{R}} q$ if $\mathbf{1}_p \leq_{\mathbb{R}} \mathbf{1}_q$.
- (c) For each $\lambda \in V_n^\Lambda$, let $p_\lambda \in P_n^\Lambda$ be the unique path in P_n^Λ such that $\omega(p_\lambda) = \lambda$ and $p_\lambda \leq_{\mathbb{R}} q$ whenever $\omega(q) = \lambda$. Set $\mathbf{1}_\lambda = \mathbf{1}_{p_\lambda}$ and $\mathbf{1}_\lambda^y = \mathbf{1}_{p_\lambda}^y$.
- (d) If $\lambda, \mu \in V_n^\Lambda$ write $\lambda \leq_{\mathbb{R}} \mu$ if $p_\lambda \leq_{\mathbb{R}} p_\mu$. Write $\lambda <_{\mathbb{R}} \mu$ if $\lambda \leq_{\mathbb{R}} \mu$ and $\lambda \neq \mu$.
- (e) If $\lambda, \mu \in V_n^{\underline{\Lambda}}$, then $\lambda \sim \mu$ if $\mu = w\lambda$, for some face permutation $w \in \mathfrak{S}_n$, and $x_{p_\lambda} = x_{p_\mu}$. Let $\dot{V}_n^\Lambda = V_n^\Lambda / \sim$ and $\dot{V}_n^{\underline{\Lambda}} = V_n^{\underline{\Lambda}} / \sim$ be the corresponding equivalence classes of vertices.

We also consider $\leq_{\mathbb{R}}$ as a total order on \dot{V}_n^Λ and $\dot{V}_n^{\underline{\Lambda}}$. We abuse notation and identify paths in V_n^Λ and $V_n^{\underline{\Lambda}}$ with their equivalence class representative in \dot{V}_n^Λ and $\dot{V}_n^{\underline{\Lambda}}$, respectively.

Example 6G.5. In [\(4B.3\)](#) we have $\nu <_{\mathbb{R}} \mu <_{\mathbb{R}} \lambda$. \diamond

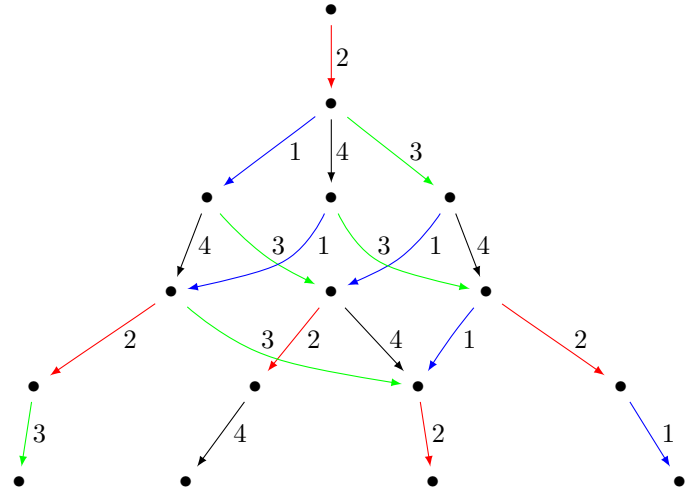
By convention, $P_n^\Lambda \subset P_n^{\underline{\Lambda}}$ and $V_n^\Lambda \subset V_n^{\underline{\Lambda}}$. The embeddings $\mathcal{G}(\Lambda) \hookrightarrow \mathcal{G}_{\otimes}(\Lambda)$ and $\mathcal{G}(\underline{\Lambda}) \hookrightarrow \mathcal{G}_{\otimes}(\underline{\Lambda})$ of [Lemma 5E.3](#) play an important role because they allow us to attach a residue sequence $\text{res}(p) \in I^{n,\ell}$ to each rooted path in these crystals. In particular, part (c) defines diagrams $\mathbf{1}_\lambda$ and $\mathbf{1}_\lambda^y$ for a choice of preferred $\lambda \in V_n^\Lambda$.

Remark 6G.6. We will see in [Lemma 7D.5.\(b\)](#) below that if $\lambda, \mu \in V_n^\Lambda$, then $\mathbf{1}_\lambda \neq \mathbf{1}_\mu$. In particular, if $\lambda \sim \mu$, then $x_\lambda = x_\mu$ but the idempotent diagrams are not equal because they have different residue sequences.

Example 6G.7. We explain how [Definition 6G.4](#) works in [Example 4B.1](#). By [\(4B.2\)](#), we can take P_5^Λ to be $\{p_\lambda, p_\mu, p_\nu\}$. In $\mathcal{G}(\Lambda_2)$, there is one path to μ , three paths to λ and one path μ . The three paths to λ , and the two paths to μ , differ by face permutations around nonadjacent squares, so there is only one equivalence class of paths to each vertex. In contrast, the paths $p_{\lambda'}$ and $p_{\lambda'}$ in [Example 4B.1.\(f\)](#) are not equivalent, so they give different elements of P_7^Λ . There are nontrivial face permutations between these paths.

Paths that are in $\mathcal{G}(\Lambda)$ and not in $\mathcal{G}(\underline{\Lambda})$ only appear when we consider paths for which the idempotent diagrams have strings that are close to the affine red strings. These paths will be used to construct the unsteady basis elements of $\mathcal{W}_n^\rho(X)$. For example, the idempotent diagram at the end of [Example 6A.2](#) corresponds to the path in $\mathcal{G}(\underline{\Lambda})$ with residue sequence $(2, 2)$. Similarly, the idempotent diagram in [Example 6C.5](#) corresponds to the path in $\mathcal{G}(\underline{\Lambda})$ with residue sequence $(1, 1)$. Neither of these paths belongs to $\mathcal{G}(\Lambda)$: even though the path p with residue sequence $(1, 1)$ starts in $\mathcal{G}(\Lambda)$ its sink $\omega(p)$ is not in $\mathcal{G}(\Lambda)$. \diamond

Example 6G.8. Let Γ be the quiver of type D_4 and let $\Lambda = \Lambda_2$ and consider $\mathcal{R}_5^\rho(x)$. The paths of length five in the crystal graph are given by:



Applying [Definition 6C.1](#), the idempotent diagrams in $\mathcal{R}_5^\rho(X)$ are:

$$\begin{aligned} \mathbf{1}_{21423} &= \begin{array}{c} 1 \\ | \\ 2 \end{array} \quad \begin{array}{c} 1 \\ || \\ 2 \end{array} \quad \begin{array}{c} 2 \\ || \\ 2 \end{array} \quad \begin{array}{c} 3 \\ || \\ 4 \end{array}, \\ \mathbf{1}_{21324} &= \begin{array}{c} 1 \\ | \\ 2 \end{array} \quad \begin{array}{c} 1 \\ || \\ 2 \end{array} \quad \begin{array}{c} 2 \\ || \\ 2 \end{array} \quad \begin{array}{c} 4 \\ || \\ 3 \end{array}, \\ \mathbf{1}_{23142} &= \begin{array}{c} 1 \\ | \\ 2 \end{array} \quad \begin{array}{c} 1 \\ || \\ 2 \end{array} \quad \begin{array}{c} 2 \\ || \\ 2 \end{array} \quad \begin{array}{c} 3 \\ || \\ 4 \end{array}, \\ \mathbf{1}_{23421} &= \begin{array}{c} 1 \\ | \\ 2 \end{array} \quad \begin{array}{c} 1 \\ || \\ 2 \end{array} \quad \begin{array}{c} 2 \\ || \\ 2 \end{array} \quad \begin{array}{c} 4 \\ || \\ 3 \end{array}. \end{aligned}$$

The idempotents for each vertex are independent of the choice of path because all paths to the same vertex differ by non-adjacent squares. In particular, note that the x -coordinates for $\mathbf{1}_{21423}$ and $\mathbf{1}_{21324}$ coincide, so these two idempotents are equivalent under [Definition 6G.4.\(e\)](#). Note that the idempotent diagrams $\mathbf{1}_{21423}$ and $\mathbf{1}_{21324}$ are not equal because they have different residue sequences. The equivalence of these two idempotents is symptomatic of $\mathcal{R}_5^\rho(X)$ not being cellular. \diamond

The next definition associates diagrams in the wKLRW algebra to the face permutations of [Definition 6G.1](#). Recall from [Definition 5D.1](#) that a two color face permutation is an equivalence class of permutations that act in the same way on the residue sequence of a given path. The next definition implicitly chooses an equivalence class representative for each face permutation. We also need to consider related 1-color relations, which correspond to the nil-Hecke case.

Definition 6G.9. Let w be a path permutation from $\mathbf{p} = (\mathbf{p}_1, \dots, \mathbf{p}_\ell)$ to $\mathbf{q} = (\mathbf{q}_1, \dots, \mathbf{q}_\ell)$, for $\mathbf{p}, \mathbf{q} \in \mathcal{G}_\otimes(\Lambda)$. Given a **basic diagrammatic path permutation** w , the corresponding diagram is given by:

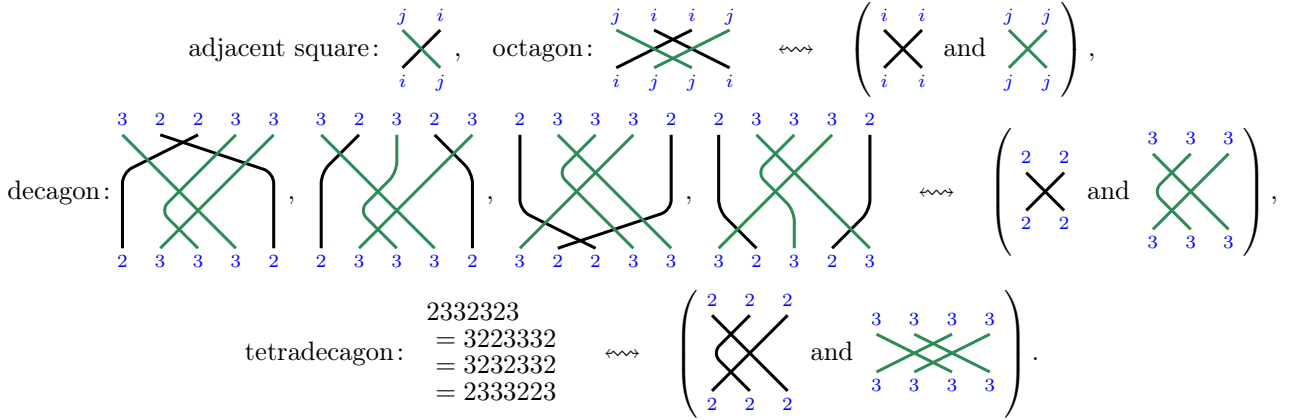
- (a) Putting the idempotent diagrams $\mathbf{1}_{\mathbf{p}}$ and $\mathbf{1}_{\mathbf{q}}$ along the top and bottom, respectively, of the permutation diagram.
- (b) Connecting all of the vertices of the same residue using a choice of representative of the longest word, for the solid strings and their ghosts, as in the permutation diagrams below. All other strings, including (affine) red strings, are vertical.
- (c) To each partial face permutation we associate the subdiagram of the corresponding basic diagrammatic face permutation.

We make the diagrams for basic face permutations more explicit. The diagrams in brackets, on the right-hand side below, show how to place these strings separately for the i and j strings in the 2-color relations, in accordance with condition (b) above.

- (i) 1-color relations: to a subsequence of consecutive solid i -strings, we attach the permutation for (a choice of representative of) the corresponding longest word. Ignoring all other strings:

$$\begin{array}{c} i \quad i \\ \times \quad \times \\ i \quad i \end{array}, \quad \begin{array}{c} i \quad i \quad i \\ \times \quad \times \quad \times \\ i \quad i \quad i \end{array}, \quad \text{etc.}$$

(ii) 2-color relations:



(iii) Multi-color relations: As in (i) and (ii), at the top and bottom of the diagram, any subsequences of repeated residues are connected by the permutation diagram on the longest word for this subsequence.

All of these diagrams are classical permutation diagrams with strings labeled by their residues. The colors in the diagrams above are only used to highlight the different residues. Although we have omitted them, there will typically be (affine) red strings in these diagrams.

Finally, a *diagrammatic face permutation* between two paths $\mathbf{p}, \mathbf{q} \in P_n^\Delta$ is a composition of basic and partial diagrammatic face permutations. Recall from [Definition 5D.1](#), that $\text{Face}_{\underline{\Delta}}(\mathbf{p}, \mathbf{q})$ is the set of face permutations from \mathbf{p} to \mathbf{q} . If $\mathbf{T} \in \text{Face}_{\underline{\Delta}}(\mathbf{p}, \mathbf{q})$ let $D_{\mathbf{T}}$ be the corresponding diagrammatic face permutation. By definition, if $\mathbf{T} \in \text{Face}_{\underline{\Delta}}(\mathbf{p}, \mathbf{q})$, then $D_{\mathbf{T}} = \mathbf{1}_{\mathbf{p}} D_{\mathbf{T}} \mathbf{1}_{\mathbf{q}}$.

The definition of a diagrammatic face permutation in [Definition 6G.9](#) involves a choice because the braid relations do not hold in $\mathcal{W}_n^\rho(X)$. The bases that we define below depend upon these choices, but our results hold for all choices. This is explained by [\[MT24, Lemma 3B.3\]](#), which says that $\mathcal{W}_n^\rho(X)$ is a filtered algebra and any two choices for $D_{\mathbf{T}}$ are equal in the associated graded algebra.

The map $\sigma \mapsto \sigma^{-1}$ gives a bijection $\text{Face}_{\underline{\Delta}}(\lambda, \mu) \xrightarrow{\sim} \text{Face}_{\underline{\Delta}}(\mu, \lambda)$. This is problematic for us because we want to associate each face permutation to a unique cell module. The next definition corrects for this overcounting.

Recall that $\lambda = \omega(\mathbf{p}) \in V_n^\Delta$ is the sink of the path \mathbf{p} and that \mathbf{p}_λ is the preferred path for λ .

Definition 6G.10. Let $\lambda \in V_n^\Delta$ and $\mu \in V_n^\Delta$. The sets of *face permutations* for λ are

$$\text{Face}_{\underline{\Delta}}(\lambda) = \bigcup_{\mathbf{p} \in P_n^\Delta, \omega(\mathbf{p}) \geq_{\mathbb{R}} \lambda} \text{Face}_{\underline{\Delta}}(\mathbf{p}_\lambda, \mathbf{p}). \quad \text{and} \quad \text{Face}_{\underline{\Delta}}(\mu) = \bigcup_{\mathbf{p} \in P_n^\Delta, \omega(\mathbf{p}) \geq_{\mathbb{R}} \mu} \text{Face}_{\underline{\Delta}}(\mathbf{p}_\mu, \mathbf{p})$$

If $\nu \in \dot{V}_n^\Delta$, set $\text{Face}_{\underline{\Delta}}(\nu) = \bigcup_{\lambda \sim \mu} \text{Face}_{\underline{\Delta}}(\lambda)$. Similarly, if $\nu \in \dot{V}_n^\Delta$ set $\text{Face}_{\underline{\Delta}}(\nu) = \bigcup_{\lambda \sim \mu} \text{Face}_{\underline{\Delta}}(\lambda)$.

By construction, if $\mu \in P_n^\Delta$, then $\text{Face}_{\underline{\Delta}}(\mu) \subseteq \text{Face}_{\underline{\Delta}}(\mu)$. Since $V_n^\Delta \subset P_n^\Delta$.

The face permutations from λ to ν are analogs of semistandard λ -tableaux of type ν in the classical types. As we already saw in [Example 6G.7](#), if $\mathbf{p} \in P_n^\Delta$ has sink λ , then $\text{Face}_{\underline{\Delta}}(\lambda)$ contains all face permutations from \mathbf{p}_λ to \mathbf{p} .

As in [Definition 5B.9](#), if $\lambda \in V_n^\Delta$ then the set of *detour permutations* in $\text{Face}_{\underline{\Delta}}(\lambda)$ is

$$(6G.11) \quad \text{Detour}(\lambda) = \bigcup_{\mathbf{p} \in P_n^\Delta, \omega(\mathbf{p}) = \lambda} \text{Face}_{\underline{\Delta}}(\mathbf{p}_\lambda, \mathbf{p}).$$

By definition, if $\mu \in V_n^\Delta$, then $\text{Detour}(\mu) \subseteq \text{Face}_{\underline{\Delta}}(\mu)$.

Example 6G.12. Using the notation of [Example 4B.1.\(d\)](#), the face permutation $(2, 3)(4, 5) \in \text{Face}_{\underline{\Delta}}(\mu)$ and $(2, 5, 4) \in \text{Face}_{\underline{\Delta}}(\nu)$, but neither of these permutations belong to $\text{Face}_{\underline{\Delta}}(\lambda)$ since $\nu \leq_{\mathbb{R}} \mu \leq_{\mathbb{R}} \lambda$. \diamond

6H. The bases. We use the usual *diagrammatic antiinvolution* $(-)^*$ given by (the R -linear extension of) reflecting diagrams bottom-to-top as illustrated by:

$$\left(\begin{array}{c} j \quad i \\ \diagup \quad \diagdown \\ \text{---} \quad \text{---} \\ i \quad \rho \quad j \end{array} \right)^* = \begin{array}{c} i \quad j \\ \diagup \quad \diagdown \\ \text{---} \quad \text{---} \\ j \quad \rho \quad i \end{array} \quad \begin{array}{c} k \\ \diagup \\ \text{---} \\ k \end{array} \quad \begin{array}{c} k \\ \diagup \\ \text{---} \\ k \end{array}.$$

Recall that we often omit the word involutive from a sandwich cell datum, but the cell data below are involutive using the diagrammatic antiinvolution $*$.

Extending [Section 6F](#), if $\sigma \in V_n^\Lambda$ set

$$A^y(\sigma) = A^y(\mathbb{p}_\sigma), \quad F^y(\sigma) = F^y(\mathbb{p}_\sigma), \quad c_m(\sigma) = c_m(\mathbb{p}_\sigma) \quad \text{and} \quad d_m(\sigma) = d_m(\mathbb{p}_\sigma),$$

for $1 \leq m \leq n$. If $\mathbf{a} \in A^y(\sigma)$ and $\mathbf{f} \in F^y(\sigma)$ set $h_{\sigma}^{\mathbf{a}, \mathbf{f}} = y^{\mathbf{a}} y^{\mathbf{f}} \mathbf{1}_{\sigma}^y$.

Now comes our main definition, which should be compared with [\(4A.1\)](#).

Definition 6H.1. Let $D_{ST}^{a,f} = (D_SE_\nu)^* h_{\sigma}^{\mathbf{a}, \mathbf{f}} \mathbf{1}_{\sigma}^y D_TE_\mu$, for $\sigma \in V_n^\Lambda$, $S \in \text{Face}_{\underline{\Lambda}}(\mathbb{p}_\sigma, \nu)$ and $T \in \text{Face}_{\underline{\Lambda}}(\mathbb{p}_\sigma, \mu)$. Define

$$(6H.2) \quad D_{\mathcal{W}_n^\rho(X)} = \{D_{ST}^{a,f} \mid \lambda \in \dot{V}_n^\Lambda, S, T \in \text{Face}_{\underline{\Lambda}}(\sigma), \mathbf{a} \in A^y(\sigma), \mathbf{f} \in F^y(\sigma), \text{ for } \sigma \in \lambda\}.$$

Similarly, let $D_{ST}^f = D_{ST}^{(0, \dots, 0), f}$, and define

$$(6H.3) \quad D_{\mathcal{R}_n^\rho(X)} = \{D_{ST}^f \mid \lambda \in \dot{V}_n^\Lambda, S, T \in \text{Face}_{\underline{\Lambda}}(\sigma), \mathbf{f} \in F^y(\sigma), \text{ for } \sigma \in \lambda\}.$$

Our choice for the sandwich cell datum $\underline{\mathcal{C}}$ for $\mathcal{W}_n^\rho(X)$ consists of:

- The middle set $\dot{V}_n^\Lambda = (\dot{V}_n^\Lambda, \leq_{\mathbb{R}})$.
- The positions of the strings at the top and bottom of the diagrams are given by the set X , from [\(3D.4\)](#). In the sandwich cellular basis, the top and bottom and top sets are equal to $\bigcup_{\lambda \in \dot{V}_n^\Lambda} \text{Face}_{\underline{\Lambda}}(\lambda)$ composed with the diagrams $E_\lambda = \sum_{\sigma \in \lambda} E_\sigma$.
- The bases of the sandwiched algebras are $B_\lambda^{\mathcal{H}} = \bigcup_{\sigma \in \lambda} \{h_{\sigma}^{\mathbf{a}, \mathbf{f}} \mid \mathbf{a} \in A^y(\sigma), \mathbf{f} \in F^y(\sigma)\}$, for $\lambda \in \dot{V}_n^\Lambda$, and the sandwiched algebras $\mathcal{H}_\lambda = \bigoplus_{\sigma \in \lambda} \mathcal{H}_{\mathbb{p}_\sigma}$ are the subalgebras of the wKLRW algebra generated by these bases.
- Our basis is the set $D = D_{\mathcal{W}_n^\rho(X)}$ from [\(6H.2\)](#), viewed as a map.
- The degree function is $S \mapsto \deg D_S$.
- The antiinvolution is the diagrammatic antiinvolution $(-)^*$.

For $\mathcal{R}_n^\rho(X)$, the sandwich cell datum of our choice \mathcal{C} is essentially the same, except that \dot{V}_n^Λ is replaced with \dot{V}_n^Λ , $\text{Face}_{\underline{\Lambda}}(\sigma)$ is replaced by $\text{Face}_{\underline{\Lambda}}(\sigma)$, and we take the set in [\(6H.3\)](#) as our basis.

Theorem 6H.4. Suppose that Γ is a quiver of finite type.

- The datum $\underline{\mathcal{C}}$ is an involutive graded affine sandwich cell datum for $\mathcal{W}_n^\rho(X)$. In particular, [\(6H.2\)](#) is a homogeneous affine sandwich cellular basis of $\mathcal{W}_n^\rho(X)$.*
- The datum \mathcal{C} is an involutive graded sandwich cell datum for $\mathcal{R}_n^\rho(X)$. In particular, [\(6H.3\)](#) is a homogeneous sandwich cellular basis of $\mathcal{R}_n^\rho(X)$.*

We prove this result in [Section 7](#).

Let \mathcal{W}_n^ρ and \mathcal{R}_n^ρ , respectively, be the KLR algebras and their cyclotomic quotients associated to the fixed Kac–Moody datum. (These are the algebras defined by Khovanov–Lauda, Rouquier and Webster in e.g. [\[KL09\]](#) and [\[Rou08\]](#).) By [\[MT24, Section 3F\]](#), the algebras $\mathcal{W}_n^\rho(X)$ and $\mathcal{R}_n^\rho(X)$ are isomorphic to the KLR algebras \mathcal{W}_n^ρ and \mathcal{R}_n^ρ , respectively; see [Proposition 7B.1](#) below for a more direct argument. Hence, [Theorem 6H.4](#) implies:

Corollary 6H.5. Suppose that Γ is a quiver of finite type. Then \mathcal{W}_n^ρ is a homogeneous affine sandwich cellular algebra and \mathcal{R}_n^ρ is a sandwich cellular algebra. \square

6I. Cellularity for general dominant weights. The definition of the wKLRW algebra labels the red strings by $i \in I$, which corresponds to labeling them with the corresponding fundamental weights Λ_i . Using more general relations, the definition of wKLRW algebras can be generalized to allow arbitrary dominant weights as labels of the red strings, see [\[Web17a, Definition 4.5\]](#). Although we will not define these algebras explicitly, our results imply that these algebras are always cellular. Given an ℓ tuple $\beta = (\beta_1, \dots, \beta_\ell)$ of dominant weights, let $\mathcal{W}_n^\beta(X)$ be the corresponding generalized wKLRW algebra and let $\mathcal{R}_n^\beta(X)$ be its cyclotomic quotient. As we now sketch, the cellularity results in this paper apply to $\mathcal{W}_n^\beta(X)$ and $\mathcal{R}_n^\beta(X)$ as well.

Theorem 6I.1. The algebra $\mathcal{W}_n^\beta(X)$ is graded affine sandwich cellular and $\mathcal{R}_n^\beta(X)$ is graded sandwich cellular.

Proof. The generalized wKLRW algebra $\mathcal{W}_n^\beta(X)$ is the idempotent truncation of a wKLRW algebra that has red strings labeled by fundamental weights. More precisely, if $\beta = a_1\Lambda_1 + \dots + a_e\Lambda_e$, for $a_i \in \mathbb{Z}_{\geq 0}$, then set

$$\Lambda = (\underbrace{\Lambda_1, \dots, \Lambda_1}_{a_1}, \dots, \underbrace{\Lambda_e, \dots, \Lambda_e}_{a_e})$$

and let $\mathcal{W}_n^\rho(X)$ be the corresponding wKLRW algebra where the red strings are placed very close together. For example:

$$\beta = 3\Lambda_1 + \Lambda_3 : \begin{array}{c} \boxed{} \boxed{} \boxed{} \\ \boxed{1} \boxed{1} \boxed{1} \boxed{3} \end{array} \xrightarrow[\text{truncation}]{\text{idempotent}} \begin{array}{c} \boxed{} \\ \boxed{\beta} \end{array} .$$

Then $\mathcal{W}_n^\beta(X)$ is an idempotent truncation of $\mathcal{W}_n^\rho(X)$ by [MT24, Proposition 3F.3]. Hence, the result follows by applying [Theorem 6H.4](#) and [Theorem 2B.1\(a\)](#). \square

7. PROOF OF SANDWICH CELLULARITY

This section proves [Theorem 6H.4](#), our sandwich cellular basis theorem for $\mathcal{W}_n^\rho(X)$ and $\mathcal{R}_n^\rho(X)$.

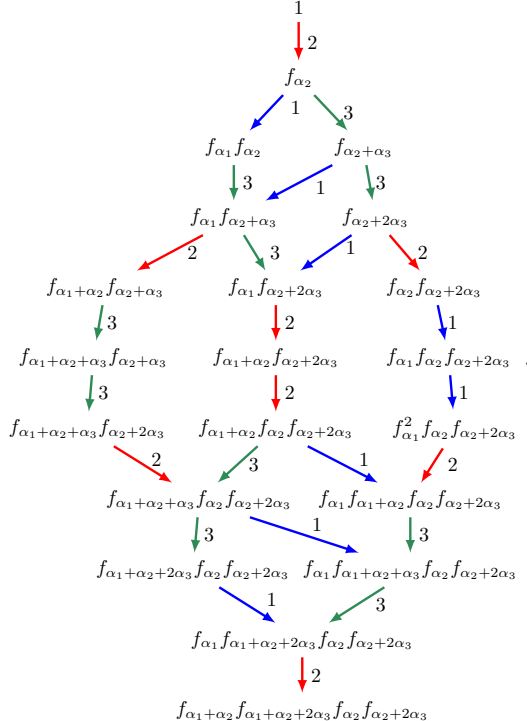
7A. Ordering in finite types. We first need a crucial lemma about the paths in a fundamental crystal graph in finite type. Let $i \in I$ and suppose that \mathbf{p} is a rooted path in $\mathcal{G}(\Lambda_i)$. A permutation in the symmetric group \mathfrak{S}_n is **\mathbf{p} -nonadjacent** if it only swaps nonadjacent residues in \mathbf{p} .

Definition 7A.1. A crystal \mathcal{B} , is **n -path ordered** if whenever \mathbf{p} and \mathbf{q} are paths in \mathcal{B} such $\text{res}(\mathbf{q}) = w\text{res}(\mathbf{p})$ for a \mathbf{p} -nonadjacent permutation w , then $\omega(\mathbf{p}) = \omega(\mathbf{q})$. The crystal graph \mathcal{B} is **path ordered** if it is n -path ordered for all $n \in \mathbb{Z}_{\geq 0}$.

That is, \mathcal{B} is path ordered if the residue sequences of paths in $\mathcal{G}(\Lambda)$ to distinct vertices are not related by permutations that swap only nonadjacent residues. Consequently, by [Proposition 5C.4](#) and [Lemma 6G.3](#), if \mathcal{B} is path ordered, then any two paths in \mathcal{B} that differ by nonadjacent permutations end at the same vertex and give the same idempotent diagram in $\mathcal{W}_n^\rho(X)$.

For this paper, being path ordered is one of the most fundamental properties of a crystal graph of finite type because it is crucial to proving that the wKLRW algebras are sandwich cellular algebras. The proof of the next result is easy but only because it invokes Lusztig's quantum PBW theorem, which is only valid in finite type. Before we give the proof, we recall some of these notions in an example.

Example 7A.2. In finite type every crystal has a PBW realization that is obtained from the \mathcal{B}_∞ crystal of PBW monomials that models Verma modules; see e.g. [BS17, Chapter 12]. For example, for type B_3 choose $w_0 = r_1 r_2 r_3 r_2 r_1 r_2 r_3 r_2 r_3$, where $\{r_i \mid i \in I\}$ is the set of Coxeter generators of the Weyl group of type B_3 . Then the crystal graph from (4B.2) in the PBW notation is



In this example the three paths λ , μ and ν from [Section 4](#) end at the vertices labeled $f_{\alpha_1+\alpha_2} f_{\alpha_2+2\alpha_3}$, $f_{\alpha_1} f_{\alpha_2} f_{\alpha_2+2\alpha_3}$ and $f_{\alpha_1+\alpha_2+\alpha_3} f_{\alpha_2+\alpha_3}$, respectively. The generating sequences of f Kashiwara operators are given by the residue sequence of the corresponding path. In general, in the PBW realization of the crystal the vertices are labeled by products $f_{\beta_1} \dots f_{\beta_k}$ of Kashiwara operators, where β_1, \dots, β_k are certain sequences of

positive roots ordered with respect to a convex order that is determined by a choice of reduced expression for w_0 , the longest element of W . \diamond

Lemma 7A.3. *Suppose that Γ is a quiver of finite type, $\Lambda \in P^+$ and let $i \in I$. Then $\mathcal{G}(\Lambda)$ is path ordered.*

Proof. As in [Example 7A.2](#), each vertex $\lambda \in \mathcal{G}(\Lambda)$ corresponds to a PBW element in $L(\Lambda)$ by applying the PBW basis given at the vertex to a highest weight vector. Moreover, every rooted path \mathbf{p} to λ corresponds to a sequence $f_{\beta_1} \dots f_{\beta_k}$ of Kashiwara operators, which gives the associated PBW basis element up to lower order terms. This depends on a choice of reduced expression for the longest word in the Coxeter group, which exists because we are in finite type, but any choice works in the same way in this proof.

The statement now follows from the PBW theorem as all different PBW elements built from the same sequence of Kashiwara operators are related by at least one nontrivial Serre relation, which involves adjacent residues in Γ . That is, as is explained in many places such as [\[Tin17, Lemma 3.3\(i\)\]](#) or [\[Jan96, Chapter 8\]](#), if \mathbf{p} and \mathbf{q} are two paths in $\mathcal{G}(\Lambda)$ such that their residue sequences $\text{res}(\mathbf{p})$ and $\text{res}(\mathbf{q})$ only differ by successive swaps of f_{β_j} and f_{β_k} , for nonadjacent $j, k \in I$, then \mathbf{p} and \mathbf{q} determine the same canonical basis element and, hence, the same vertex of $\mathcal{G}(\Lambda)$. \square

Corollary 7A.4. *The crystals $\mathcal{G}(\underline{\Lambda})$, $\mathcal{G}_{\otimes}(\underline{\Lambda})$ and $\mathcal{G}_{\otimes}(\underline{\Lambda})$ are all path ordered.* \square

Proof. The crystal graph $\mathcal{G}(\underline{\Lambda})$ is path ordered by [Lemma 7A.3](#). As remarked already, $\mathcal{G}_{\otimes}(\underline{\Lambda})$ and $\mathcal{G}_{\otimes}(\underline{\Lambda})$ are both direct sums of highest weight crystals. Hence, the result again follows from [Lemma 7A.3](#). \square

7B. Steady diagrams in level one. We now use standard arguments to connect the wKLRW algebras with the quantum groups. In this section we assume that $\ell = 1$ and that $\underline{\Lambda} = (\Lambda_j)$, for some $j \in I$.

Recall from [Section 6H](#) that \mathcal{W}_n^{ρ} and \mathcal{R}_n^{ρ} are the infinite and finite dimensional KLR algebras attached to the quiver Γ .

Proposition 7B.1. *As graded algebras, $\mathcal{W}_n^{\rho}(X) \cong \mathcal{W}_n^{\rho}$ and $\mathcal{R}_n^{\rho}(X) \cong \mathcal{R}_n^{\rho}$.*

Proof. The proof is similar to [\[MT24, Proposition 3F.1\]](#), so we only sketch the details. The algebra \mathcal{W}_n^{ρ} is generated by elements ψ_r , Y_s and e_i , where $1 \leq r < n$, $1 \leq s \leq n$ and $i \in I^n$, so it is enough to define a map $f: \mathcal{W}_n^{\rho} \rightarrow \mathcal{W}_n^{\rho}(X)$ on the generators of \mathcal{W}_n^{ρ} , show that this map respects the relations of \mathcal{W}_n^{ρ} and then define an inverse map. Write $X = \{\mathbf{x}\}$ and define

$$(7B.2) \quad f(e_i) = \mathbf{1}_{\mathbf{x},i}, \quad f(\psi_r e_i) = D_{s_r} \mathbf{1}_{\mathbf{x},i}, \quad f(Y_s e_i) = y_s \mathbf{1}_{\mathbf{x},i},$$

for $i \in I^n$ and all admissible r, s as above. By definition, the images of the generators of \mathcal{W}_n^{ρ} are diagrams in the subalgebra $\mathcal{W}_n^{\rho}(X)$, which is spanned by diagrams that have all of their solid and ghost strings, except for the rightmost ghost string, to the left of the red strings. As discussed in [\[MT24, Proposition 3F.1\]](#), this follows using the arguments of [\[Bow22, Proposition 6.19\]](#). Strictly speaking Bowman is working in type $A_e^{(1)}$ but the argument applies, essentially without change, to quivers of all types. Once it is known that f is an isomorphism it is straightforward to check that it induces an isomorphism between the cyclotomic quotients. \square

Let q be an indeterminate over \mathbb{Q} . For $a \in \mathbb{Z}$ and $i \in I$ define the **quantum integer** $[a]_i = (q_i^a - q_i^{-a})/(q_i - q_i^{-1})$, where $q_i = q^{d_i}$. If $a \in \mathbb{Z}_{\geq 0}$ set $[a]_i! = [a]_i [a-1]_i \dots [1]_i$. For $a \in \mathbb{Z}$ and $b \in \mathbb{Z}_{\geq 0}$ set $\begin{bmatrix} a \\ b \end{bmatrix}_i = \frac{[a]_i [a-1]_i \dots [a-b+1]_i}{[b]_i [b-1]_i \dots [1]_i}$. By convention, empty products are 1, so $[0]_i = 0 = \begin{bmatrix} a \\ 0 \end{bmatrix}_i$.

Recall from [Section 3A](#) that $(a_{ij})_{i,j=1}^e$ is the Cartan matrix of Γ . Moreover, let Q^+ be the positive root lattice associated to Γ . Following Lusztig [\[Lus10, Section 1\]](#), define $\mathbf{f} = \bigoplus_{\alpha \in Q^+} \mathbf{f}_{\alpha}$ to be the $\mathbb{Q}(q)$ -algebra generated by $\{\theta_i \mid i \in I\}$ with relations

$$\sum_{k=0}^{1-a_{ij}} \begin{bmatrix} 1-a_{ij} \\ k \end{bmatrix}_i \theta_i^{1-a_{ij}-k} \theta_j \theta_i^k = 0, \quad \text{for } i, j \in I.$$

Define the divided powers $\theta_i^{(k)} = \theta_i^k / [k]_i!$, for $i \in I$ and $k \in \mathbb{Z}_{>0}$.

Using the nil-Hecke algebra, Khovanov–Lauda define a projective \mathcal{W}_n^{ρ} -module P_i , which is a summand of $\mathcal{W}_n^{\rho} e_i$ for each $i \in I^+$. Abusing notation, we consider P_i as a $\mathcal{W}_n^{\rho}(X)$ -module using the isomorphism of [Proposition 7B.1](#).

If A is a graded algebra let $[\text{Proj } A]$ be the Grothendieck group of finitely generated graded projective A -modules. If P is a projective A -module, let $[P]$ be its image in $[\text{Proj } A]$. By extension of scalars, consider $[\text{Proj } A]$ as a $\mathbb{Q}(q)$ -module, where v acts as the grading shift functor. We are interested in the cases when A is a wKLRW algebra $\mathcal{W}_n^{\rho}(X)$, a KLR algebra \mathcal{W}_n^{ρ} or a cyclotomic quotient $\mathcal{R}_n^{\rho}(X)$ and \mathcal{R}_n^{ρ} of one of these algebras.

Let $L(\Lambda_j)$ be the Weyl \mathbf{f} -module of highest weight Λ_j .

Using what are by now standard results for KLR algebras, we can use [Proposition 7B.1](#) to give an f -action on $[\text{Proj } \mathcal{W}_\oplus^\rho] = \bigoplus_{n \geq 0} [\text{Proj } \mathcal{W}_n^\rho(X)]$ and $[\text{Proj } \mathcal{R}_\oplus^\rho] = \bigoplus_{n \geq 0} [\text{Proj } \mathcal{R}_n^\rho(X)]$. Similarly, set $[\text{Proj } \mathcal{W}_\oplus^\rho] = \bigoplus_{n \geq 0} [\text{Proj } \mathcal{W}_n^\rho(X)]$ and $[\text{Proj } \mathcal{R}_\oplus^\rho] = \bigoplus_{n \geq 0} [\text{Proj } \mathcal{R}_n^\rho(X)]$.

Lemma 7B.3. *Suppose that a steady diagram D in $\mathcal{R}_n^\rho(X)$ factors through an idempotent diagram $\mathbf{1}_{\mathbf{x}, \mathbf{i}}$. Then D factors through an idempotent diagram that has all of its strings to the left of the red j -string.*

Proof. Suppose that $\mathbf{1}_{\mathbf{x}, \mathbf{i}}$ has a solid j -string s to the right of the red j -string. If s is steady then there is a sequence of strings $s_1, \dots, s_k = s$ such that s_{r+1} is blocked by s_r , for $1 \leq r < k$, and s_1 is blocked by the red j -string. Let s_r be an i_r -string. Since s_1 is blocked by the red string $i_1 = j$, and $i_r \rightsquigarrow i_{r+1}$ since s_{r+1} is blocked by s_r . Therefore, $j = i_1 \rightsquigarrow i_2 \rightsquigarrow \dots \rightsquigarrow i_k = j$. However, this is impossible because Dynkin diagrams of finite type do not contain cycles.

Therefore, all of the solid j -strings in a steady idempotent diagram are to the left of the red j -string. Hence, applying the relations, all of the strings in $\mathbf{1}_{\mathbf{x}, \mathbf{i}}$ can be pulled to the left of the red j -string, proving the lemma. \square

Proposition 7B.4. *Then there is an injective algebra homomorphism $\pi: f \rightarrow [\text{Proj } \mathcal{W}_\oplus^\rho(X)]$ of $\mathbb{Q}(q)$ -algebras such that $\pi(\theta_i) = [P_i]$, for $\mathbf{i} \in I^n$. Moreover, f acts on $[\text{Proj } \mathcal{R}_n^\rho(X)]$ and $L(\Lambda_j) \cong [\text{Proj } \mathcal{R}_\oplus^\rho]$ as f -modules.*

Proof. By [\[KL11, Theorem 8\]](#), we have $f \cong [\text{Proj } \mathcal{W}_\oplus^\rho]$ as algebras, where the isomorphism sends θ_i to P_i , for $i \in I$. Hence, the first isomorphism follows in view of [Proposition 7B.1](#). By [\[LV11, Theorem 7.8\]](#) or [\[KK12, Theorem 6.2\]](#), we have $L(\Lambda_j) \cong [\text{Proj } \mathcal{R}_\oplus^\rho]$ as f -modules. Applying [Proposition 7B.1](#) again, the highest weight module $L(\Lambda_j)$ is isomorphic to $[\text{Proj } \mathcal{R}_\oplus^\rho]$. More explicitly by [Lemma 7B.3](#), the solid strings in a steady idempotent diagram can always be pulled to the left of the red j -string. Therefore, every projective $\mathcal{R}_n^\rho(X)$ -module can be identified with a projective \mathcal{R}_n^ρ -module under the isomorphism of [Proposition 7B.1](#). \square

[Section 6C](#) associates an idempotent diagram $\mathbf{1}_{\mathbf{p}}$ to each path \mathbf{p} in the crystal graph $\mathcal{G}(\Lambda_j)$. This section shows how face permutations in the crystal are related to permutation diagrams in the wKLRW algebras.

Lemma 7B.5. *Let $\mathbf{i} \in I^n$ and $\mathbf{x} \in X$. Then $\mathbf{1}_{\mathbf{x}, \mathbf{i}}$ is steady if and only if $\mathbf{i} = \text{res}(\mathbf{p})$ where \mathbf{p} is a rooted path in $\mathcal{G}(\Lambda_j)$.*

Proof. By [Lemma 7B.3](#), we can assume that all solid strings are to the left of the red j -string. We argue by induction on n . If $n = 1$, then $\mathbf{1}_{\mathbf{x}, \mathbf{i}}$ is steady if and only if $\mathbf{i} = (j)$ and $x_1 = \kappa_1 - \varepsilon$. As the first edge in the crystal graph $\mathcal{G}(\Lambda_j)$ is labeled j , the result holds in this case. Now assume that $n > 1$ and let $\mathbf{y} = (x_1, \dots, x_{n-1})$ and $\mathbf{j} = (i_1, \dots, i_{n-1})$. By assumption, $\mathbf{1}_{\mathbf{y}, \mathbf{j}}$ is steady so, by induction, \mathbf{j} is a path in $\mathcal{G}(\Lambda_j)$. By the proof of [Proposition 7B.4](#), adding an i_n -string to the left of the diagram $\mathbf{1}_{\mathbf{y}, \mathbf{j}}$ is equivalent to tensoring with P_{i_n} , which gives an action of θ_{i_n} on $\mathbf{1}_{\mathbf{y}, \mathbf{j}}$. By [\[LV11, Theorem 7.5\]](#), the crystal graph $\mathcal{G}(\Lambda_j)$ categorifies the simple \mathcal{R}_n^ρ -modules, for $n \geq 0$. Therefore, θ_{i_n} is nonzero on $\mathbf{1}_{\mathbf{y}, \mathbf{j}}$ if and only if \mathbf{i} is the residue sequence of a path in $\mathcal{G}(\Lambda_j)$, giving the result. \square

As a special case of face permutations, [Definition 5B.9](#) defines detour permutations to be the face permutations in $\text{Face}_{\underline{\Lambda}}(\mathbf{p}_\lambda, \mathbf{p}_\lambda)$, for $\lambda \in V_n^\Lambda$. To understand the detour permutations we use the plactic relations of [Lemma 3G.6](#) and the plactic monoid moves of [Section 6D](#).

Proposition 7B.6. *Let $\mathbf{T} \in \text{Face}_{\underline{\Lambda}}(\lambda)$ be a detour permutation, for $\lambda \in V_n^\Lambda$. Then $D_{\mathbf{T}}$ is invertible up to more dominant diagrams. That is, there exists a diagram $E_{\mathbf{T}}$ such that $E_{\mathbf{T}}D_{\mathbf{T}} = \mathbf{1}_\lambda + F$, where F is linear combination of diagrams that dominate $\mathbf{1}_\lambda$.*

Proof. Let $i, j \in I$ with $i \neq j$. It is enough to consider the case when \mathbf{T} is a basic face permutation between two paths \mathbf{p} and \mathbf{q} with sink λ . To prove the lemma it is enough to show that the idempotent diagrams $\mathbf{1}_{\mathbf{p}}$ and $\mathbf{1}_{\mathbf{q}}$ factor through each other, up to more dominant diagrams. By [Definition 5D.1](#) and [Proposition 5C.4](#), the basic face permutations are of the form

$$ij \rightsquigarrow ji \text{ with } i, j \text{ nonadjacent,}$$

$$i \dots ij \rightsquigarrow i \dots ji \text{ with } i, j \text{ simply laced adjacent, } \quad i j j i \rightsquigarrow j i i j \text{ with } i, j \text{ doubly laced adjacent,}$$

except in type F_4 where there are two additional cases, which we consider at the end of the proof. We consider each of the basic face permutations in turn.

Case 1: $ij \rightsquigarrow ji$, with i and j nonadjacent. The claim is easy to verify in this case. On the one hand, if i, j are not fishtail vertices, then $\mathbf{1}_{\mathbf{p}} = \mathbf{1}_{\mathbf{q}}$ on the nose by our string placement strategy in [Definition 6C.1](#). On the other hand, if i, j are fishtail vertices, then

$$\begin{array}{c|c} | & | \\ \hline i & j \end{array} = \begin{array}{c} \diagup \quad \diagdown \\ i \quad j \end{array}$$

and its partner relation hold by the honest Reidemeister II relation. Hence, this local picture verifies the claim.

Case 2: $ij \rightsquigarrow ji$, with i and j adjacent. This is the only place where we use [Proposition 6D.10](#), which says that the crystal $\mathcal{G}(\Lambda_j)$ is plactic. First assume that the local situation is $iij \rightsquigarrow iji$, which corresponds to part (a) of [Definition 6D.5](#). Assume first that $i \rightarrow j$, we can use [Lemma 3G.6](#) which reads

Note that this relates iji and iij modulo jii , and jii is always more dominant. A similar argument works for its partner relation and for the case when $i \leftarrow j$. This verifies the claim when $iij \rightsquigarrow iji$.

Now consider the case when $ij \rightsquigarrow ji$ is not preceded by i or j , which corresponds to [Definition 6D.5\(b\)](#). By [Lemma 6D.4](#), we can use weighted plactic monoid moves to reduce to the case when $ij \rightsquigarrow ji$ is not preceded by i or j . Thus, it remains to show that the weighted plactic moves are realized by invertible operations up to more dominant diagrams. For the first case we can simply use an honest Reidemeister II relation [Lemma 3G.5.\(b\)](#), e.g.

At the equator of these diagrams is the sequence ji , showing that the corresponding weighted plactic move is realized by an invertible operation. Similarly, for the other case applying a Reidemeister III relation [\(3D.8\)](#), and looking at the equators proves the claim.

Case 3: $ijji \rightsquigarrow jiji$ and $i \rightarrow j$. By [Lemma 3G.5](#) and [Lemma 3G.5](#),

or its partner relation. Hence, we have related $jiji$ and $ijji$ up to higher order terms. We can now use the plactic relations from [Lemma 3G.6](#) to relate $jiji$ to $ijji$ and $jjii$, with $jjii$ being a more dominant term. The argument when $j \rightarrow i$ is identical.

Case 4: $ijji \rightsquigarrow jiji$ and $i \Rightarrow j$. If i and j are doubly laced adjacent then essentially the same argument applies except that we make use of the fact that the rightmost of the two middle strings carries a dot by [Section 6E](#). More precisely, as above, we can relate $ijji$ to $jiji$ up to more dominant terms since [Lemma 3G.5.\(b\)](#) gives

and the same diagrammatic argument used above works (the more dominant terms will have two dots, but this does not affect the argument). Note that in the diagram the strings with residues jij are such that the i -string has a dot, so using [Lemma 3G.5.\(b\)](#) we can relate this to ijj up to higher order terms. Hence, we have related $ijji$ to $jiji$ up to higher order terms.

Case 5: the decagon in type F_4 . We consider only the case when the basic diagrammatic face permutation is:

From Lemma 3G.5.(a) and the Reidemeister II relation we get

$$\begin{aligned}
 \begin{array}{c} 3 \\ \vdots \\ 2 \end{array} \quad \begin{array}{c} 3 \\ \vdots \\ 2 \end{array} \quad \begin{array}{c} 3 \\ \vdots \\ 2 \end{array} &= \begin{array}{c} 3 \\ \vdots \\ 2 \end{array} \quad \begin{array}{c} 3 \\ \vdots \\ 2 \end{array} \quad \begin{array}{c} 3 \\ \vdots \\ 2 \end{array} - \begin{array}{c} 3 \\ \vdots \\ 2 \end{array} \quad \begin{array}{c} 3 \\ \vdots \\ 2 \end{array} \quad \begin{array}{c} 3 \\ \vdots \\ 2 \end{array} - \begin{array}{c} 3 \\ \vdots \\ 2 \end{array} \quad \begin{array}{c} 3 \\ \vdots \\ 2 \end{array} + \begin{array}{c} 3 \\ \vdots \\ 2 \end{array} \quad \begin{array}{c} 3 \\ \vdots \\ 2 \end{array} \\
 &= \begin{array}{c} 3 \\ \vdots \\ 2 \end{array} \quad \begin{array}{c} 3 \\ \vdots \\ 2 \end{array} \quad \begin{array}{c} 3 \\ \vdots \\ 2 \end{array} + \text{more dominant terms},.
 \end{aligned}$$

Now Lemma 3G.5.(a) implies that

$$\begin{array}{c} 3 \\ \vdots \\ 2 \end{array} \quad \begin{array}{c} 3 \\ \vdots \\ 2 \end{array} \quad \begin{array}{c} 3 \\ \vdots \\ 2 \end{array} + \text{more dominant terms} = \begin{array}{c} 3 \\ \vdots \\ 2 \end{array} \quad \begin{array}{c} 3 \\ \vdots \\ 2 \end{array} \quad \begin{array}{c} 3 \\ \vdots \\ 2 \end{array} + \text{more dominant terms},$$

which is what we needed to establish, up to symmetry. The argument when $j \Rightarrow i$ is identical.

Case 6: The tetradecagon in type F_4 . Similar to the previous case, we use Lemma 3G.5.(a) and the Reidemeister II relation on close strings of the same residue. The details are omitted. \square

7C. Steady diagrams and crystals. We now return to the case where Λ is of arbitrary level $\ell \geq 1$. Recall from Section 5E that we write each rooted path $\mathbf{p} \in P_n^\Lambda$ as a tuple $\mathbf{p} = (\mathbf{p}_1, \dots, \mathbf{p}_\ell)$, where \mathbf{p}_m is a rooted path in $\mathcal{G}(\Lambda_{\rho_m})$, for $1 \leq m \leq \underline{\ell}$.

Lemma 7C.1. *Suppose that $\mathbf{p} = (\mathbf{p}_1, \dots, \mathbf{p}_\ell) \in P_n^\Lambda$. Then the solid strings in $\mathbf{1}_\mathbf{p}$ corresponding to \mathbf{p}_m are anchored around the m th (affine) red string, for $1 \leq m \leq \underline{\ell}$. Moreover, $\mathbf{1}_\mathbf{p}$ is steady if and only if \mathbf{p}_m is empty for $\ell < m \leq \underline{\ell}$.*

Proof. By Lemma 5E.4, \mathbf{p}_m is a rooted path in $\mathcal{G}(\Lambda_{\rho_m})$. By Proposition 7B.1, $\mathcal{R}_n^\rho \cong \mathcal{R}_n^\Lambda$ is isomorphic to the wKLRW algebra obtained by putting n solid strings to the left of the m th red string using an appropriate modification of (7B.2). In view of Lemma 6B.7, we can apply Lemma 7B.5 locally to the strings anchored on each (affine) red string. Hence, the strings in $\mathbf{1}_\mathbf{p}$ that correspond to the edges of the path \mathbf{p}_m in $\mathcal{G}(\Lambda_{\rho_m})$ are anchored on the m th (affine) red string by Lemma 7B.5. Finally, to show that $\mathbf{1}_\mathbf{p}$ is steady if and only if \mathbf{p}_m is empty for $\ell < m \leq \underline{\ell}$ first note that $\mathbf{1}_\mathbf{p}$ is not steady if \mathbf{p}_m is not empty for any $m > \ell$. Conversely, if \mathbf{p}_m is empty for $\ell < m \leq \underline{\ell}$ then all of the strings anchored on the k th red string, for $1 \leq k \leq \ell$, are steady by Lemma 7B.5, so no string in $\mathbf{1}_\mathbf{p}$ can be pulled arbitrarily far to the right. Hence, $\mathbf{1}_\mathbf{p}$ is steady. \square

A diagram D **factors through** a diagram B if $D = D'BD''$ for some diagrams D' and D'' . The diagram D **dominates** $\mathbf{1}_\lambda$ if D factors through an idempotent diagram $\mathbf{1}_\mu$ such that $\lambda \leq_{\mathbb{R}} \mu$. We do not require that B belongs to the wKLRW algebra $\mathcal{R}_n^\rho(X)$, only that it is a wKLRW diagram.

Proposition 7C.2. *Let $\mathbf{i} \in I^n$. Then $\mathbf{1}_{\mathbf{x}, \mathbf{i}}$ factors through $\mathbf{1}_\mathbf{p}$ for some path \mathbf{p} in $\mathcal{G}(\Lambda)$ such that $\mathbf{1}_{\mathbf{x}, \mathbf{i}} \leq_{\mathbb{R}} \mathbf{1}_\mathbf{p}$. Moreover, $\mathbf{1}_{\mathbf{x}, \mathbf{i}}$ is steady if and only if $\mathbf{p} \in \mathcal{G}(\Lambda)$.*

Proof. By pulling strings to the right, we can assume that every string is anchored on a red string or an affine red string. Therefore, $\mathbf{1}_{\mathbf{x}, \mathbf{i}}$ factors through a diagram $\mathbf{1}_\mathbf{j}$, where $\mathbf{j} = (j_1, \dots, j_{\underline{\ell}}) \in I^{n, \underline{\ell}}$ and j_m correspond to the strings anchored on the (affine) red ρ_m -string with coordinate κ_m . By construction, $\mathbf{1}_{\mathbf{x}, \mathbf{i}} \leq_{\mathbb{R}} \mathbf{1}_\mathbf{j}$. By Lemma 7B.5, $j_m = \text{res}(\mathbf{p}_m)$ is the residue sequence of a rooted path \mathbf{p}_m in $\mathcal{G}(\Lambda_{\rho_m})$. Therefore, by Lemma 5E.5, we can find a rooted path $\mathbf{p} \in \mathcal{G}(\Lambda)$ with $\mathbf{p} = (\mathbf{p}_1, \dots, \mathbf{p}_\ell)$. Finally, $\mathbf{1}_{\mathbf{x}, \mathbf{i}}$ is steady if and only if $\mathbf{1}_\mathbf{p}$ is steady, which is if and only if \mathbf{p}_m is empty for $\ell < m \leq \underline{\ell}$ by Lemma 7C.1. Hence, $\mathbf{1}_{\mathbf{x}, \mathbf{i}}$ is steady if and only if $\mathbf{p} \in \mathcal{G}(\Lambda)$ by Lemma 5E.5. \square

Remark 7C.3. In fact, the argument of Proposition 7C.2 shows that if Γ is a symmetrizable quiver, then an idempotent diagram $\mathbf{1}_{\mathbf{x}, \mathbf{i}}$ in the wKLRW algebra $\mathcal{W}_n^\rho(X)$ is steady if and only if \mathbf{i} is the residue sequence of a rooted path in the quiver $\mathcal{G}(\Lambda)$.

Let $\mathbf{p} \in I^{n, \ell}$. Recall from Definition 6E.1 that $d_m(\mathbf{p}) + 1$ is the length of a dotted i -sequence in $\text{res}(\mathbf{p})$ and $c_m(\mathbf{p}) = d_i - d_m - 1$ is the maximal number of finite sandwich dots by Definition 6F.1.

Corollary 7C.4. *Let \mathbf{p} be a rooted path in the crystal graph $\mathcal{G}(\Lambda)$. Then*

$$d_m(\mathbf{p}) \leq \begin{cases} 2 & \text{in types } F_4 \text{ and } G_2, \\ 1 & \text{in types } B_{e>1}, C_{e>2}, D_{e>3} \text{ and } E_k, \\ 0 & \text{in type } A_e. \end{cases}$$

In particular, $\mathbf{1}_{\mathbf{p}}^y = \mathbf{1}_{\mathbf{p}}$ in type A_e . □

Proof. Since every string in $\mathbf{1}_{\mathbf{p}}$ is anchored on some (affine) red string, it is enough to consider rooted paths in $\mathcal{G}(\Lambda_i)$, for $i \in I$. By definition, $d_m(\mathbf{p})$ is determined by the crystal graph of $\mathcal{G}(\Lambda_i)$. The Serre relations show that $F_j^{1-a_{jk}}$ annihilates $L(\Lambda_i)$, for $j, k \in I$. Therefore, no path in $\mathcal{G}(\Lambda_i)$ has a dotted j -subsequence of length $1 - a_{jk}$, so if $i_m = j$, then $d_m(\mathbf{p}) \leq \max\{|a_{jk}| \mid k \in I\}$. This gives all of the bounds above except for types A_e , B_{e+1} , C_{e+2} and G_2 , where we can do better. In the classical cases, these bounds can be verified using tableaux combinatorics, as in the proof of [Proposition 5C.4](#). For type G_2 , the bound follows directly from [\(5C.6\)](#). □

Recall that [Section 6G](#) associates a permutation diagram $D_{\mathbf{T}}$ to each face permutation $\mathbf{T} \in \text{Face}_{\underline{\Lambda}}(\mathbf{p}, \mathbf{q})$, for $\mathbf{p}, \mathbf{q} \in P_n^{\Lambda}$. By [Definition 5D.1](#), a face permutation $\mathbf{T} \in \text{Face}_{\underline{\Lambda}}(\mathbf{p}, \mathbf{q})$ is an equivalence class of permutations, and [Definition 6G.9](#) defines the diagrammatic face permutation $D_{\mathbf{T}}$ for \mathbf{T} .

Lemma 7C.5. *Let $\mathbf{T} \in \text{Face}_{\underline{\Lambda}}(\mathbf{p}, \mathbf{q})$, for $\mathbf{p}, \mathbf{q} \in P_n^{\Lambda}$. If $w \in \mathbf{T}$, then D_w can be obtained from $D_{\mathbf{T}}$, up to more dominant terms, by applying crossings and dots.*

Proof. As all of the relations in [Definition 3D.5](#) are bilocal, we can ignore the red strings in the relations below. By definition, the basic diagrammatic face permutations permute the minimal number of strings with different residues and the maximal number of strings with the same residue. Thus, if the permutation diagram D_w has more i - j crossings, then we can apply these crossings to $D_{\mathbf{T}}$ to give all of the i - j crossings in D_w . On the other hand, we can remove i - i crossings from $D_{\mathbf{T}}$ by successively applying relation [\(3D.6\)](#), which gives

$$(7C.6) \quad \text{Diagram} = \text{Diagram} + \text{Diagram} \quad \text{and} \quad \text{Diagram} = \text{Diagram} + \text{Diagram} .$$

more dominant

more dominant

That the rightmost diagrams in these equations are more dominant follows by pulling strings and jumping dots to the right, as in [Lemma 3G.5](#). For example, in the simplified notation as in [Definition 6G.9](#):

$$\text{Diagram} = \text{Diagram} + \underbrace{\text{Diagram} + \text{Diagram} + \text{Diagram}}_{\text{more dominant}} + \text{Diagram} .$$

So, we get the diagram with only two crossings from the left-hand one by applying dots. □

Proposition 7C.7. *Let D be a steady permutation diagram in $\mathcal{W}_n^{\rho}(X)$. Then D is a linear combination of diagrams of the form $E_{\mathbf{p}}^* D_{\mathbf{T}} E_{\mathbf{q}}$, for $\mathbf{p}, \mathbf{q} \in P_n^{\Lambda}$ and face permutations $\mathbf{T} \in \text{Face}_{\underline{\Lambda}}(\mathbf{p}, \mathbf{q})$.*

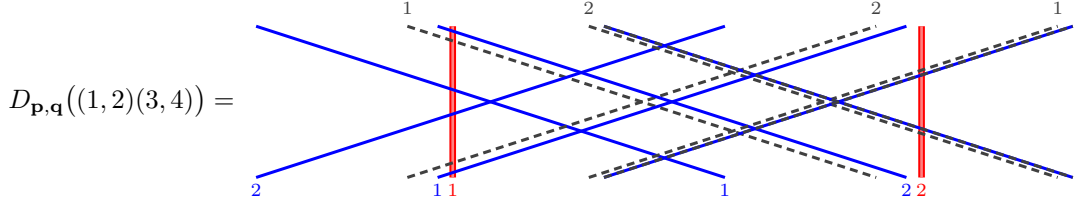
Proof. Any diagram can be factored through an idempotent diagram by making a horizontal cut through the diagram. By [Proposition 7C.2](#), we can pull the strings of D to the right until each string becomes blocked. This gives paths $\mathbf{p}, \mathbf{q} \in P_n^{\Lambda}$ such that D is a linear combination of diagrams of the form $E_{\mathbf{p}}^* D' E_{\mathbf{q}}$, for some diagram D' . In particular, the residues along the top and bottom of a nonzero diagram uniquely determine paths \mathbf{p} and \mathbf{q} in P_n^{Λ} by [Proposition 7C.2](#). Each diagram D' determines a permutation $w = w_{D'} \in \mathfrak{S}_n$ such that $\text{res}(\mathbf{p}) = w \text{res}(\mathbf{q})$. By [Lemma 5D.4](#) and [Proposition 5D.6](#), $w = \mathbf{T}$ is a face permutation in $\text{Face}_{\underline{\Lambda}}(\mathbf{p}, \mathbf{q})$, so $D' = D_{\mathbf{T}}$ in view of [Lemma 7C.5](#). (As noted after [Definition 6G.9](#), the definition of diagrammatic face permutations involves several choices, but these give the same diagrams modulo more dominant terms.) □

To summarize the results so far:

- ▷ In all finite types the path idempotents $\mathbf{1}_{\mathbf{X}}$ are ordered by how far strings are to the right.
- ▷ The end points of steady diagrams correspond to paths in crystals.
- ▷ Up to more dominant terms, the steady permutation diagrams are compositions of diagrammatic face permutations, where diagrammatic face permutations correspond to face permutations in the crystals.
- ▷ In level one, the weighted plactic monoid moves were used to show that steady permutation diagrams for detour permutations are the same up to more dominant terms.

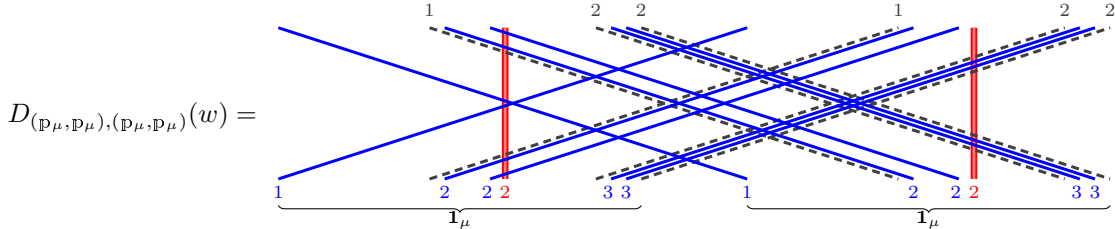
Example 7C.8. Let Γ be a quiver of type A_5 and set $\Lambda = \Lambda_1 + \Lambda_2$, $\rho = (1, 2)$, and $\kappa = (0, 3)$. Then $\mathbf{p} = (1, 2, 2, 1)$ and $\mathbf{q} = (2, 1, 1, 2)$ are both paths in $\mathcal{G}(\Lambda)$. Using the notation of [Section 5E](#), $\mathbf{p} = (12, 21)$ and $\mathbf{q} = (12, 21)$. Hence, $\mathbf{1}_{\mathbf{p}} = \mathbf{1}_{\mathbf{q}}$. There are two face permutations in $\text{Face}_{\underline{\Lambda}}(\mathbf{p}, \mathbf{q})$. Namely, the trivial

permutation $\mathbf{1}_p$ and the permutation



The face permutation $D_{p,q}((1,2)(3,4))$ has degree zero and is invertible. \diamond

Example 7C.9. Extending [Example 4B.1](#), let Γ be the quiver of type B_3 and let $\Lambda = (\Lambda_2, \Lambda_2)$. Let $n = 10$, $\ell = 2$, $\kappa = (0, 3)$ and $\rho = (2, 2)$. Let $w = (1, 6)(2, 7)(3, 8)(4, 9)(5, 10)$, Then



Looking at the equator of this diagram, and comparing with the crystal graph in [Example 4B.1](#), this diagram is unsteady in view of [Proposition 7C.2](#). In particular, this diagram is not the diagram of a face path permutation by [Lemma 5D.4](#) and [Proposition 7C.7](#). \diamond

7D. Combinatorics of diagrams in finite types. As in [\[MT24\]](#) and [\[MT23\]](#), in [Theorem 6I.1](#) the basis theorem for the infinite dimensional wKLRW algebra $\mathcal{W}_n^\rho(X)$ implies the result for the cyclotomic quotient $\mathcal{R}_n^\rho(X)$, so we focus on the infinite dimensional algebra in this section. In this setting we have the following *standard basis* and *polynomial module*.

Recall from [Definition 6G.9](#) that each permutation $w \in \mathfrak{S}_n$ defines a diagram $D_w \mathbf{1}_{\mathbf{x}, \mathbf{i}}$, for $\mathbf{x} \in X$ and $\mathbf{i} \in I^n$.

Proposition 7D.1. *The algebra $\mathcal{W}_n^\rho(X)$ is free as an R -module with homogeneous basis*

$$(7D.2) \quad \mathcal{B}_{\mathcal{W}_n^\rho(X)} = \{D_w y_1^{a_1} \dots y_n^{a_n} \mathbf{1}_{\mathbf{x}, \mathbf{i}} \mid a_1, \dots, a_n \in \mathbb{Z}_{\geq 0}, w \in \mathfrak{S}_n, \mathbf{x} \in X, \mathbf{i} \in I^n\}.$$

Proof. See [\[MT24\]](#), Proposition 3B.12]. \square

Similarly to [\(4A.1\)](#), the mnemonic for [\(7D.2\)](#) is

$$D_w y_1^{a_1} \dots y_n^{a_n} \mathbf{1}_{\mathbf{x}, \mathbf{i}} \quad \rightsquigarrow \quad \begin{array}{c} D_w \\ \diagdown \quad \diagup \\ d \end{array}, \quad \text{where} \quad \begin{array}{c} D_w \\ \diagdown \quad \diagup \\ d \end{array} \text{ a permutation diagram,} \\ \begin{array}{c} d \\ \boxed{d} \end{array} \text{ dots on an idempotent.}$$

Importantly, the algebra $\mathcal{W}_n^\rho(X)$ has a faithful polynomial representation. To define it, let y_1, \dots, y_n be indeterminates over R and set

$$P_n(X) = \bigoplus_{\mathbf{x} \in X, \mathbf{i} \in I^n} R[y_1, \dots, y_n] \mathbf{1}_{\mathbf{x}, \mathbf{i}}.$$

The symmetric group \mathfrak{S}_n acts on $P_n(X)$ by place permutations. Let $\partial_{r,s} = \frac{(r,s)-1}{y_s - y_r}$ be the **Demazure operator**. By [\[MT24\]](#), Lemma 3B.11], $\mathcal{W}_n^\rho(X)$ acts on $P_n(X)$ by:

$$(7D.3) \quad \mathbf{1}_{\mathbf{y}, \mathbf{j}} \cdot f(y) \mathbf{1}_{\mathbf{x}, \mathbf{i}} = \delta_{\mathbf{x}\mathbf{y}} \delta_{\mathbf{i}\mathbf{j}} f(y) \mathbf{1}_{\mathbf{x}, \mathbf{i}}, \quad \begin{array}{c} \bullet \\ i_r \end{array} \mapsto y_r, \quad \begin{array}{c} \bullet \\ i_r \end{array} \mapsto 1,$$

and all crossings act as the identity except that

$$\begin{array}{c} \times \\ i_r \quad i_s \end{array} \mapsto \begin{cases} \partial_{r,s} & \text{if } i_r = i_s, \\ (r,s) & \text{if } i_r \neq i_s, \end{cases} \quad \begin{array}{c} \times \\ i_r \quad i_s \end{array} \mapsto \begin{cases} x_r & \text{if } i_r = i_s, \\ 1 & \text{if } i_r \neq i_s, \end{cases} \quad \begin{array}{c} \diagup \quad \diagdown \\ i_r \quad i_s \end{array} \mapsto \begin{cases} Q_{i_r, i_s}(y_r, y_s) & \text{if } i \rightsquigarrow j, \\ 1 & \text{otherwise.} \end{cases}$$

Proposition 7D.4. *The algebra $\mathcal{W}_n^\rho(X)$ acts faithfully on $P_n(X)$.*

Proof. See [\[MT24\]](#), Corollary 3B.13]. \square

Recall from [Definition 6G.4](#) that P_n^Δ is a fixed choice of paths in $\mathcal{G}(\mathcal{B})$ of length of n .

Lemma 7D.5. *Let $\mathbf{p}, \mathbf{q} \in P_n^\Delta$. Then $\mathbf{1}_p = \mathbf{1}_q$ if and only if $\mathbf{p} = \mathbf{q}$.*

Proof. One direction is clear, so let us assume that $\mathbf{p} \neq \mathbf{q}$. We will show that $\mathbf{1}_{\mathbf{p}} \neq \mathbf{1}_{\mathbf{q}}$.

Case 1: $\text{res}(\mathbf{p}) = \text{res}(\mathbf{q})$. This case does not arise because paths in irreducible crystals are uniquely determined by the sequence of their labels.

Case 2: $\text{res}(\mathbf{p}) \neq w \text{res}(\mathbf{q})$ for any $w \in \mathfrak{S}_n$. In this case the idempotent diagrams $\mathbf{1}_{\mathbf{p}}$ and $\mathbf{1}_{\mathbf{q}}$ have different residues of their solid strings. Hence, [Proposition 7D.1](#) ensures that $\mathbf{1}_{\mathbf{p}} \neq \mathbf{1}_{\mathbf{q}}$.

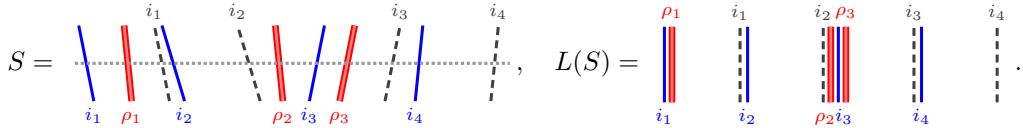
Case 3: $\text{res}(\mathbf{p}) = w \text{res}(\mathbf{q})$ for some $1 \neq w \in \mathfrak{S}_n$. The permutation w necessarily swaps solid strings of different residues $i \neq j$ since otherwise $\text{res}(\mathbf{p}) = \text{res}(\mathbf{q})$. By [Lemma 5E.5](#), we can write $\mathbf{p} = (\mathbf{p}_1, \dots, \mathbf{p}_\ell)$ and $\mathbf{q} = (\mathbf{q}_1, \dots, \mathbf{q}_\ell)$. By [Lemma 6C.8](#), we can assume that w permutes the residues in just one component, so that $\mathbf{p}_m = w\mathbf{q}_m$, for some m . The crystal graph $\mathcal{G}(\Lambda_{\rho_m})$ is path ordered by [Lemma 7A.3](#), so $\omega(\mathbf{p}_m) = \omega(\mathbf{q}_m)$. Hence, w is a face permutation by [Lemma 5D.4](#) and we can assume that w only permutes two non-adjacent residues i and j . As i and j are not adjacent in the quiver Γ , then $\mathbf{1}_{\mathbf{p}} = \mathbf{1}_{\mathbf{q}}$ by the construction of [Definition 6C.1](#). \square

A *straight line diagram* is a diagram without crossings. For example, every idempotent diagram is a straight line diagram. As for idempotent diagrams, a diagram D **factors through** a straight line diagram S if $D = ESF$, for some $E, F \in \mathcal{W}_n^{\rho}(X)$. Here, E and F are allowed to be linear combinations of diagrams.

Definition 7D.6. Let S be a straight line diagram. The **left justification** of S is an idempotent diagram $L(S)$ such that S factors through $L(S)$, and $L(S)$ has its solid strings in admissible parking positions that are as far to the left as possible.

By successively pulling strings as far to the left as possible, it follows that every straight line diagram has a unique left justification; cf. [\[MT24, Lemma 5D.9\]](#).

Example 7D.7. The notions from [Definition 7D.6](#) can be illustrated by



The left justification $L(S)$ can be thought of as being in a collar neighborhood of the points on the dashed line through the middle of S , so S factors through $L(S)$. (Recall that a **collar neighborhood** of a set is the Cartesian product of the set with a half-open interval.) \diamond

Once our main theorem is established, the general theory of sandwich cellular algebras defines the two-sided ideals $\mathcal{W}_n^{\rho}(X)^{\geq_{\mathbb{R}} \lambda}$ for $\lambda \in \dot{V}_n^{\Delta}$. However, we need to define these ideals now even though we do not yet have a sandwich cellular basis. For $\lambda \in \dot{V}_n^{\Delta}$ let $\mathcal{W}_n^{\rho}(X)^{\geq_{\mathbb{R}} \lambda}$ be the R -submodule of $\mathcal{W}_n^{\rho}(X)$ spanned by all diagrams D such that D factors through a straight line diagram S with $L(S) \geq_{\mathbb{R}} \mathbf{1}_{\lambda}$. Define $\mathcal{W}_n^{\rho}(X)^{>_{\mathbb{R}} \lambda}$ in the same way.

The next two results imply that $\mathcal{W}_n^{\rho}(X)^{\geq_{\mathbb{R}} \lambda}$ and $\mathcal{W}_n^{\rho}(X)^{>_{\mathbb{R}} \lambda}$ are two-sided ideals of $\mathcal{W}_n^{\rho}(X)$.

Lemma 7D.8. Suppose that $D \in \mathcal{W}_n^{\rho}(X)$ and that D factors through the idempotent diagram S . Then there exists $\lambda \in \dot{V}_n^{\Delta}$ such that D factors through $\mathbf{1}_{\lambda}^y$ and $L(S) \geq_{\mathbb{R}} \mathbf{1}_{\lambda}^y$ modulo $\mathcal{W}_n^{\rho}(X)^{\geq_{\mathbb{R}} \lambda}$.

Proof. Without loss of generality we can assume that $D = S$. Using the results in [Section 3G](#) to pull strings to the right, if necessary, we can replace D with a linear combination of more $\geq_{\mathbb{R}}$ -dominant diagrams in which every string is anchored on some (affine) red string. With respect to $\geq_{\mathbb{R}}$, let $T = L(T)$ be the minimal straight line diagram such that one of the summands of D factors through T . By construction, $T \geq_{\mathbb{R}} L(S)$ and every string in T is anchored on an (affine) red string. By [Lemma 7B.5](#), the strings anchored around the red ρ_i -string correspond to the path \mathbf{p} in $\mathcal{G}(\Lambda_i)$, so T naturally corresponds to an ℓ -tuple $(\mathbf{p}_1, \dots, \mathbf{p}_\ell)$, where $\mathbf{p}_k \in \mathcal{G}(\Lambda_{\rho_k})$. Note that this argument also applies to the affine red strings because, by definition, the strings anchored around the affine red strings are blocked by the affine red strings. By construction each component of T is anchored around an (affine) red string so, up to conjugation by straight line diagrams, $T = \mathbf{1}_{\mathbf{p}}$ by [Lemma 7B.5](#), for some $\mathbf{p} \in P_n^{\Delta}$. Let $\lambda = \omega(\mathbf{p})$. In view of [Lemma 7C.5](#), we can assume that $\mathbf{p} = \mathbf{p}_{\lambda}$. By [Lemma 3G.5.\(a\)](#), the dots on dotted idempotents are invertible, modulo higher terms, so D factors through $\mathbf{1}_{\lambda}^y$ as claimed. \square

From here on we can use almost the same arguments as in [\[MT24, Sections 6D and 7E\]](#).

For the next lemma, recall from [Definition 6F.1](#) that $c_k(\lambda)$ is the maximum number of dots allowed on the k th solid string in the sandwich algebra \mathcal{H}_{λ} . The next lemma says that the idempotent diagram $\mathbf{1}_{\lambda}^y$ is a minimal diagram in $\mathcal{W}_n^{\rho}(X)^{\geq_{\mathbb{R}} \lambda}$, with respect to the $<_{\mathbb{R}}$ -order, and adding dots or crossings gives a linear combination of more dominant diagrams.

Lemma 7D.9.

- (a) Suppose that $\lambda \in \dot{V}_n^\Delta$ and $1 \leq k \leq n$ such that the k th string is not immediately adjacent to an affine string of the same residue. Then $y_k y_k^{c_k(\lambda)} \mathbf{1}_\lambda^y \in \mathcal{W}_n^\rho(X)^{>_\mathbb{R} \lambda}$.
- (b) Suppose that $\lambda \in \dot{V}_n^\Delta$ and $w \in \text{Face}_\Delta(\mathbf{p}_\lambda, \mathbf{p})$ for $\mathbf{1}_\mathbf{p} >_\mathbb{R} \mathbf{1}_\lambda^y$. Then $D_w \mathbf{1}_\lambda^y, \mathbf{1}_\lambda^y D_w^* \in \mathcal{W}_n^\rho(X)^{>_\mathbb{R} \lambda}$.

Proof. (a). By the construction of $\mathbf{1}_\lambda^y$ in (6H.2), putting a dot on the k th solid string allows us to pull the string to the right by Lemma 3G.5, applied to the k th solid string or its ghosts. Now apply Lemma 7D.8.

(b). This follows directly from Proposition 7C.7 and Lemma 7D.8. \square

Lemma 7D.10. *The diagrams in (6H.2) form an R -basis of $\mathcal{W}_n^\rho(X)$.*

Proof. Spanning. By Proposition 7D.1, $\mathcal{W}_n^\rho(X)$ is spanned by the diagrams $D_w^* y^b \mathbf{1}_\lambda D_v$, for $w, v \in \mathfrak{S}_n$ and $b \in \mathbb{Z}_{\geq 0}$. Lemma 7D.9(a) implies that we can restrict the dots y^b to $b = \mathbf{a} + \mathbf{f}$, where $\mathbf{a} \in A^y(\lambda)$ and $\mathbf{f} \in F^y(\lambda)$ as in (6H.2). By Proposition 7C.7, we can assume that D_w and D_v are diagrammatic face permutations. By Lemma 7D.9(b), we can further assume that $w, v \in \bigcup_{\nu \leq_\mathbb{R} \lambda} \text{Face}_\Delta(\lambda, \nu)$. Hence, the diagrams in (6H.2) span $\mathcal{W}_n^\rho(X)$.

Linear independence. Using Proposition 7D.4, it is enough to show that the images of the elements from (6H.2) in the endomorphism algebra of the polynomial module $P_n(X)$ are linearly independent. Note that it suffices to check linear independence of the elements from (6H.2) in the associated graded algebra of $\mathcal{W}_n^\rho(X)$, see [MT24, Section 3B] for details. To this end, for $\mathbf{S}, \mathbf{T} \in \text{Face}_\Delta(\lambda)$ let $\mathbf{1}_\mathbf{S}$ and $\mathbf{1}_\mathbf{T}$ be the idempotents whose endpoints are determined by the top of $D_\mathbf{S}^* \mathbf{1}_\lambda$ and the bottom of $\mathbf{1}_\lambda D_\mathbf{T}$, i.e.

$$D_\mathbf{S}^* \mathbf{1}_\lambda \rightsquigarrow \begin{array}{c} D_\mathbf{S}^* \\ \backslash \quad / \\ \mathbf{1}_\lambda \end{array} \leftarrow \text{endpoints} \quad , \quad \mathbf{1}_\lambda D_\mathbf{T} \rightsquigarrow \begin{array}{c} \mathbf{1}_\lambda \\ \backslash \quad / \\ D_\mathbf{T} \end{array} \leftarrow \text{endpoints} .$$

The action of these elements on the polynomial module is given by (7D.3). Hence, in the associated graded, $D_\mathbf{T}$ acts on $\mathbf{1}_\mathbf{T} P_n(X)$ by sending $\mathbf{1}_\mathbf{T} f(y_1, \dots, y_n)$ to $\mathbf{1}_\lambda f(y_{w_\mathbf{T}(1)}, \dots, y_{w_\mathbf{T}(n)})$, and $D_\mathbf{S}^*$ acts similarly except that the permutation is $w_\mathbf{S}^{-1}$. Thus, in the associated graded module, the element $D_{\mathbf{S}\mathbf{T}}^{\mathbf{a}, \mathbf{f}}$ from in (6H.2) acts as the endomorphism

$$\mathbf{1}_\mathbf{S} f(y_1, \dots, y_n) \mapsto \mathbf{1}_\mathbf{T} y^{\mathbf{a}} y^{\mathbf{f}} f(y_{w_\mathbf{S}^{-1} w_\mathbf{T}(1)}, \dots, y_{w_\mathbf{S}^{-1} w_\mathbf{T}(n)}).$$

Linear independence follows. \square

Proof of Theorem 6H.4. (a). By the results and definitions above, the only statement that is not immediate is (AC₃). In (AC₃) it is sufficient to let x be a crossing or a dot since, up to isotopy, these generate $\mathcal{W}_n^\rho(X)$. The x will be on top of the diagram $D_{\mathbf{S}\mathbf{T}}^{\mathbf{a}, \mathbf{f}}$.

If x is a crossing, then (AC₃) is immediate from Proposition 7C.7 and Lemma 7D.9(b).

Now suppose that x is a dot. This follows almost immediately from Lemma 7D.9(a) with the caveat that we first need to pull the dot x to the equator. Let $i, j, k \in I$ with $i \neq j$, and recall from Section 3D that we have

$$\begin{array}{c} \text{error term} \\ \text{---} \end{array} = \begin{array}{c} \text{---} \\ \text{---} \end{array} + \underbrace{\begin{array}{c} | & | \\ i & i \end{array}}_{\text{error term}} , \quad \begin{array}{c} \text{---} \\ \text{---} \end{array} = \begin{array}{c} \text{---} \\ \text{---} \end{array} , \quad \begin{array}{c} \text{---} \\ \text{---} \end{array} = \begin{array}{c} \text{---} \\ \text{---} \end{array} , \quad \begin{array}{c} \text{---} \\ \text{---} \end{array} = \begin{array}{c} \text{---} \\ \text{---} \end{array} ,$$

and all the partner relations. In other words, we can slide dots freely to the equator up to additional error terms for (i, i) -crossings. Let us first ignore these error terms, and first consider the case when x reaches the equator, and say it does so on the k th solid string. If k is in the unsteady part of the diagram, or if k is in the steady part of the diagram and number of dots on the equator with x is strictly smaller than $c_k(\lambda)$, then we just park the dot where it is to obtain another basis element. In all other cases Lemma 7D.9(a) applies, giving (AC₃). Finally, for the error terms we use Lemma 3G.5 to pull strings to the right, again showing that (AC₃) holds.

(b). By Proposition 7C.2, a diagram in (6H.2) is steady if and only if is in (6H.3). Hence, the sandwich cellularity result for $\mathcal{R}_n^\rho(X)$ follows immediately from Theorem 6H.4.(a), the corresponding result for the algebra $\mathcal{W}_n^\rho(X)$. \square

8. SOME CONSEQUENCES OF SANDWICH CELLULARITY

This section proves results for $\mathcal{W}_n^\rho(X)$ and $\mathcal{R}_n^\rho(X)$ that follow from Theorem 6H.4. Some results are restricted to level one. We remind the reader that we are using the labeling of the Dynkin diagrams given in Section 5A.

8A. **Maximal number of strings.** We now focus on $\mathcal{R}_n^\rho(X)$. We start by observing that $\mathcal{R}_n^\rho(X)$ is zero for most n .

Definition 8A.1. Attach the following numbers $n(i)$, for $i \in I$ to the fundamental weights in finite types:

Type	$n(i)$ for $i \in I$
A_e	$i(e - i + 1)$
$B_{e>1}$	$(e + i)(e - i + 1)$ for $i \neq e$, $\frac{e(e+1)}{2}$ otherwise
$C_{e>2}$	$(e + i - 1)(e - i + 1)$
$D_{e>3}$	$2ie - i(i + 1)$ for $i \notin \{e - 1, e\}$, $\frac{e(e-1)}{2}$ otherwise
E_6	$16, 30, 42, 22, 30, 16$
E_7	$34, 66, 96, 51, 75, 52, 27$
E_8	$92, 182, 270, 136, 220, 168, 114, 58$
F_4	$22, 42, 30, 16$
G_2	$10, 6$

where we list $n(i)$ starting from $i = 1$ for the exceptional types.

Proposition 8A.2. Let $\Lambda = (\Lambda_{\rho_1}, \dots, \Lambda_{\rho_\ell})$. Then $\mathcal{R}_n^\rho(X) \not\cong 0$ if and only if $1 \leq n \leq n(\rho_1) + \dots + n(\rho_\ell)$.

Proof. The numbers in [Definition 8A.1](#) appear as

$$\Lambda_i = \sum_{j=1}^e m_{ij} \cdot \alpha_j, \quad n(i) = 2 \sum_{j=1}^e m_{ij},$$

see e.g. [\[Bou02, Plates I–IX\]](#), with the slight caveat that the numbers for some types need to be permuted because of our differences in labeling in [Section 5A](#). Since Λ_i and $-\Lambda_i$ correspond to the highest and lowest weight vectors in the representation for $\mathcal{G}(\Lambda_i)$, it follows that the paths in $\mathcal{G}(\Lambda_i)$ have length at most $n(i) - 1$. Therefore, $\mathcal{R}_n^\rho(X) \cong 0$ by [Theorem 6H.4](#) if and only if $n > n(\rho_1) + \dots + n(\rho_\ell)$ or $n < 1$. \square

In particular, [Proposition 8A.2](#) implies that for each fixed rank e there are only finitely many n such that $\mathcal{R}_n^\rho(X)$ is nonzero.

Example 8A.3. Let $\ell = 1$ and assume that the rank of Γ is strictly less than nine. Then the maximal number of solid strings in a nonzero diagram is 270, which happens in type E_8 . \diamond

8B. Classification of simples.

Remark 8B.1. By comparing [Theorem 6H.4](#) and [Corollary 6H.5](#), all the results below have obvious analogs for \mathcal{W}_n^ρ and \mathcal{R}_n^ρ . We omit details for the sake of brevity.

Let $\lambda \in V_n^\Lambda$ and let $a(\lambda)$ be the number of unsteady strings in $\mathbf{1}_\lambda$. Equivalently, $a(\lambda)$ is the number of strings in $\mathbf{1}_\lambda$, or the number of positions in $A^y(\lambda)$, that can carry arbitrarily many dots. In the following result, simple modules are counted up to homogeneous isomorphism.

Proposition 8B.2. Let R be a field.

- (a) The set of apexes of $\mathcal{W}_n^\rho(X)$ and $\mathcal{R}_n^\rho(X)$ are in 1:1-correspondence with V_n^Λ and V_n^Λ , respectively. In other words, $\mathcal{P}^{\neq 0} = \mathcal{P}$ in the notation of [Theorem 2B.1\(b\)](#).
- (b) There is a 1:1-correspondence between simple $\mathcal{W}_n^\rho(X)$ -modules with apex $\lambda \in V_n^\Lambda$ and $\bigoplus_{\sigma \in \lambda} R^{a(\sigma)}$. For every $\lambda \in V_n^\Lambda$, there are $\#\lambda$ isomorphism classes of simple $\mathcal{R}_n^\rho(X)$ -modules with apex λ .
- (c) There is exactly one graded simple $\mathcal{W}_n^\rho(X)$, and one graded simple $\mathcal{R}_n^\rho(X)$ -module, for each vertex in V_n^Λ , or V_n^Λ , respectively.

Proof. (a). Suppose that a simple $\mathcal{W}_n^\rho(X)$ -module has apex $\lambda \in V_n^\Lambda$. Then $\mathcal{H}_\lambda = \bigoplus_{\sigma \in \lambda} \mathcal{H}_{\mathbf{p}_\sigma}$ is a direct sum of polynomial rings. Hence, by [Theorem 2B.1\(b\)](#), the number of simple \mathcal{H}_λ -modules is equal $\#\lambda$, which is the size of the equivalence class of λ . Hence, it is enough to show that if $\sigma \in V_n^\Lambda$ then there is a simple $\mathcal{W}_n^\rho(X)$ -module with apex σ . Similarly, we need to show that if $\sigma \in V_n^\Lambda$ then there is a simple $\mathcal{R}_n^\rho(X)$ -module with apex σ .

Assume first that we are not in type G_2 and fix $\sigma \in V_n^\Lambda$ or $\sigma \in V_n^\Lambda$. If there are no repeated residues, then $\mathbf{1}_\sigma^y = \mathbf{1}_\sigma$ is the idempotent associated with σ . In the case of repeated residues, first recall that σ has at most two consecutive residues by [Corollary 7C.4](#), and secondly note that the relation

$$\left(\begin{smallmatrix} \times & \times \\ i & i \end{smallmatrix} \right)^2 = - \begin{smallmatrix} \times & \times \\ i & i \end{smallmatrix}$$

and its partner relation follow from the dot sliding relation (3D.6). Thus, the crossing with a dot is a pseudo idempotent. By [Definition 6G.9](#) we always flank $\mathbf{1}_\sigma^y$ with crossings for repeated residues. Since all $\sigma \in V_n^\Lambda$ and all $\sigma \in V_n^{\dot{\Lambda}}$ have an associated idempotent by the above discussion, the statement is a direct consequence of the basis theorems [Theorem 6H.4](#) and [Corollary 6H.5](#), combined with the classification of simple modules in sandwich cellular algebras from [Theorem 2B.1\(b\)](#) and [\[TV23, Theorem 2.16\]](#).

In type G_2 we can use essentially the same argument, with the only difference being that three repeated residues are possible by [Corollary 7C.4](#). To deal with these one checks that



is a pseudo idempotent, after which the rest of the argument works verbatim.

(b)+(c). By [Theorem 6H.4](#) and [Corollary 6H.5](#), the sandwiched algebras are

$$\begin{aligned}\mathcal{H}_\lambda &\cong \bigoplus_{\sigma \in \lambda} R[X_1, \dots, X_{a(\sigma)}] \otimes R[Y_1, \dots, Y_{f(\sigma)}]/(Y_1^{z_1}, \dots, Y_{f(\sigma)}^{z_{f(\sigma)}}), \\ \mathcal{F}_\lambda &\cong \bigoplus_{\sigma \in \lambda} R[Y_1, \dots, Y_{f(\sigma)}]/(Y_1^{z_1}, \dots, Y_{f(\sigma)}^{z_{f(\sigma)}}),\end{aligned}$$

where the exponents z_i are either two or three, depending on the type. Here, $f(\lambda)$ is the number of dots on the steady strings, or the possible nonzero positions in $F^y(\lambda)$. Thus, both claims follow from [Theorem 2B.1\(b\)](#). \square

For the next statement, recall the notions of *quasi-hereditary* from [\[CPS88\]](#) and *affine quasi-hereditary* as in [\[Kle15\]](#).

Proposition 8B.3. *Let R be a field and suppose that $V_n^\Lambda = \dot{V}_n^\Lambda$. The algebras $\mathcal{W}_n^\rho(X)$ and $\mathcal{R}_n^\rho(X)$ are affine quasi hereditary algebras. If Γ is of type A_e , then $\mathcal{R}_n^\rho(X)$ is quasi-hereditary.*

Proof. That $\mathcal{W}_n^\rho(X)$ is affine quasi hereditary follows by combining [Theorem 6H.4](#) and [Proposition 8B.2](#), and similarly for $\mathcal{R}_n^\rho(X)$. For the second claim, the assumption that Γ is of type A_e implies that the sandwiched algebras are isomorphic to R , see the proof of [Proposition 8B.2](#) and combine this with [Corollary 7C.4](#). Thus, $\mathcal{R}_n^\rho(X)$ is actually an honest cellular algebra. Hence, the result follows by [Corollary 6H.5](#), [Proposition 8B.2](#) and [\[KX99b, Lemma 2.1\]](#). \square

Remark 8B.4. Maintain the assumptions of [Proposition 8B.3](#).

- (a) Since the sandwiched algebras are often nontrivial, the algebra $\mathcal{R}_n^\rho(X)$ is in general not quasi-hereditary.
- (b) By [Proposition 8B.3](#), $\mathcal{W}_n^\rho(X)$ is affine quasi-hereditary. This generalizes [\[KL15, Main theorem\]](#), which proves that the infinite dimensional KLR algebras of finite type are affine quasi-hereditary algebras.
- (c) In affine type A , [\[Web17b, Corollary 2.26\]](#) and [\[Bow22, Corollary 6.24\]](#) prove that $\mathcal{R}_n^\rho(X)$ is quasi-hereditary. Using a similar argument to that above, [\[MT24, Corollary 5C.2\]](#) gives another proof that $\mathcal{R}_n^\rho(X)$ is quasi-hereditary in this case.

Proposition 8B.5. *Let R be a field. Then $\mathcal{R}_n^\rho(X)$ and \mathcal{R}_n^ρ are graded Morita equivalent.*

Proof. By [\[LV11, Theorem 7.5\]](#) the simple \mathcal{R}_n^ρ -modules are indexed by the crystal graph $\mathcal{G}(\Lambda)$. Therefore, by [Proposition 8B.2](#), the isomorphism of [Proposition 7B.1](#) gives a truncation functor that maps simple modules to simple modules, which makes it an equivalence. \square

8C. Semisimplicity. We will now show that $\mathcal{R}_n^\rho(X)$ is rarely semisimple outside of A_e .

Definition 8C.1. A crystal graph $\mathcal{G}(\Lambda_i)$ is *entirely semisimple* if Λ_i is in the following list:

Type	Λ_i
A_e	$\Lambda_i, i \in \{1, \dots, e\}$
$B_{e>1}$	Λ_1, Λ_e
$C_{e>2}$	Λ_e
$D_{e>3}$	$\Lambda_1, \Lambda_{e-1}, \Lambda_e$
E_6	Λ_1, Λ_6
E_7	Λ_7
E_8	None
F_4	None
G_2	None

With the exception of Λ_e in type $B_{e>1}$, the entirely semisimple crystal graphs are the crystal graphs for minuscule weights (Λ_1 is not minuscule in type $B_{e>1}$).

Proposition 8C.2. *Let R be a field.*

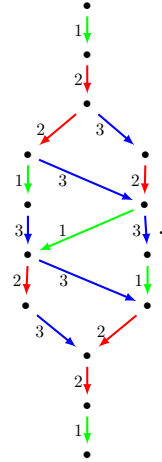
- (a) *Let $\ell = 1$ (so that we have a level one crystal graph $\mathcal{G}(\Lambda_i)$). The algebra $\mathcal{R}_n^{\rho}(X)$ is semisimple for all $n \geq 0$ if and only if $\mathcal{G}(\Lambda_i)$ is an entirely semisimple crystal graph.*
- (b) *In general, the algebra $\mathcal{R}_n^{\rho}(X)$ is semisimple for all $n \geq 0$ if and only if the components of Λ are pairwise distinct entirely semisimple crystal graphs.*

Proof. We will use [Theorem 2B.1.\(c\)](#) silently below.

(a). By the proof of [Proposition 8B.2](#) and [Proposition 8B.3](#) it follows that $\mathcal{R}_n^{\rho}(X)$ is semisimple if and only if the all sandwich algebras are trivial and the paths in $\mathcal{G}(\Lambda_i)$ of length n are in different blocks, in the sense of [Definition 5D.5](#). For the duration of this proof, we call the first condition the sandwich property and the second one the block property.

Suppose that $\mathcal{G}(\Lambda_i)$ is entirely semisimple. In [Definition 6G.4](#) we fixed a choice of paths, say $\mathbf{p}_1, \dots, \mathbf{p}_k$, for the vertices of $\mathcal{G}(\Lambda_i)$. For entirely semisimple crystal graphs, the paths $\text{res}(\mathbf{p}_1), \dots, \text{res}(\mathbf{p}_k)$ are never related by face permutations by the explicit tableau realization of these crystal graphs outlined in the proof of [Proposition 5C.4](#) and described in detail, for example, in [\[BS17, Section 5.4\]](#). For A_e this is immediate from [Proposition 5C.4.\(a\)](#), which says that the crystal graph $\mathcal{G}(\Lambda_i)$ only contains nonadjacent squares, whereas for types $B_{e>1}$, $C_{c>2}$ and $D_{e>3}$ only one box tableaux appear in the entirely semisimple crystal graphs, so they also contain only nonadjacent squares. The type E_6 and E_7 crystal graphs can be inspected, for example using SageMath [\[Sag23\]](#) or [\[BS17, Section 5.6\]](#). Hence, the block property holds for all entirely semisimple crystal graphs. Moreover, it also follows from these descriptions of the entirely semisimple crystal graphs, and our construction of the bases of $\mathcal{R}_n^{\rho}(X)$ in [Section 6H](#), that the sandwiched algebras are trivial in these cases. Therefore, if $\mathcal{G}(\Lambda_i)$ is semisimple, then $\mathcal{R}_n^{\rho}(X)$ is semisimple for $n \geq 0$.

Conversely, suppose that $\mathcal{G}(\Lambda_i)$ is not entirely semisimple. In classical types, except for Λ_1 in C_3 , the tableau model for the crystals shows that $\mathcal{G}(\Lambda_i)$ contains a $ijji = jiji$ octagon, so the block property fails since we have a partial face permutation to different vertices in the octagon. In types F_4 and the E_k the block property fails by observation (we used SageMath [\[Sag23\]](#)). For type G_2 we can use [\(5C.6\)](#): in $\mathcal{G}(\Lambda_1)$ the block property fails while in $\mathcal{G}(\Lambda_2)$ the sandwich property does not hold. The remaining case is Λ_1 for type C_3 , which has the crystal graph:



The result follows because the consecutive 2-strings have a sandwich dot. Hence, if $\mathcal{G}(\Lambda_i)$ is not entirely semisimple, then $\mathcal{R}_n^{\rho}(X)$ is not semisimple for some n .

(b). If the components of Λ are pairwise distinct, entirely semisimple crystal graphs, then the argument of part (a) proves that $\mathcal{R}_n^{\rho}(X)$ is semisimple for all n . Conversely, again by (a), having a component of Λ that is not entirely semisimple implies that $\mathcal{R}_n^{\rho}(X)$ is not semisimple. Having repeated components also implies that $\mathcal{R}_n^{\rho}(X)$ is not semisimple since the block property fails. \square

Except in the case of Λ_1 for type C_3 and in type G_2 , the proof of [Proposition 8C.2](#) shows that $\mathcal{R}_n^{\rho}(X)$ is semisimple for all n if and only if $\mathcal{G}(\Lambda_i)$ does not contain an octagon.

For the next statement we need the following lower and upper bound formulas.

Definition 8C.3. We define $l(i)$, for $i \in I$ as follows:

Type	$l(i)$ for $i \in I$
A_e	∞
$B_{e>1}$	∞ for $i \in \{1, e\}$ and $2e - 2i + 3$ otherwise
$C_{e>2}$	8 for $i = 1$, $2i$ for $i \in \{2, \dots, e-1\}$, and ∞ if $i = e$
$D_{e>3}$	∞ for $i \in \{1, e, e-1\}$ and $2e - 2i + 1$ otherwise
E_6	$\infty, 7, 5, 11, 7, \infty$
E_7	$17, 7, 5, 11, 7, 9, \infty$
E_8	$17, 7, 5, 11, 7, 9, 11, 29$
F_4	$11, 5, 4, 8$
G_2	7, 5

where we list $l(i)$ starting from $i = 1$ for the exceptional types. We also set $u(i) = n(i) - l(i)$, where $n(i)$ is as in [Definition 8A.1](#).

By convention, $\{l(i), l(i) + 1, \dots, u(i)\}$ is empty if $l(i) > u(i)$. This happens only if $i = 3$ in type C_3 , or $i = 2$ in type G_2 . If $l(i) = \infty$, then the crystal graph $\mathcal{G}(\Lambda_i)$ is entirely semisimple.

The following statement is in level one.

Proposition 8C.4. *Let R be a field and $\ell = 1$. Let $\mathcal{G}(\Lambda_i)$ be a crystal graph that is not entirely semisimple and suppose that $n \notin \{l(i), l(i) + 1, \dots, u(i)\}$. Then every block of $\mathcal{R}_n^p(X)$ contains a unique simple module.*

Proof. The simple $\mathcal{R}_n^p(X)$ -modules correspond to the vertices of $\mathcal{G}(\Lambda_i)$ by [Proposition 8B.2](#). We need to show that if $n \notin \{l(i), l(i) + 1, \dots, u(i)\}$, then the vertices $\alpha \in \mathcal{G}(\Lambda_i)$ with $d(\alpha) = n$ belong to distinct permutation classes of residue sequences.

By [Lemma 5B.14](#) and [Proposition 8A.2](#) we only need to prove that the lower bound holds. Moreover, for $i = 1$ the lower bound follows from [Example 5B.4](#), while the case $i = 3$ in type C_3 is easily verified, so we assume that we are not in these cases.

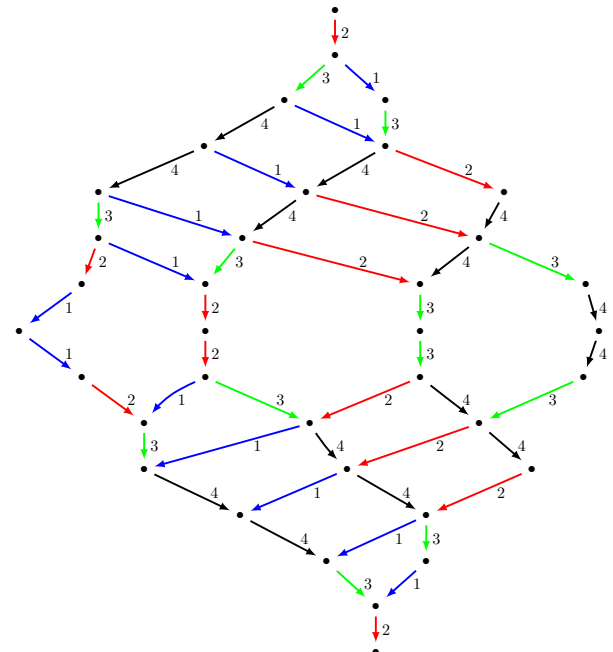
To verify the lower bound in the classical types we will use the Young diagrams combinatorics as in the proof of [Proposition 5C.4](#). We consider only type $B_{e>1}$, with types $C_{e>2}$ and $D_{e>3}$ being similar. The first situation where it is possible to have two vertices $\lambda, \mu \in \mathcal{G}(\Lambda_i)$ with $\lambda \neq \mu$ that have two paths \mathbf{p} and \mathbf{q} whose residue sequences are permutations of one another is when the last two nodes in the column tableau of shape (1^i) are:

$$i \neq 1, e: \lambda \rightsquigarrow \begin{array}{c} i \\ \hline \bar{i} \end{array} \text{ and } \mu \rightsquigarrow \begin{array}{c} i+1 \\ \hline \bar{i+1} \end{array}.$$

Counting, using the tableau crystal graphs described in [\(5C.5\)](#), shows that this happens at precisely $l(i) = 2e - 2i + 3$ steps, for each $i \in I$. The other classical cases are similar and are omitted.

The exceptional types were verified with the code that can be found in [\[MT22\]](#). \square

Example 8C.5. Consider the crystal graph $\mathcal{G}(\Lambda_2)$ in type B_4 :



In this case we have $l(2) = 7 = u(2)$ and indeed, only in the middle of the crystal graph do we find different vertices with residue sequences that are related by face permutations. For example, there is a nontrivial face

permutation between the paths with residue sequences 2344321 and 2344312. As a more complicated example, there is a nontrivial face permutation between the paths with residue sequences 2344321 and 2132434.

Note that the sandwiched algebras are not necessarily trivial because having only one block does not imply that $\mathcal{R}_n^\rho(X)$ is semisimple. Explicitly, if $n = 3$, then every vertex corresponds to a unique block, but the idempotent $\mathbf{1}_{\mathbb{P}_\lambda}$ for the path with residue sequence $\text{res}(\lambda) = 234$ can get a sandwich dot on the solid 4-string:

$$h_\lambda^f = \left\{ \begin{array}{c} \text{Diagram 1} \\ \text{Diagram 2} \\ \text{Diagram 3} \end{array} \right. , \quad \left. \begin{array}{c} \text{Diagram 4} \\ \text{Diagram 5} \\ \text{Diagram 6} \end{array} \right\}.$$

In this case, the sandwiched algebra is isomorphic to $R[Y]/(Y^2)$, so $\mathcal{R}_3^\rho(X)$ is not semisimple. \diamond

Example 8C.6. Using the code from [MT22], Proposition 8C.4 for E_6 was verified using the code:

```
sage: ! ! .join(f"{{CheckForRepeatedPositiveRoots(['E', 6], [i], minlength=True)}}"
....: for i in range(1,7))
+Infinity 11 7 5 7 +Infinity
```

Adjusting for the differences in different labeling conventions between Section 5A and SageMath, this agrees with Definition 8C.3. \diamond

8D. Projective modules in level one. Throughout this and the next section we work only with the cyclotomic quotients $\mathcal{R}_n^\rho(X)$ in level one such that $V_n^\Lambda = \dot{V}_n^\Lambda$.

For $\lambda \in V_n^\Lambda$ set $P_\lambda^\mathcal{R} = \mathcal{R}_n^\rho(X)\mathbf{1}_\lambda$, which is a projective $\mathcal{R}_n^\rho(X)$ -module, and let $\Delta_\lambda^\mathcal{R}$ and $L_\lambda^\mathcal{R}$ be the corresponding cell module and graded simple with apex λ , respectively.

Since $\mathbf{1}_\lambda$ is an idempotent, as graded algebras $\text{End}_{\mathcal{R}_n^\rho}(P_\lambda^\mathcal{R}) \cong \mathbf{1}_\lambda \mathcal{R}_n^\rho \mathbf{1}_\lambda$. Each choice of $S, T \in \text{Face}_{\underline{\Lambda}}(\lambda)$ and $f \in F^y(\lambda)$ defines an endomorphism of these modules, given by $\theta_{ST}^f(\mathbf{1}_\lambda) = D_{ST}^f$.

Proposition 8D.1. *Let R be a field and set $\Lambda = (\Lambda_i)$, for some i . Assume that $V_n^\Lambda = \dot{V}_n^\Lambda$.*

If $\lambda \in V_n^\Lambda$, then $\text{End}_{\mathcal{R}_n^\rho(X)}(P_\lambda^\mathcal{R}) \cong \mathbf{1}_\lambda \mathcal{R}_n^\rho(X) \mathbf{1}_\lambda$, which has an R -basis given by $\{D_{ST}^f \mid S, T \in \text{Face}_{\underline{\Lambda}}(\lambda), f \in F^y(\lambda)\}$. Moreover, $P_\lambda^\mathcal{R}$ is the projective cover of $L_\lambda^\mathcal{R}$.

Proof. First note that $P_\lambda^\mathcal{R} \supset \mathcal{R}_n^\rho \mathbf{1}_\lambda^y$ by (7C.6). The endomorphism algebra of $P_\lambda^\mathcal{R}$ is, by construction, given by all steady diagrams with bottom and top $\mathbf{1}_\lambda$. Hence, $\text{End}_{\mathcal{R}_n^\rho}(P_\lambda^\mathcal{R}) \cong \mathbf{1}_\lambda \mathcal{R}_n^\rho \mathbf{1}_\lambda$. Recall that we have classified all possible steady permutations as face permutations in Proposition 7C.7. In particular, the detour permutations to λ and partial face permutations belong to the endomorphism algebra of $P_\lambda^\mathcal{R}$. Moreover, the sandwiched algebras are contained in the endomorphism algebra by construction. By Theorem 6H.4, P_λ has no other endomorphisms, so $\text{End}_{\mathcal{R}_n^\rho}(P_\lambda^\mathcal{R})$ is generated as an R -module by the detour and face permutations, and the sandwich dots, as in the statement of the proposition.

As we are in level one, we can assume that all of the strings in the diagrams are to the left of the red strings by Lemma 7B.3, so all detour permutations in $\text{End}_{\mathcal{R}_n^\rho}(P_\lambda^\mathcal{R})$ are invertible, modulo more dominant terms by Proposition 7B.6. Hence, the endomorphism algebra of $P_\lambda^\mathcal{R}$ is a local ring by the explicit description of its basis given by Proposition 7C.7. Therefore, the projective module $P_\lambda^\mathcal{R} = \mathcal{R}_n^\rho(X)\mathbf{1}_\lambda$ is indecomposable. Hence, $P_\lambda^\mathcal{R}$ is the projective cover of $L_\lambda^\mathcal{R}$ by Theorem 6H.4 and Proposition 8B.2. \square

Corollary 8D.2. *Suppose that R is a field, Γ is a quiver of type A_e , $\Lambda = (\Lambda_i)$ and $V_n^\Lambda = \dot{V}_n^\Lambda$. Let $\lambda \in V_n^\Lambda$. Then $\text{End}_{\mathcal{R}_n^\rho(X)}(P_\lambda^\mathcal{R})$ is concentrated in degree 0.*

Proof. This follows from Definition 6G.9 because all diagrammatic face permutations are compositions of (partial) face permutations around nonadjacent squares by Proposition 5C.4, since Γ is of type A_e . The associated permutation diagrams are thus of degree 0. Hence, $\text{End}_{\mathcal{R}_n^\rho(X)}(P_\lambda)$ is in degree 0. \square

Recall from Section 4B that v is our grading parameter. Let $[\Delta_\lambda^\mathcal{R} : L_\mu^\mathcal{R}]_v$ be the *graded decomposition multiplicity* of $L_\mu^\mathcal{R}$ in $\Delta_\lambda^\mathcal{R}$.

Corollary 8D.3. *Suppose that R is a field, $V_n^\Lambda = \dot{V}_n^\Lambda$, $\Lambda = (\Lambda_i)$ and let $\lambda, \mu \in V_n^\Lambda$. Then*

$$[\Delta_\lambda^\mathcal{R} : L_\mu^\mathcal{R}]_v = \text{rk}_R^v(\mathbf{1}_\mu \Delta_\lambda^\mathcal{R}) = \sum_{T \in \text{Face}_{\underline{\Lambda}}(\mathbb{P}_\lambda, \mathbb{P}_\mu)} v^{\deg D_T}.$$

In particular, $[\Delta_\lambda^\mathcal{R} : L_\mu^\mathcal{R}]_v$ is independent of the characteristic of R .

Proof. By Proposition 8D.1, $P_\mu^\mathcal{R} = \mathcal{R}_n^\rho(X)\mathbf{1}_\mu$ is the projective cover of $L_\mu^\mathcal{R}$. Since $\mathbf{1}_\mu$ is an idempotent,

$$[\Delta_\lambda^\mathcal{R} : L_\mu^\mathcal{R}]_v = \text{rk}_v \text{Hom}_{\mathcal{R}_n^\rho(X)}(P_\mu^\mathcal{R}, \Delta_\lambda^\mathcal{R}) = \text{rk}_v \mathbf{1}_\mu \Delta_\lambda^\mathcal{R}.$$

Hence, the result follows from Theorem 6I.1. \square

Recall from Section 7B that $L(\Lambda) \cong [\text{Proj } \mathcal{R}_{\oplus}^{\rho}]$ as $U_v(\mathfrak{g})$ -modules, where $[\text{Proj } \mathcal{R}_{\oplus}^{\rho}] = \bigoplus_{n \geq 0} [\text{Proj } \mathcal{R}_n^{\rho}]$. Hence, by Proposition 8B.5, $L(\Lambda) \cong [\text{Proj } \mathcal{R}_{\oplus}^{\rho}]$ as $U_v(\mathfrak{g})$ -modules. Henceforth, we identify these two modules. Note that $[\text{Rep } \mathcal{R}_{\oplus}^{\rho}]$ and $[\text{Proj } \mathcal{R}_{\oplus}^{\rho}]$ are finite dimensional $\mathbb{Q}(v)$ -modules since $\mathcal{R}_n^{\rho}(X) = 0$ for $n \gg 0$ by Proposition 8A.2.

Let $[\text{Rep } \mathcal{R}_{\oplus}^{\rho}] = \bigoplus_{n \geq 0} [\text{Rep } \mathcal{R}_n^{\rho}(X)]$. There is a natural inclusion $[\text{Proj } \mathcal{R}_{\oplus}^{\rho}] \hookrightarrow [\text{Rep } \mathcal{R}_{\oplus}^{\rho}]$, so we can consider $L(\Lambda)$ as a submodule of $[\text{Rep } \mathcal{R}_{\oplus}^{\rho}]$. If M is a $\mathcal{R}_n^{\rho}(X)$ -module, then let $[M]$ be its image in $[\text{Rep } \mathcal{R}_{\oplus}^{\rho}]$.

Lemma 8D.4. *The Grothendieck group $[\text{Rep } \mathcal{R}_{\oplus}^{\rho}]$ has basis $\{[\Delta_{\lambda}^{\mathcal{R}}] \mid \lambda \in \dot{V}_n^{\Lambda}\}$.*

Proof. The simple $\mathcal{R}_n^{\rho}(X)$ -modules, for $n \geq 0$, give a basis of $[\text{Rep } \mathcal{R}_{\oplus}^{\rho}]$ and the graded decomposition matrices of these algebras are unitriangular by Corollary 8D.3. \square

Let \mathcal{L}_{Λ} be the $\mathbb{Z}[v]$ -lattice of $[\text{Rep } \mathcal{R}_{\oplus}^{\rho}]$ spanned by $\{[\Delta_{\lambda}^{\mathcal{R}}] \mid \lambda \in V_n^{\Lambda}\}$ and let $\mathcal{B}_{\Lambda} = \{[P_{\lambda}^{\mathcal{R}}] + v\mathcal{L}_{\Lambda} \mid \lambda \in V_n^{\Lambda}\}$. Then $[\text{Rep } \mathcal{R}_{\oplus}^{\rho}] \cong \mathbb{Q}(v) \otimes_{\mathbb{Z}[v]} \mathcal{L}_{\Lambda}$ and \mathcal{B}_{Λ} is a \mathbb{Q} -basis of $\mathcal{L}_{\Lambda}/v\mathcal{L}_{\Lambda}$ by Lemma 8D.4. We will show that $(\mathcal{L}_{\Lambda}, \mathcal{B}_{\Lambda})$ is a 0-crystal base of $L(\Lambda)$ in the sense of [Kas91]. Unlike [Kas91], we work with lattices over $\mathbb{Z}[v]$. However, by base change, we obtain lattices over the ring of rational functions in $\mathbb{Q}(v)$, which gives the setting used by Kashiwara.

For $i \in I$ let F_i^{Λ} be the i -induction functor, which is given by adding an i -string to the left of a diagram.

Theorem 8D.5. *Suppose that R is a field, $\Lambda = (\Lambda_i)$, $V_n^{\Lambda} = \dot{V}_n^{\Lambda}$, and that Γ is not of type F_4 . Let $\lambda, \mu \in V_n^{\Lambda}$. Then*

$$[\Delta_{\lambda}^{\mathcal{R}} : L_{\mu}^{\mathcal{R}}]_v \in \delta_{\lambda\mu} + v\mathbb{Z}_{\geq 0}[v].$$

Consequently, under categorification P_{λ} corresponds to a canonical basis element in $L(\Lambda)$.

Proof. If $\lambda = \mu$, then $[\Delta_{\lambda}^{\mathcal{R}} : L_{\mu}^{\mathcal{R}}]_v = 1$ by Corollary 8D.3, so there is nothing to prove. If $\lambda \neq \mu$ and $D_T \in \text{Face}_{\Lambda}(\mathbf{p}_{\lambda}, \mathbf{p}_{\mu})$, then D_T is a product of basic face permutations around adjacent squares and octagons together with at least one partial face permutation around an octagon. This follows from Proposition 5C.4 and our assumption that Γ is not of type F_4 . As all of the basic diagrammatic face permutations have nonnegative degree, and the partial diagrammatic face permutations have positive degree, it follows that $[\Delta_{\lambda}^{\mathcal{R}} : L_{\mu}^{\mathcal{R}}]_v \in \delta_{\lambda\mu} + v\mathbb{Z}_{\geq 0}[v]$.

It remains to prove that $P_{\lambda}^{\mathcal{R}}$ corresponds to the canonical basis under Kang–Kashiwara’s [KK12] categorification of the highest weight module $L(\Lambda)$. By Proposition 7B.4 and Corollary 6H.5, if $\nu \in V_{n-1}^{\Lambda}$ and $i \in I$, then

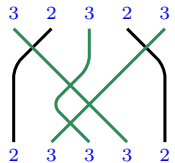
$$F_i^{\Lambda}[P_{\nu}^{\mathcal{R}}] = \begin{cases} [P_{\lambda}^{\mathcal{R}}] & \text{if } \nu \xrightarrow{i} \lambda \text{ is a path in } \mathcal{G}(\Lambda), \\ 0 & \text{if } \text{res}(\mathbf{p}_{\nu})i \text{ is not a path in } \mathcal{G}(\Lambda). \end{cases}$$

It follows from the usual yoga that $P_{\lambda}^{\mathcal{R}}$ has a filtration with subquotients $\Delta_{\mu}^{\mathcal{R}} \otimes \mathcal{H}_{\mu}$ appearing with multiplicity $[\Delta_{\mu}^{\mathcal{R}} : L_{\lambda}^{\mathcal{R}}]_v$ for $\mu \in V_n^{\Lambda}$. Therefore, using the positivity property $[\Delta_{\lambda}^{\mathcal{R}} : L_{\mu}^{\mathcal{R}}]_v \in \delta_{\lambda\mu} + v\mathbb{Z}_{\geq 0}[v]$ from the first paragraph, and working modulo $v\mathcal{L}_{\Lambda}$,

$$F_i^{\Lambda}[P_{\nu}^{\mathcal{R}}] \equiv \begin{cases} [\Delta_{\lambda}^{\mathcal{R}}] & \text{if } \nu \xrightarrow{i} \lambda \text{ is a path in } \mathcal{G}(\Lambda), \\ 0 & \text{otherwise.} \end{cases}$$

Therefore, $(\mathcal{L}_{\Lambda}, \mathcal{B}_{\Lambda})$ is a 0-crystal base for $L(\Lambda)$ in the sense of Kashiwara [Kas91, Definition 2.3.1]. By [Kas93, Theorem 1], this crystal base uniquely determines the lower global basis $\{G_{\lambda} \mid \lambda \in V_n^{\Lambda}, n \geq 0\}$, or canonical basis, of $L(\Lambda)$ as the unique bar invariant basis of $L(\Lambda)$ such that $G_{\lambda} \equiv \Delta_{\lambda}^{\mathcal{R}} \pmod{v\mathcal{L}_{\Lambda}}$, for $\lambda \in V_n^{\Lambda}$. Hence, $\{[P_{\lambda}^{\mathcal{R}}] \mid \lambda \in V_n^{\Lambda}, n \geq 0\}$ is the canonical basis of $[\text{Rep } \mathcal{R}_{\oplus}^{\rho}]$, as claimed. \square

Example 8D.6. The argument in the proof of Theorem 8D.5 does not work for type F_4 . To see this take the basic face permutation given by



This diagram is of degree -2 . If the idempotent diagram is to the north of this diagram, then Definition 6E.1 does not add extra dots, so the degree is negative. \diamond

Remark 8D.7. The results in this section, and the next, follow from the fact that detour permutations in level one are invertible. This may still be true in level two, but this is difficult to check (compare Example 7C.8). In general, even in type A_e , detour permutations are not invertible because this would imply that the decomposition matrices of $\mathcal{R}_n^{\rho}(X)$ are independent of the characters, contradicting [Wil14] (see also [Mat15, Example 3.7.10]).

Remark 8D.8. Example 8D.6 can be extended to show that the proof Theorem 8D.5 only works in simply laced types for the more general wKLRW algebras that have red strings labeled by arbitrary dominant weights. More, precisely, according to [Ste07], the analog Proposition 5C.4 for nonfundamental dominant weights has decagons appearing in types $B_{e>1}$, $C_{e>2}$ and G_2 , so the argument in the first paragraph of Theorem 8D.5 does not work for these types. This is consistent with [VV11, Theorem 4.4] and [Web15, Paragraph after Corollary B].

Tsuchioka [Tsu10] shows that the structure constants of the canonical bases can have negative coefficients in nonsimply laced types, which implies that the projective indecomposable modules for the infinite KLR algebras cannot coincide with the Lusztig–Kashiwara canonical basis in general. This does not contradict Theorem 8D.5 because we are looking only at projective modules for wKLRW algebras attached to fundamental weights.

Example 8D.9. Let Γ be a quiver of type G_2 . Set $\Lambda = (\Lambda_1, \Lambda_1, \Lambda_2)$ and consider the tensor crystal $\mathcal{G}_\otimes(\Lambda)$. Given a path \mathbf{p} in the crystal graph $\mathcal{G}_\otimes(\Lambda)$, let $G(\mathbf{p})$ be the corresponding canonical basis element. Tsuchioka [Tsu10] computes that

$$\begin{aligned} F_2 G(121112211) &= G(1211122211) + [2]_v \cdot G(1111222211) + G(2111112221) + [2]_v \cdot G(1211112221) \\ &\quad + G(1111122221) \quad \text{---} \quad G(1112211122) + [2]_v \cdot G(1122111122) \end{aligned}$$

Then $\mathcal{G}_\otimes(\Lambda)$ has a path \mathbf{p} with residue sequence 121112211 but it does not have a path with residue sequence 1112211122. Hence, the wKLRW algebras $\mathcal{R}_n^\rho(X)$ are not able to detect this negative multiplicity. \diamond

8E. Simple modules in level one. We are still in level one. For the next proposition recall from Proposition 8B.2 that $\mathcal{R}_n^\rho(X)$ has simple modules L_λ^ρ indexed by $\lambda \in V_n^\Lambda$.

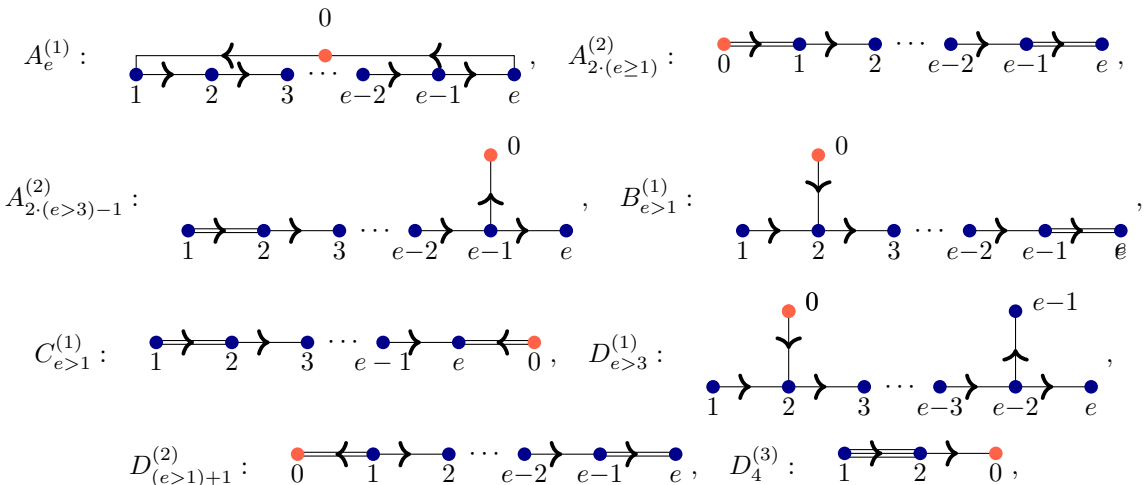
Proposition 8E.1. *Let R be a field and suppose that $\Lambda = (\Lambda_i)$ and $V_n^\Lambda = \dot{V}_n^\Lambda$. Then $\text{rk}_R^v L_\lambda^\rho$ is equal to the number of detour permutations in $\text{Face}_\Lambda(\lambda)$.*

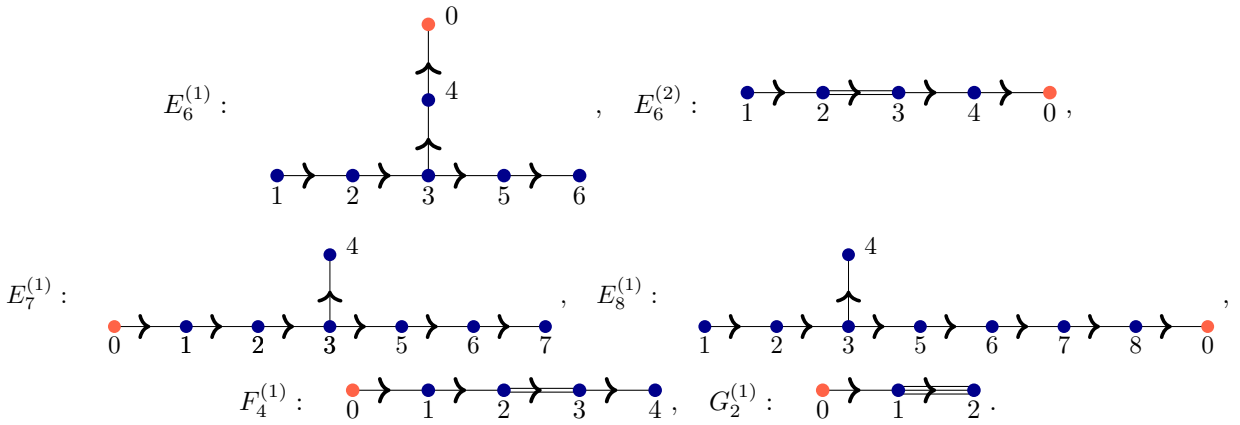
Proof. As noted already in the proof of Proposition 8D.1, the action of every a detour permutation $\mathbf{T} \in \text{Face}_\Lambda(\lambda)$ on Δ_λ^ρ is invertible by Lemma 7B.3 and Proposition 7B.6, so its image in L_λ^ρ is nonzero. Conversely, any face permutation $\mathbf{T} \in \text{Face}_\Lambda(\mu, \mu)$ for $\mu \neq \lambda$ is in the image of a map from $P_\mu^\rho \rightarrow \Delta_\lambda^\rho$, so the image of this permutation in L_λ^ρ is zero. Hence, the detour permutations index a basis of L_λ^ρ . Finally, as in the proof of Theorem 8D.5, the detour permutations have degree zero, so L_λ^ρ is concentrated in degree zero and $\text{rk}_R^v L_\lambda^\rho$ is equal to the number of detour permutations. \square

Example 8E.2. Let Γ be a quiver of type A_e . Then L_λ^ρ is one dimensional for all $\lambda \in V_n^\Lambda$. This follows because the only nontrivial faces of $\mathcal{G}(\Lambda)$ are nonadjacent squares by Proposition 5C.4, which are excluded by Definition 6G.4.(c). By (6D.7), if Γ is a quiver of type C_3 and $\Lambda = \Lambda_1$, then \mathcal{R}_4^ρ is semisimple and it has a two dimensional simple module with residue sequence 1232. \diamond

Example 8E.3. For a quiver of type B_2 and suppose that $\Lambda = \Lambda_2$ as in Example 4B.1. If $0 \leq n \leq 10$, then the simple modules of $\mathcal{R}_n^\rho(X)$ are one dimensional unless $n = 7$ in which case they are two dimensional. \diamond

8F. Sandwich cellularity in affine types. Fix $e \in \mathbb{Z}_{\geq 1}$. The *affine types* are:





The affine node is the red node with label 0. The choices of orientation for the simply laced edges are not needed below, but we expect that these choices give the nicest ghost combinatorics.

Remark 8F.1. As in [Remark 5A.1](#), with a few exceptions our conventions above follow SageMath [\[Sag23\]](#).

The definitions in [Section 3D](#) gives a wKLRW algebra $\mathcal{R}_n^\rho(X)$ for each affine quiver. We start with a slightly disappointing fact:

Proposition 8F.2. *Let R be a field of characteristic $\neq 2$ and suppose that Γ of type $D_{e>3}^{(1)}$, $E_6^{(1)}$, $E_7^{(1)}$ or $E_8^{(1)}$. Then $\mathcal{R}_n^\rho(X)$ is not cellular for some n .*

Proof. According to [\[KM19, Section 5\]](#), the direct summand of the cyclotomic KLR algebras indexed by the null root in these types is Morita equivalent to the so-called zigzag algebra for the graph obtained by removing the affine node. These zigzag algebras are not cellular by [\[ET20, Theorem A\]](#), so the corresponding cyclotomic KLR algebra is not cellular by Morita invariance of cellularity [\[KX99a, Section 5\]](#). The cyclotomic KLR algebra is an idempotent truncation of $\mathcal{R}_n^\rho(X)$ so, because taking idempotent truncations preserves cellularity by [Theorem 2B.1\(a\)](#), the statement follows. \square

Remark 8F.3. We suspect that the restriction to odd characteristic in [Proposition 8F.2](#) is not necessary. We add this condition only because it is required by [\[KX99a, Section 5\]](#). We expect that this condition is not needed because we have weakened the condition on the antiinvolution in (AC₅).

Remark 8F.4. Robert Muth computed the zigzag-type algebras for $B_{e>1}^{(1)}$ and $C_{e>1}^{(1)}$ for the null root, following the ideas of [\[KM19, Section 5\]](#). It appears that these algebras are not cellular in type $B_{e>2}^{(1)}$, but the zigzag algebras are probably cellular in types $B_2^{(1)}$ and $C_{e>1}^{(1)}$. Extending these ideas, Robert Muth's computations imply that finite types B and D are not cellular in general, see also [Example 6G.8](#).

In general, we hope that our methods give a sandwich cellular basis for all types. However, we expect that these bases are only honestly cellular in general in types A and C (affine and finite).

REFERENCES

- [Ari96] S. Ariki. On the decomposition numbers of the Hecke algebra of $G(m, 1, n)$. *J. Math. Kyoto Univ.*, 36(4):789–808, 1996. [doi:10.1215/kjm/1250518452](https://doi.org/10.1215/kjm/1250518452).
- [Bou02] N. Bourbaki. *Lie groups and Lie algebras. Chapters 4–6*. Elements of Mathematics (Berlin). Springer-Verlag, Berlin, 2002. Translated from the 1968 French original by Andrew Pressley. [doi:10.1007/978-3-540-89394-3](https://doi.org/10.1007/978-3-540-89394-3).
- [Bow22] C. Bowman. The many integral graded cellular bases of Hecke algebras of complex reflection groups. *Amer. J. Math.*, 144(2):437–504, 2022. URL: <https://arxiv.org/abs/1702.06579>, [doi:10.1353/ajm.2022.0008](https://doi.org/10.1353/ajm.2022.0008).
- [Bro90] M. Broué. Isométries parfaites, types de blocs, catégories dérivées. *Astérisque*, 181–182(181–182):61–92, 1990.
- [Bro55] W.P. Brown. Generalized matrix algebras. *Canadian J. Math.*, 7:188–190, 1955. [doi:10.4153/CJM-1955-023-2](https://doi.org/10.4153/CJM-1955-023-2).
- [BK09a] J. Brundan and A. Kleshchev. Blocks of cyclotomic Hecke algebras and Khovanov–Lauda algebras. *Invent. Math.*, 178(3):451–484, 2009. URL: <https://arxiv.org/abs/0808.2032>, [doi:10.1007/s00222-009-0204-8](https://doi.org/10.1007/s00222-009-0204-8).
- [BK09b] J. Brundan and A. Kleshchev. Graded decomposition numbers for cyclotomic Hecke algebras. *Adv. Math.*, 222(6):1883–1942, 2009. URL: <https://arxiv.org/abs/0901.4450>, [doi:10.1016/j.aim.2009.06.018](https://doi.org/10.1016/j.aim.2009.06.018).
- [BS17] D. Bump and A. Schilling. *Crystal bases*. World Scientific Publishing Co. Pte. Ltd., Hackensack, NJ, 2017. Representations and combinatorics. [doi:10.1142/9876](https://doi.org/10.1142/9876).
- [CR08] J. Chuang and R. Rouquier. Derived equivalences for symmetric groups and \mathfrak{sl}_2 -categorification. *Ann. of Math.* (2), 167(1):245–298, 2008. URL: <http://dx.doi.org/10.4007/annals.2008.167.245>, [doi:10.4007/annals.2008.167.245](https://doi.org/10.4007/annals.2008.167.245).
- [CPS88] E. Cline, B. Parshall, and L. Scott. Finite-dimensional algebras and highest weight categories. *J. Reine Angew. Math.*, 391:85–99, 1988.
- [ET20] M. Ehrig and D. Tubbenhauer. Algebraic properties of zigzag algebras. *Comm. Algebra*, 48(1):11–36, 2020. URL: <https://arxiv.org/abs/1807.11173>, [doi:10.1080/00927872.2019.1632325](https://doi.org/10.1080/00927872.2019.1632325).
- [ET21] M. Ehrig and D. Tubbenhauer. Relative cellular algebras. *Transform. Groups*, 26(1):229–277, 2021. URL: <https://arxiv.org/abs/1710.02851>, [doi:10.1007/S00031-019-09544-5](https://doi.org/10.1007/S00031-019-09544-5).

- [GG11] F.M. Goodman and J. Graber. Cellularity and the Jones basic construction. *Adv. in Appl. Math.*, 46(1-4):312–362, 2011. URL: <https://arxiv.org/abs/0906.1496>, doi:10.1016/j.aam.2010.10.003.
- [GL96] J.J. Graham and G. Lehrer. Cellular algebras. *Invent. Math.*, 123(1):1–34, 1996. doi:10.1007/BF01232365.
- [HL17] P. Hersh and C. Lenart. From the weak Bruhat order to crystal posets. *Math. Z.*, 286(3-4):1435–1464, 2017. URL: <https://arxiv.org/abs/1510.05636>, doi:10.1007/s00209-016-1808-5.
- [HM10] J. Hu and A. Mathas. Graded cellular bases for the cyclotomic Khovanov–Lauda–Rouquier algebras of type A. *Adv. Math.*, 225(2):598–642, 2010. URL: <https://arxiv.org/abs/0907.2985>, doi:10.1016/j.aim.2010.03.002.
- [HS24] J. Hu and L. Shi. Graded dimensions and monomial bases for the cyclotomic quiver Hecke algebras. *Commun. Contemp. Math.*, 26(8):Paper No. 2350044, 44, 2024. URL: <https://arxiv.org/abs/2108.05508>, doi:10.1142/S021919972350044X.
- [Jan96] J.C. Jantzen. *Lectures on quantum groups*, volume 6 of *Graduate Studies in Mathematics*. American Mathematical Society, Providence, RI, 1996.
- [Kac90] V.G. Kac. *Infinite-dimensional Lie algebras*. Cambridge University Press, Cambridge, third edition, 1990. doi:10.1017/CBO9780511626234.
- [Kas93] M. Kashiwara. Global crystal bases of quantum groups. *Duke Math. J.*, 69(2):455–485, 1993. doi:10.1215/S0012-7094-93-06920-7.
- [Kas91] M. Kashiwara. On crystal bases of the q -analogue of universal enveloping algebras. *Duke Math. J.*, 63(2):465–516, 1991. URL: <http://dx.doi.org/10.1215/S0012-7094-91-06321-0>, doi:10.1215/S0012-7094-91-06321-0.
- [KK12] S.-J. Kang and M. Kashiwara. Categorification of highest weight modules via Khovanov–Lauda–Rouquier algebras. *Invent. Math.*, 190(3):699–742, 2012. URL: <https://arxiv.org/abs/1102.4677>, doi:10.1007/s00222-012-0388-1.
- [KL09] M. Khovanov and A.D. Lauda. A diagrammatic approach to categorification of quantum groups. I. *Represent. Theory*, 13:309–347, 2009. URL: <https://arxiv.org/abs/0803.4121>, doi:10.1090/S1088-4165-09-00346-X.
- [KL11] M. Khovanov and A.D. Lauda. A diagrammatic approach to categorification of quantum groups II. *Trans. Amer. Math. Soc.*, 363(5):2685–2700, 2011. URL: <https://arxiv.org/abs/0804.2080>, doi:10.1090/S0002-9947-2010-05210-9.
- [Kle15] A.S. Kleshchev. Affine highest weight categories and affine quasihereditary algebras. *Proc. Lond. Math. Soc. (3)*, 110(4):841–882, 2015. URL: <https://arxiv.org/abs/1405.3328>, doi:10.1112/plms/pdv004.
- [KL15] A.S. Kleshchev and J.W. Loubert. Affine cellularity of Khovanov–Lauda–Rouquier algebras of finite types. *Int. Math. Res. Not. IMRN*, (14):5659–5709, 2015. URL: <https://arxiv.org/abs/1310.4467>, doi:10.1093/imrn/rnu096.
- [KLM13] A.S. Kleshchev, J.W. Loubert, and V. Miemietz. Affine cellularity of Khovanov–Lauda–Rouquier algebras in type A. *J. Lond. Math. Soc. (2)*, 88(2):338–358, 2013. URL: <https://arxiv.org/abs/1210.6542>, doi:10.1112/jlms/jdt023.
- [KM19] A. Kleshchev and R. Muth. Affine zigzag algebras and imaginary strata for KLR algebras. *Trans. Amer. Math. Soc.*, 371(7):4535–4583, 2019. URL: <https://arxiv.org/abs/1511.05905>, doi:10.1090/tran/7464.
- [KX12] S. König and C. Xi. Affine cellular algebras. *Adv. Math.*, 229(1):139–182, 2012. doi:10.1016/j.aim.2011.08.010.
- [KX99a] S. König and C. Xi. Cellular algebras: inflations and Morita equivalences. *J. London Math. Soc. (2)*, 60(3):700–722, 1999. doi:10.1112/S0024610799008212.
- [KX98] S. König and C. Xi. On the structure of cellular algebras. In *Algebras and modules, II (Geiranger, 1996)*, volume 24 of *CMS Conf. Proc.*, pages 365–386. Amer. Math. Soc., Providence, RI, 1998.
- [KX99b] S. König and C. Xi. When is a cellular algebra quasi-hereditary? *Math. Ann.*, 315(2):281–293, 1999. doi:10.1007/s002080050368.
- [LLT96] A. Lascoux, B. Leclerc, and J.-Y. Thibon. Hecke algebras at roots of unity and crystal bases of quantum affine algebras. *Comm. Math. Phys.*, 181(1):205–263, 1996.
- [LV11] A.D. Lauda and M. Vazirani. Crystals from categorified quantum groups. *Adv. Math.*, 228(2):803–861, 2011. URL: <https://arxiv.org/abs/0909.1810>, doi:10.1016/j.aim.2011.06.009.
- [Lus10] G. Lusztig. *Introduction to quantum groups*. Modern Birkhäuser Classics. Birkhäuser/Springer, New York, 2010. Reprint of the 1994 edition. doi:10.1007/978-0-8176-4717-9.
- [LM07] S. Lyle and A. Mathas. Blocks of cyclotomic Hecke algebras. *Adv. Math.*, 216 (2007), no. 2, 854–878. URL: <https://arxiv.org/abs/math/060745>, doi:10.1016/j.aim.2007.06.00.
- [Mat15] A. Mathas. Cyclotomic quiver Hecke algebras of type A. In G.W. Teck and K.M. Tan, editors, *Modular representation theory of finite and p -adic groups*, volume 30 of *National University of Singapore Lecture Notes Series*, chapter 5, pages 165–266. World Scientific, 2015. URL: <https://arxiv.org/abs/1310.2142>, doi:10.1142/9789814651813_0005.
- [MT23] A. Mathas and D. Tubbenhauer. Cellularity for weighted KLRW algebras of types B, $A^{(2)}$, $D^{(2)}$. *J. Lond. Math. Soc. (2)*, 107(3):1002–1044, 2023. URL: <https://arxiv.org/abs/2201.01998>, doi:10.1112/jlms.12706.
- [MT22] A. Mathas and D. Tubbenhauer. SageMath code on GitHub to compute dimensions of cyclotomic KLR algebras; and tikz macro on GitHub to display weighted KLRW idempotent diagrams. 2022. <https://github.com/AndrewMathas/GradedDimKLR>, <https://github.com/AndrewMathas/KLRWAlgebras> and <https://github.com/dtubbenhauer/KLRWdimensions>.
- [MT24] A. Mathas and D. Tubbenhauer. Subdivision and cellularity for weighted KLRW algebras. *Math. Ann.*, 389(3):3043–3122, 2024. URL: <https://arxiv.org/abs/2111.12949>, doi:10.1007/s00208-023-02660-4.
- [Rou08] R. Rouquier. 2-Kac–Moody algebras. 2008. URL: <http://arxiv.org/abs/0812.5023>.
- [Rou12] R. Rouquier. Quiver Hecke algebras and 2-Lie algebras. *Algebra Colloq.*, 19(2):359–410, 2012. URL: <https://arxiv.org/abs/1112.3619>, doi:10.1142/S1005386712000247.
- [Sag23] Sage Developers. *SageMath, the Sage Mathematics Software System*. The Sage Development Team, 2023. URL: <http://www.sagemath.org>.
- [Ste03] J.R. Stembridge. A local characterization of simply-laced crystals. *Trans. Amer. Math. Soc.*, 355(12):4807–4823, 2003. doi:10.1090/S0002-9947-03-03042-3.
- [Ste07] P. Sternberg. On the local structure of doubly laced crystals. *J. Combin. Theory Ser. A*, 114(5):809–824, 2007. URL: <https://arxiv.org/abs/math/0603547>, doi:10.1016/j.jcta.2006.09.003.
- [Tin17] P. Tingley. Elementary construction of Lusztig’s canonical basis. In *Groups, rings, group rings, and Hopf algebras*, volume 688 of *Contemp. Math.*, pages 265–277. Amer. Math. Soc., Providence, RI, 2017. URL: <https://arxiv.org/abs/1602.04895>, doi:10.1090/conm/688.
- [Tsu10] S. Tsuchioka. When does Lusztig’s canonical basis have non-positive structure coefficients? MathOverflow, 30 September 2010. URL: <https://mathoverflow.net/a/40577>.

- [Tub22] D. Tubbenhauer. Sandwich cellularity and a version of cell theory. *Rocky Mountain J. Math.*, 54(6):1733–1773, 2024. URL: <https://arxiv.org/abs/2206.06678>, doi:10.1216/rmj.2024.54.1733.
- [TV23] D. Tubbenhauer and P. Vaz. Handlebody diagram algebras. *Rev. Mat. Iberoam.*, 39(3):845–896, 2023. URL: <https://arxiv.org/abs/2105.07049>, doi:10.4171/RMI/1356.
- [VV11] M. Varagnolo and E. Vasserot. Canonical bases and KLR-algebras. *J. Reine Angew. Math.*, 659:67–100, 2011. URL: <https://arxiv.org/abs/0901.3992>, doi:10.1515/CRELLE.2011.068.
- [Web15] B. Webster. Canonical bases and higher representation theory. *Compos. Math.*, 151(1):121–166, 2015. URL: <https://arxiv.org/abs/1209.0051>, doi:10.1112/S0010437X1400760X.
- [Web17a] B. Webster. Knot invariants and higher representation theory. *Mem. Amer. Math. Soc.*, 250(1191):v+141, 2017. URL: <https://arxiv.org/abs/1309.3796>, doi:10.1090/memo/1191.
- [Web17b] B. Webster. Rouquier’s conjecture and diagrammatic algebra. *Forum Math. Sigma*, 5:e27, 71, 2017. URL: <https://arxiv.org/abs/1306.0074>, doi:10.1017/fms.2017.17.
- [Web19] B. Webster. Weighted Khovanov–Lauda–Rouquier algebras. *Doc. Math.*, 24:209–250, 2019. URL: <https://arxiv.org/abs/1209.2463>, doi:10.25537/dm.2019v24.209–250.
- [Wil14] G. Williamson. On an analogue of the James conjecture. *Represent. Theory*, 18:15–27, 2014. URL: <https://arxiv.org/abs/1212.0794>, doi:10.1090/S1088-4165-2014-00447-3.

A.M.: THE UNIVERSITY OF SYDNEY, SCHOOL OF MATHEMATICS AND STATISTICS F07, OFFICE CARSLAW 718, NSW 2006, AUSTRALIA, WWW.MATHS.USYD.EDU.AU/U/MATHAS/, ORCID 0000-0001-7565-5798

Email address: andrew.mathas@sydney.edu.au

D.T.: THE UNIVERSITY OF SYDNEY, SCHOOL OF MATHEMATICS AND STATISTICS F07, OFFICE CARSLAW 827, NSW 2006, AUSTRALIA, WWW.DTUBBENHAUER.COM, ORCID 0000-0001-7265-5047

Email address: daniel.tubbenhauer@sydney.edu.au